

ADVANCEMENTS IN THE EVALUATION OF HETEROGENEITY FOR NUCLEAR CRITICALITY SAFETY IN  
HIGH-ASSAY LOW-ENRICHED URANIUM SYSTEMS

A Dissertation

Presented in Partial Fulfillment of the Requirements for the

Degree of Doctor of Philosophy

with a

Major in Nuclear Engineering

in the

College of Graduate Studies

University of Idaho

by

Joseph Abraham Christensen

Approved by:

Major Professor: R.A. Borrelli, Ph.D.

Committee Members: Lee Ostrom, Ph.D.; Leslie Kerby, Ph.D.; John Bess, Ph.D.

Department Administrator: Indraji Charit, Ph.D.

May 2023

## ABSTRACT

A review of historical nuclear criticality accidents and critical experiments is conducted to evaluate the effects of heterogeneity in uranium-water critical systems. Advanced modeling methods are developed and described which generate and evaluate data to determine correlated effects between heterogeneity and other nuclear parameters. The described methods are validated against existing historical data using statistical methods.

## TABLE OF CONTENTS

ABSTRACT . . . . .	ii
TABLE OF CONTENTS . . . . .	iii
LIST OF TABLES . . . . .	iv
LIST OF FIGURES . . . . .	vi
LIST OF EQUATIONS . . . . .	vii
LIST OF ACRONYMS . . . . .	viii
STATEMENT OF CONTRIBUTION . . . . .	ix
CHAPTER 1: INTRODUCTION . . . . .	1
CHAPTER 2: TRIANGULAR LATTICES OF 2.49-CM DIAMETER LEU (4.948) RODS IN WATER . . . . .	11
CHAPTER 3: PARAMETRIC STUDY OF MINIMUM CRITICAL VOLUME FOR HIGH-ASSAY LOW-ENRICHED URANIUM (20%) IN SPHERICAL GEOMETRY AGAINST PARTICLE SIZE . . . . .	52
CHAPTER 4: NUCLEAR CRITICALITY SAFETY ASPECTS FOR THE FUTURE OF HALEU: EVALUATING HETEROGENEITY IN INTERMEDIATE-ENRICHMENT URANIUM USING CRITICAL BENCHMARK EXPERIMENTS . . . . .	74
CHAPTER 5: EVALUATIONS OF THE EFFECT OF HETEROGENEITY IN HALEU SYSTEMS USING MODIFIED CRITICAL BENCHMARKS . . . . .	92
CHAPTER 6: SUMMARY AND CONCLUSIONS . . . . .	119
APPENDIX A: TYPICAL INPUT LISTINGS . . . . .	127
APPENDIX B: SELECTED PORTIONS OF THE LETTER FROM E. B. JOHNSON TO G. E. WHITESIDES	
137	
APPENDIX C: MATERIAL DATA SHEET FOR STAINLESS STEEL . . . . .	139
APPENDIX D: EXPERIMENTER HAND CALCULATIONS FOR METAL MASS . . . . .	141
APPENDIX E: PLEXIGLAS TABLE ASSEMBLY DRAWING . . . . .	142
APPENDIX F: LATTICE PLATE ASSEMBLY DRAWING . . . . .	143
APPENDIX G: LATTICE PLATE ASSEMBLY DRAWING . . . . .	144
APPENDIX H: LATTICE PLATE ASSEMBLY DRAWING . . . . .	145

## LIST OF TABLES

2.1	LEU-MET-THERM-004 Average Experimental Rod Diameters . . . . .	12
2.2	LEU-MET-THERM-004 Experimental Lattice Specifications . . . . .	16
2.3	LEU-MET-THERM-004 Recorded Experimental Data . . . . .	19
2.4	LEU-MET-THERM-004 Reported Atom Densities . . . . .	20
2.5	LEU-MET-THERM-004 Uranium Metal Analysis . . . . .	20
2.6	LEU-MET-THERM-004 Reported Mass Data . . . . .	21
2.7	LEU-MET-THERM-004 Critical Arrangement Reflector Properties . . . . .	22
2.8	LEU-MET-THERM-004 Evaluated Critical Configurations . . . . .	24
2.9	LEU-MET-THERM-004 Summary of Mass Uncertainty . . . . .	25
2.10	LEU-MET-THERM-004 Mass Perturbation Results . . . . .	25
2.11	LEU-MET-THERM-004 Summary of Dimensional Uncertainty . . . . .	26
2.12	LEU-MET-THERM-004 Radius Perturbation Results . . . . .	27
2.13	LEU-MET-THERM-004 Fuel Height Perturbation Results . . . . .	27
2.14	LEU-MET-THERM-004 Lattice Pitch Perturbation Results . . . . .	28
2.15	LEU-MET-THERM-004 Nominal Fuel Composition . . . . .	28
2.16	LEU-MET-THERM-004 Enrichment Perturbation Results . . . . .	29
2.17	LEU-MET-THERM-004 U-234 Content Perturbation Results . . . . .	29
2.18	LEU-MET-THERM-004 Fuel Impurity Concentration . . . . .	30
2.19	LEU-MET-THERM-004 Impurity Content Perturbation Results . . . . .	30
2.20	LEU-MET-THERM-004 Plexiglas Sheet Dimensional Uncertainty . . . . .	32
2.21	LEU-MET-THERM-004 Plexiglas Lattice Plate Thickness Perturbation Results . . . . .	32
2.22	LEU-MET-THERM-004 Plexiglas Table Thickness Perturbation Results . . . . .	33
2.23	LEU-MET-THERM-004 Stainless Steel Support Thickness Perturbation Results . . . . .	33
2.24	LEU-MET-THERM-004 Plexiglas Lattice Plate Density Perturbation Results . . . . .	34
2.25	LEU-MET-THERM-004 Plexiglas Table Density Perturbation Results . . . . .	34
2.26	LEU-MET-THERM-004 Nominal PMMA Atom Densities . . . . .	35
2.27	LEU-MET-THERM-004 Plexiglas Impurity Uncertainty Results . . . . .	35
2.28	LEU-MET-THERM-004 Lattice Plate Height Bounding Uncertainty Results . . . . .	36
2.29	LEU-MET-THERM-004 Temperature Perturbation Results . . . . .	36
2.30	LEU-MET-THERM-004 Bottom Reflector Perturbation Results . . . . .	37
2.31	LEU-MET-THERM-004 Side Reflector Perturbation Results . . . . .	38

2.32	LEU-MET-THERM-004 Water Height Perturbation Results . . . . .	38
2.33	LEU-MET-THERM-004 Stainless Steel Composition . . . . .	39
2.34	LEU-MET-THERM-004 Total Experimental Uncertainty, Cases 1-4 . . . . .	44
2.35	LEU-MET-THERM-004 Total Experimental Uncertainty, Cases 5-8 . . . . .	45
2.36	LEU-MET-THERM-004 Bias Summary, Cases 1-4 . . . . .	46
2.37	LEU-MET-THERM-004 Bias Summary, Cases 5-8 . . . . .	47
2.38	LEU-MET-THERM-004 Holding Tank Removal Bias . . . . .	47
2.39	LEU-MET-THERM-004 Support Assembly Removal Bias . . . . .	48
2.40	LEU-MET-THERM-004 Reflector Temperature Bias . . . . .	48
2.41	LEU-MET-THERM-004 Fuel Impurity Removal Bias . . . . .	48
2.42	LEU-MET-THERM-004 Summary of Benchmark Experiment Parameters . . . . .	49
2.43	LEU-MET-THERM-004 Benchmark Model Fuel Atom Densities . . . . .	49
2.44	LEU-MET-THERM-004 Benchmark Model Reflector Atom Density . . . . .	49
2.45	LEU-MET-THERM-004 Experimental and Benchmark $k_{\text{eff}}$ . . . . .	49
2.46	LEU-MET-THERM-004 MCNP Sample Calculation Results . . . . .	50
2.47	LEU-MET-THERM-004 KENO Sample Calculation Results . . . . .	50
3.1	Modeling Input Parameters . . . . .	56
3.2	Uranium Minimum Volume . . . . .	59
3.3	Test Case 1 WHISPER Results . . . . .	61
4.1	Selected IEU-MET-FAST Benchmarks . . . . .	82
4.2	IEU-MET-FAST Transformation Bias . . . . .	83
5.1	IEU-COMP-INTER-003 Results and Parameters . . . . .	102
5.2	IEU-COMP-MIXED-002 Results and Parameters . . . . .	103
5.3	IEU-COMP-THERM-001 Results and Parameters . . . . .	103
5.4	IEU-COMP-THERM-015 Results and Parameters . . . . .	104
5.5	Correlation Results . . . . .	110

## LIST OF FIGURES

2.1	LEU-MET-THERM-004 Experimental Assembly . . . . .	14
2.2	LEU-MET-THERM-004 Co-axially Stacked Lattice . . . . .	15
2.3	LEU-MET-THERM-004 Experimental Lattice Arrangements, Cases 1-4 . . . . .	17
2.4	LEU-MET-THERM-004 Experimental Lattice Plate Arrangements, Cases 5-8 . . . . .	18
2.5	LEU-MET-THERM-004 Simplified Model Lattice Arrangements . . . . .	42
3.1	Calculated Minimum Critical Volume for Uranium-Water Systems . . . . .	65
3.2	Cross-sectional View of the Heterogeneous Model . . . . .	66
3.3	Critical Volume Versus Particle Size (6-15 kg) . . . . .	67
3.4	Critical Volume Versus Particle Size (8-25 kg) . . . . .	68
3.5	Homogeneous and Minimum Critical Volume Versus Mass . . . . .	69
3.6	WHISPER Correlation Coefficients (Case 1) . . . . .	70
3.7	WHISPER Correlation Coefficients (Case 2) . . . . .	71
4.1	Simplified Tokai-Mura Procedural Deviations . . . . .	77
4.2	Minimum Spherical Critical Volume Versus Enrichment . . . . .	80
4.3	Calculated Minimum Critical Volume Versus Enrichment . . . . .	88
5.1	ICI-003-01 . . . . .	105
5.2	ICM-002-02 . . . . .	106
5.3	ICM-002-01 . . . . .	106
5.4	ICT-001-01 . . . . .	107
5.5	ICT-015-01 . . . . .	107
5.6	ICM-002-03 . . . . .	108
5.7	ICI-003-02 . . . . .	109
5.8	ICM-002-04 . . . . .	109
5.9	LA-10860 Figure 22 . . . . .	111
5.10	LA-10860 Figure 23 . . . . .	112
5.11	PNNL-19176 Figure 11 . . . . .	114

## LIST OF EQUATIONS

2.1	Standard Uncertainty . . . . .	23
2.2	U-234 Weight Percent . . . . .	28
3.3	Lattice Parameter for Transformations . . . . .	56
3.4	Atomic Weight of Uranium . . . . .	57
5.5	Transformation of Material Specifications . . . . .	98
5.6	Calculation of Fuel Sphere Quantity . . . . .	98
5.7	Moderating Material Volume . . . . .	98
5.8	Differential $k_{\text{eff}}$ . . . . .	99
5.9	Pearson's Correlation Coefficient . . . . .	100

## LIST OF ACRONYMS

ANECEP	average energy of neutrons causing fission
HALEU	high-assay, low-enriched uranium
HEU	high-enriched uranium
ICSBEP	International Criticality Safety Benchmark Evaluation Project
IEU	intermediate-enrichment uranium
LEU	low-enriched uranium
LWR	light-water reactor
NCS	nuclear criticality safety
ORCEF	Oak Ridge Critical Experiments Facility
ORNL	Oak Ridge National Laboratory
PMMA	polymethyl methacrylate
SMR	small modular reactor



## STATEMENT OF CONTRIBUTION

The benchmark experiment evaluation published as Chapter 2 was authored by Joseph A. Christensen in its entirety, including the construction of models, analysis of data, and overall evaluation. The study was performed for the International Criticality Safety Benchmark Evaluation Project (ICSBEP) in accordance with the format and content guidance used for the handbook. Dr. John D. Bess, of the Idaho National Laboratory, provided comparative modeling to validate the study results as discussed in the report, and served as the internal reviewer for the entire work. An independent technical review was performed prior to submission by Mr. Davis A. Reed, of the Oak Ridge National Laboratory.

Chapters 3 through 5 were primarily authored in their entirety by Joseph A. Christensen under the direct supervision of Prof. R.A. Borrelli of the University of Idaho. Mr. Christensen was responsible for all research, modeling, analysis, and evaluation tasks as well as authorship of the final report. Dr. Borrelli performed technical review of all report content and provided feedback necessary to ensure overall research quality.

# CHAPTER 1: INTRODUCTION

## 1.1 PROJECT SUMMARY

This project seeks to address a gap in the research literature and an important question for practitioners of nuclear criticality safety (NCS): How much margin needs to be added for safe handling of heterogeneous high-assay, low-enriched uranium (HALEU) relative to safe sub-critical limits for homogeneous HALEU. This question is of growing importance due to the widespread industrial interest in small modular reactors, nuclear power systems for space applications, and non-light-water reactors (LWRs), for which HALEU will be needed as fuel. To address this question, through a series of exercises, methods were developed to examine the effects of heterogeneity and to estimate the magnitude of differences in multiplication factor ( $k_{\text{eff}}$ ) between similar heterogeneous and homogeneous uranium systems at twenty percent enrichment. The methods were developed using critical benchmark models from the International Handbook of Evaluated Criticality Safety Benchmark Experiments [1], including the evaluation and documentation of a benchmark experiment for this work. For each scope of work, a specific objective is established and a method is described to accomplish it. Taken together, these combined works show consistent progress toward creating a uniform validated methodology which can be used to evaluate the effects of heterogeneity in HALEU systems, with the ultimate intent of making operations with this category of nuclear material safer.

## 1.2 MOTIVATION

The interest in nuclear reactor systems utilizing HALEU in the United States is growing dramatically. Small modular reactors (SMRs), nuclear power systems for space applications, and non-LWRs currently under development all plan to utilize uranium enriched beyond five percent U-235 by weight. In order to support this industry expansion, new fuel cycle facilities will need to be designed, licensed, and built. Nuclear criticality safety is a very important part of the design, licensing, and operation of nuclear fuel cycle facilities, and the effect of heterogeneity in these facilities is extremely important to NCS.

## 1.3 OVERALL OBJECTIVE

The objective of this work is to examine the effects of heterogeneity as it applies to HALEU systems. It starts by establishing a general framework from which such an evaluation can take place by formal evaluation of an historical critical experiment. This benchmark evaluation demonstrates the use of tools which are used in follow-on examinations. The second step of this work critically evaluates several

parameters identified in the literature as important to heterogeneity for NCS applications using a rigorous modeling approach. Finally, the tools and algorithms developed in the early project stages are applied to a series of previously-published benchmark evaluations to determine if any effects of heterogeneity are present and if they can be effectively quantified. The results of each phase of the project are peer-reviewed and published.

## 1.4 BACKGROUND

### 1.4.1 HISTORY

Knowledge of the effect of heterogeneity has been known since virtually the beginning of nuclear science and engineering. In fact, prior to the development of enrichment technology to increase the amount of U-235 available in uranium to be used for fuel, nuclear chain reactions were quite impossible to obtain without the influence of heterogeneity. Proof of this fact was successfully demonstrated in 1942 by Enrico Fermi and his “Chicago Pile No. 1” [2].

Following the Manhattan Project, the questions surrounding heterogeneity in the early days were primarily focused on reducing the amount of nuclear fuel needed to create a reactor [3]. At that time, it was believed that uranium was relatively scarce. Therefore, it was desirable to minimize the amount of fuel needed for reactors in order to achieve economic goals, particularly given the energy cost of enrichment. An analytic solution was developed and described by Goertzel in his work, *Minimum Critical Mass and Flat Flux* [3] which describes a condition where a non-uniform fuel distribution (a heterogeneous fuel distribution) resulting in a uniform thermal neutron flux produces the minimum critical mass for a reactor. His solution forms a cornerstone in reactor analysis which has driven reactor design for decades.

Goertzel’s analytic solution was demonstrated experimentally by J.W. Morfitt. The experiment and its results are described in detail in an Atomic Energy Commission de-classified report which was also submitted as a Ph.D. thesis at the University of Tennessee [4]. In this report, concentric cylinders of highly-enriched uranyl nitrate solution of varying concentration are used as an experimental assembly. The assembly was brought critical and nuclear measurements were made. The conclusions of this experiment clearly validated Goertzel’s analytical solution and demonstrated that the critical mass of a non-uniform fuel distribution in a critical system is lower than the mass of a similar system with uniform fuel distribution.

### 1.4.2 CRITICALITY ACCIDENTS

Following the early days of reactor development, the lesson of heterogeneity was learned painfully on at least four occasions [5]. On April 21, 1957 at the Mayak Production Association in the Soviet Union, a criticality accident occurred due to unforeseen accumulation of fissile material in a solution processing tank. The accumulated material was two different forms of highly-enriched uranium compounds: a thin, hard crust and flocculant precipitate with variable concentration inside the vessel. This accident resulted in the death of a worker and caused several nearby workers to become ill with acute radiation sickness.

The second occasion in which heterogeneity played a clear role in an accident occurred on July 14, 1961 at the Siberian Chemical Combine, also in the Soviet Union. This accident involved a slow accumulation of 22.6 percent enriched uranium in an oil reservoir for a vacuum pump. The precise concentration, volume, and material configuration at the time of the accident are not known, and the accident only resulted in one worker experiencing non-fatal radiation sickness.

On November 3, 1965, another criticality accident occurred at the Electrostal Machine Building Plant in the Soviet Union. This accident was caused by the slow settling of 6.5 percent enriched uranium oxide particles inside a vacuum system supply vessel after the vacuum pump was turned off. Fortunately, there were no injuries caused by this accident. Notably, however, this accident occurred at the facility during a time of transition. The facility had previously been used for deconversion of uranium hexafluoride to uranium oxide at two percent enrichment and was being upgraded to handle the higher 6.5 percent enrichment. This fact is important when considering the larger context of the industry transition being discussed in the United States from low-enriched uranium (LEU) to HALEU.

The final criticality accident in which heterogeneity played a clear role happened on May 15, 1997 at the Novosibirsk Chemical Concentration plant. The accident occurred in a ‘favorable geometry’ collection vessel downstream of an etching process. Over a 13-year period, solid deposits of uranium oxide had collected inside the vessel as both a solid crust and a particle slurry. This unanticipated change in material form, combined with an unreviewed change in the process enrichment from 36 percent to 90 percent, allowed the ‘favorable geometry’ vessel to achieve criticality. Six super-critical excursions occurred over two days before the system was brought under control. No significant radiation dose occurred during this incident.

Two common threads emerge when evaluating these four historical criticality accidents: (1) the effects of heterogeneity can play a significant role in the sequence of events which lead to a criticality, and (2) changes, both anticipated and unanticipated, in a fissile material process must be carefully evaluated in order to prevent accidents from occurring. In each of these accidents, the fissile material configuration

was found, post hoc, to be very different than the conditions analyzed for the process. The effects of process chemistry on material composition should always be carefully evaluated, and the evaluation should be approached with conservatism to account for uncertainties.

### 1.4.3 APPLICATIONS

In the field of modern nuclear criticality safety, analysts use available data to establish sub-critical limits on systems containing fissile material. These limits are intended to allow operations with fissile material outside reactors while preventing the occurrence of a nuclear chain-reaction, sometimes referred to as a “criticality”. The preferred hierarchy for selection of sub-critical limits is (1) by derivation from directly applicable experiments, or, if experimental data are not available, (2) by calculations using a validated method [6]. At issue for nuclear criticality safety practitioners today is the general lack of relevant experimental data for particular applications, in this case HALEU.

Previously, the relative lack of data for HALEU has not been a significant issue. Substantial data exist for both LEU and high-enriched uranium (HEU) applications such that interpolation between the two is trivial for simple applications, and there has been little or no need in the last few decades for data on HALEU outside of academic discussion. Typically, handbooks and regulatory guidance provide information that NCS practitioners are able to use to provide safe sub-critical limits. However, the current literature contains a significant caveat that becomes the focus of this work: many of the limits provided apply to single, homogeneous units—when considering systems which contain heterogeneity, additional margin must be applied. This creates a question without a convincing answer: ‘how much margin?’ It is from this particular query that the need for a refreshed look at the subject arises. If the answer provided by NCS practitioners is too much, production processes will become too restricted to be economical due to small batches and low throughput; if the answer is too little, a nuclear accident could result.

Heterogeneity, generally, is the property where fissionable material is dispersed in a moderating medium in discrete units, rather than uniformly throughout a given volume. From the literature, it is not even immediately clear what systems qualify as heterogeneous. Various safety guides ([7], [8]) provide one possible answer:

...if the particles constituting a mixture are uniformly distributed and are larger than 127 microns (i.e.. not capable of being passed through a 120-mesh screen), the mixture must be considered as heterogeneous.

Interestingly, this particular restriction seems to be quite arbitrary. Its derivation appears to have come from a pins-in-water experiment where the pin size was 0.02 inches (508 microns) [9]. The 127-micron restriction is precisely one-fourth of the 508 and was probably selected as ‘conservative’, although the basis for such a selection is not clear. It is precisely these sort of parameters that this project intends to address directly using more modern methods.

#### 1.4.4 PROJECT

This project focuses on particular aspects of heterogeneity in NCS with unique application to HALEU systems. In the literature, it is known that the effects of heterogeneity for uranium systems with less than six percent enrichment reduce both the critical volume and mass [8], and between six and thirty-four percent enrichment, only the critical volume is reduced. The effect tends to disappear above thirty-four percent enrichment [10], where the critical volume of homogeneous uranium-water systems is bounded by single-unit metal systems. Therefore it is of significant interest to explore the range between six percent and thirty-four percent enrichment for applications relevant to the use, handling, and storage of HALEU.

Existing NCS methodologies are dichomatic in that they have been developed to support and are focused on the two historical applications of nuclear reactions: LWRs using low-enriched uranium at or below five percent U-235 and nuclear weapons using HEU. Consequently, there is a gap in knowledge and methods for the safe handling of uranium enriched between these values. This isn’t to say that there is no information or that application of the current methodologies is inadequate for safety purposes, but there are opportunities to improve the methods and potentially gain efficiencies through the reduction of overly-conservative safety margins. Such efficiencies are important; the financial costs associated with new fuel cycle facilities are likely to be significantly higher than existing facilities because new equipment, techniques, and materials are needed to handle higher-enrichment fuel.

Another aspect of heterogeneity to be addressed is the size of the solid units dispersed within the moderating medium. Again, some guidance exists which creates an upper bound on the particle size which can be considered negligible (127 microns) [8], but robust explorations of the effect of particle size on heterogeneity in NCS have not been conducted. For this work, it is of interest to examine the origin of the stated upper bound, test its veracity, and determine if there are opportunities to extend this value to particles of larger size. There is a general lack of experimental data which examines the effect of small particles. This project will demonstrate methods which can be used to adapt existing benchmark experimental data in a way which provides insight into the problem.

## 1.5 LOGICAL PATH, WORK SCOPE, AND DESCRIPTION OF TASKS

A formal exploration of the effect of heterogeneity in HALEU systems requires division of the work into specific, discrete scope. The selection of the individual scopes of work was accomplished to ensure that the overall research question is evaluated with sufficient rigor such that the results are appropriate and relevant.

### 1.5.1 SCOPE OF WORK 1 - ESTABLISH RESEARCH BASELINE FOR USE OF NUCLEAR CRITICALITY SAFETY BENCHMARKS

The first scope of work accomplished as part of the overall research goal is the establishment of a baseline understanding of the nature and scope of a heterogeneous nuclear system. This scope was accomplished by the formal evaluation of an historical criticality experiment and documentation of the results of this evaluation in the ICSBEP handbook.

To complete this work, an evaluation of an historical critical experiment series performed at the Oak Ridge National Laboratory in the 1960s was conducted. The experimental series evaluates the effect of lattice spacing on critical mass in a LEU and water system. The experiments used a collection of LEU metal rods in a water tank. The benchmark evaluation is a report documenting the physical and analytical uncertainties in the experiment and generates a simplified model which can be used to approximate the experiment. These benchmarks are often currently used to evaluate nuclear data and nuclear simulation codes.

This work is shown in Chapter 2. The benchmark evaluation report documents statistical evaluations of experimental and modeling uncertainty, provides simplified benchmark model specifications, and demonstrates the accuracy of the benchmark model across a variety of Monte Carlo codes and nuclear data libraries. This scope of work was divided into discrete tasks in order to guide the completion of work and to establish supporting milestones:

#### *Task I. Develop Detailed Experimental Model*

Using historical experiment records and available literature, develop a detailed MCNP model of the subject experimental configurations.

#### *Task II. Evaluate Experimental Uncertainties*

Using appropriate statistical methods and ICSBEP handbook guidance, evaluate and quantify the effect of parametric uncertainties in the detailed experimental model.

*Task III. Develop Simplified Benchmark Model*

Develop a simplified model of the subject experiments which meets acceptance criteria established in the ICSBEP handbook.

*Task IV. Quantify and Evaluate Benchmark Simplification Biases*

Using the detailed and simplified experimental models, quantify and evaluate simplification biases, including an analysis of the overall simplification bias.

### 1.5.2 SCOPE OF WORK 2 - COMPLETE AN EVALUATION OF HISTORICAL DATA TO DEMONSTRATE THE EFFECTS OF HETEROGENEITY

In support of the need for a detailed review of the effects of heterogeneity, a scope of work was developed to evaluate relevant data available in literature. This scope examined specific parameters related to NCS evaluations of heterogeneous uranium systems and compared them to the results in literature, with the specific purpose of developing and testing methods which might yield a resolution to the overall research goal. This work is shown in Chapter 3. The scope of work was divided into discrete tasks in order to guide the completion of work and to establish supporting milestones:

*Task V. Describe a methodology by which the minimum critical volume of uranium-water systems may be systematically examined in both homogeneous and heterogeneous systems.*

The methodology automates the process of input deck generation for use in Monte Carlo neutron transport codes to improve the efficiency of evaluations.

*Task VI. Using the described methodology, examine the effect of uranium mass and particle size on the minimum critical volume of uranium-water systems of 20% enriched uranium.*

This examination is intended to identify the minimum critical volume for heterogeneous and homogeneous systems and to compare the two systems with respect to percent relative change.

*Task VII. Compare the results of the examination to previous results presented in technical literature and propose recommendations.*

Several assumptions present in current literature regarding particle size and the difference in critical volume between homogeneous and heterogeneous systems are tested and compared to the results derived using the described algorithms.



### 1.5.3 SCOPE OF WORK 3 - INVESTIGATE THE EFFECTS OF HETEROGENEITY USING CRITICAL BENCHMARKS

This project scope is accomplished in two stages. In the first stage, a thorough examination of available source material is conducted and the candidate benchmark evaluations are identified. In the second, the selected benchmarks are evaluated using the tools described previously.

#### 1.5.3.1 SCOPE OF WORK 3A - IDENTIFY CANDIDATE BENCHMARKS

As a starting point, it was necessary to down-select relevant benchmark evaluations from the ICSBEP handbook. The handbook contains thousands of evaluated benchmark experiments, of which only a small fraction are intermediate-enrichment uranium, and only a fraction of those are relevant to the evaluation of heterogeneity. Consequently, a focused effort was made to develop rigorous selection criteria which could be used to select precisely which benchmark evaluations would be used to test the new methodologies and to justify the selection. This work is shown in Chapter 4. The scope of work was divided into discrete tasks in order to guide the completion of work and to establish supporting milestones:

*Task VIII. Establish and explain selection criteria for the identification of candidate benchmark evaluations.*

*Task IX. Identify and describe the selected benchmarks.*

*Task X. Propose modifications to the evaluated benchmark models that will aid in the evaluation of the effects of heterogeneity.*

#### SCOPE OF WORK 3B - EVALUATE SELECTED BENCHMARKS

Using the selected benchmark evaluations, a detailed investigation into the effects of heterogeneity in the evaluated critical systems was undertaken. This investigation used the previously-developed tools and methods to modify the specified benchmarks to induce a known degree of heterogeneity into the critical system and evaluate the effects. The information gathered from the previous work was used to guide the investigation, and the results of the investigation were evaluated using statistical methods to form reasonable conclusions which may be used by NCS professionals to formulate rules for the safe handling of HALEU. This work is shown in Chapter 5. The scope of work was divided into discrete tasks in order to guide the completion of work and to establish supporting milestones:

*Task XI. Using evaluated critical benchmarks, determine whether or not a change in the fuel geometry from homogeneous to heterogeneous produces a meaningful change in system multiplication.*

*Task XII. If a change in multiplication is determined to exist, evaluate the magnitude of the change against other system parameters in search of useful correlations.*

*Task XIII. Evaluate the presence or lack of correlation.*

The aggregate outcome of these scopes of work is a comprehensive methodology which can be used to evaluate the effects of heterogeneity in HALEU systems for NCS applications. The methodology is based on principles established in the critical benchmark evaluation process and is validated against data which exists in the currently-available literature.

## REFERENCES

- [1] Nuclear Energy Agency. *International Handbook of Evaluated Criticality Safety Benchmark Experiments*. NEA No. 7520. Paris: OECD Nuclear Energy Agency, July 2020.
- [2] U.S. Department of Energy - Office of History and Heritage Resources. *The Manhattan Project, An Interactive History, "CP-1 Goes Critical"*. n.d. URL: [https://www.osti.gov/opennet/manhattan-project-history/Events/1942-1944\\_pu/cp-1\\_critical.htm](https://www.osti.gov/opennet/manhattan-project-history/Events/1942-1944_pu/cp-1_critical.htm) (visited on 09/23/2022).
- [3] Gerald Goertzel. "Minimum Critical Mass and Flat Flux". In: *Journal of Nuclear Energy (1954)* 2.3 (1956), pp. 193–201. ISSN: 0891-3919. DOI: [https://doi.org/10.1016/0891-3919\(55\)90034-6](https://doi.org/10.1016/0891-3919(55)90034-6). URL: <https://www.sciencedirect.com/science/article/pii/0891391955900346>.
- [4] J.W. Morfitt. *Minimum Critical Mass and Uniform Thermal Neutron Core Flux in an Experimental Reactor*. Ph.D. Thesis. Report number Y-1023. Declassified November 22, 1957. Oak Ridge, TN: United States Atomic Energy Commission, Dec. 1953.
- [5] Thomas P. McLaughlin et al. *A Review of Criticality Accidents*. Technical Report LA-13638. Los Alamos, NM: Los Alamos National Laboratory, May 2000.
- [6] *Nuclear Criticality Safety in Operations with Fissionable Material Outside Reactors*. Standard. La Grange Park, IL: American Nuclear Society, Nov. 2018.
- [7] Norman L. Pruvost, Hugh C. Paxton, eds. *Nuclear Criticality Safety Guide*. Technical Report LA-12808. Los Alamos, NM: Los Alamos National Laboratory, Sept. 1996.
- [8] J.T. Thomas, ed. *Nuclear Safety Guide. TID-7016, Revision 2*. Tech. rep. NUREG/CR-0095. U.S. Nuclear Regulatory Commission, May 1978. DOI: 10.2172/6231577. URL: <https://www.osti.gov/biblio/6231577>.
- [9] C.E. Newlon. *The Effect of Uranium Density on the Safe U-235 Enrichment Criterion*. Technical Report K-1550. Oak Ridge, TN: Oak Ridge Gaseous Diffusion Plant, Oct. 1962.
- [10] E.D. Clayton et al. *Anomalies of Nuclear Criticality, Revision 6*. Tech. rep. PNNL-19176. Pacific Northwest National Lab, Richland, WA, 2010.

## CHAPTER 2: TRIANGULAR LATTICES OF 2.49-CM DIAMETER LEU (4.948) RODS IN WATER

**Joseph A. Christensen. “Triangular Lattices of 2.49 cm Diameter LEU (4.948) Rods in Water”. In: *International Handbook of Evaluated Criticality Safety Benchmark Experiments*. LEU-MET-THERM-004. Paris: OECD Nuclear Energy Agency, 2020**

### 2.1 DETAILED DESCRIPTION

#### 2.1.1 OVERVIEW OF EXPERIMENT

A series of critical experiments were performed at the Oak Ridge Critical Experiments Facility (ORCEF) in the late 1960s involving square and triangular lattices of different spacing with unclad LEU (4.948) metal rods in water. The experiments were performed by Ms. Elizabeth B. Johnson of Oak Ridge National Laboratory (ORNL). The purpose of the experimental series was to determine critical mass of uranium for various rod diameters and pitches with water as the moderator and reflector. The set of experiments evaluated in this report consists of triangular lattice arrangements of 2.495 cm (0.982 in) diameter metal rods reflected in water [2]. This set of experiments was performed between January 4 and February 23, 1967. Additional information supporting this series is found in the experiment logbook ([3], pp 9-27). A total of fifteen configurations were reported in this experimental set, with eight critical arrangements evaluated. All eight configurations were determined to represent acceptable benchmark experiments.

The rods were enriched to  $4.948 \pm 0.05$  wt%  $^{235}\text{U}$  and had at least 15 cm (5.98 in) of water reflection on all sides, except the top (Appendix G of [4]). The rods were held in place by Plexiglas<sup>®</sup> grid plates with holes cut out for the placement of the rods. The grid plates were supported by bolts in the corners of the plates. The measurements included positive and negative period, as well as “just critical.” The control parameter for these experiments was the water height in the tank, which was varied along with the number of rods and the rod arrangement to produce a critical configuration.

Other experiments in the series included rods of various sizes in similar configurations. The series includes rods of 0.094, 0.3, 0.5, 0.75, and 1.0 in nominal diameters and various square and triangular

pitch and arrangements. The 0.3-in diameter rods in square-pitched arrays were previously evaluated in LEU-MET-THERM-007 [4].

## 2.1.2 DESCRIPTION OF EXPERIMENTAL CONFIGURATION

### 2.1.2.1 LEU RODS

The experiments in this series consisted of triangular arrangements of solid  $30.00 \pm 0.01$  cm ( $11.811 \pm 0.004$  in) long, 0.982 in (2.495 cm) diameter LEU rods. All of the experiments used between 31 and 78 rods per configuration, and some configurations stacked lattices co-axially, creating a 60-cm total rod length (Appendix B). Corrosion was inhibited by wiping the rods with a “light machine oil” soaked cloth. This method of corrosion prevention was described as a common laboratory practice by Calvin M. Hopper, of ORNL.

A sample of rods was measured to determine the average diameter, with three measurements being taken and averaged per rod. These data were recorded in the logbooks ([5], p.300). The rod diameters are given in Table 2.1. These average rod diameters were generated by a random sample of the fuel rods used in the experiments. Each number recorded in the table is the average of three measurements on each rod—each end and the center. Records of the uranium mass per individual rod were not available; the experimenter’s specification for manufacture of the rods stated dimensional requirements only.

Table 2.1. Average Rod Diameters for the Evaluated Experiments.

	Measurement (inches)
	0.928
	0.990
“1.0 inches”	0.987
	0.983
	0.970
	0.981
Average	0.982

### 2.1.2.2 LATTICE PLATES AND SUPPORTING STRUCTURE

A 0.5 in (1.27 cm) thick Plexiglas grid plate was used at the center-line to support the configurations that were co-axially stacked. This same grid plate was used as the upper support plate for the non-stacked configurations. At the top of the co-axially-stacked (60 cm) configurations, a 0.25 in (0.635 cm)

thick Plexiglas grid plate was used to stabilize the LEU metal rods. The height of the lattice plates was maintained by 9/16 in (1.429 cm) diameter carbon steel bolts held in place by wing nuts at the top and bottom of each lattice plate. The bottoms of the fuel rods were supported by a 1 in thick Plexiglas support plate. A 2 in stainless steel support was used under the bottom support plate, and was stacked on top of a 3 in slab (Appendix E) of Plexiglas with drainage holes and slots to allow water to drain from the assembly during tank draining. The bottom of this support was held off the bottom of the tank by spacers, approximately 1/2 in high. The bottom of the fuel rods was approximately 6.5 in (16.51 cm) from the bottom of the tank. The holes in the lattice plates for the fuel rods were 1-1/64 in (2.580 cm) in diameter (Appendix F).

### 2.1.2.3 WATER REFLECTOR

The reflector was approximately 15 cm (6 in) thick in all directions except above the rods, where the water height was varied for each experimental configuration (Appendix G of [4]). The experiment was established as exactly critical by changing the water height. The measured and recorded water heights are in reference to the bottom of the uranium rods. The experimenter also notes that this was considered an “infinite water reflector”. Water level measurements were taken with a mirror scale on a sloped manometer sight glass to minimize meniscus effects giving the uncertainty in the water level of  $\pm 0.05$  cm.

### 2.1.2.4 EXPERIMENT ROOM AND TANK

These experiments were performed in the West Cell of the ORCEF. A photograph of an assembly is shown in Figure 2.1; the tank was approximately 6 ft by 6 ft square. Nothing other than the fuel rods, support structure, and neutron detectors with lead anchoring bricks was present in the tank.

### 2.1.2.5 ASSEMBLY DESCRIPTION

The experiment used triangular arrays of two different heights. Sketches were provided in the logbook [3] and in other documents (Appendix B). Figure 2.1 shows a similar experimental arrangement to those evaluated in this report. Figure 2.2 shows a cross sectional view of an example experimental arrangement for a co-axially-stacked lattice.

There were fifteen configurations, seven with a single-height assembly, and eight with a coaxial stack of two fuel rods (for a total height of 60 cm). Of these fifteen configurations, eight were critical. Data

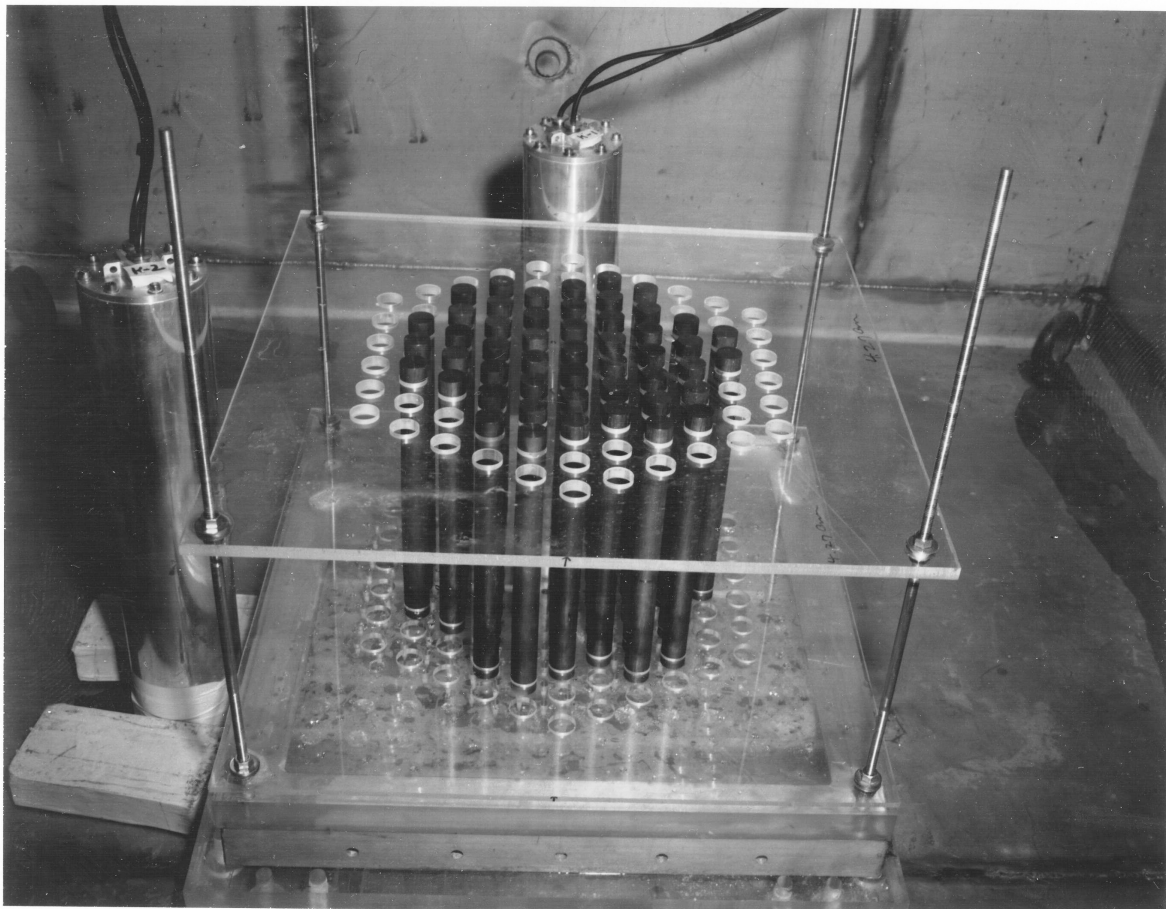


Figure 2.1. An undated photograph of the experimental assembly for a 30-cm-high array of uranium fuel rods. This particular assembly is evaluated as Case 2..

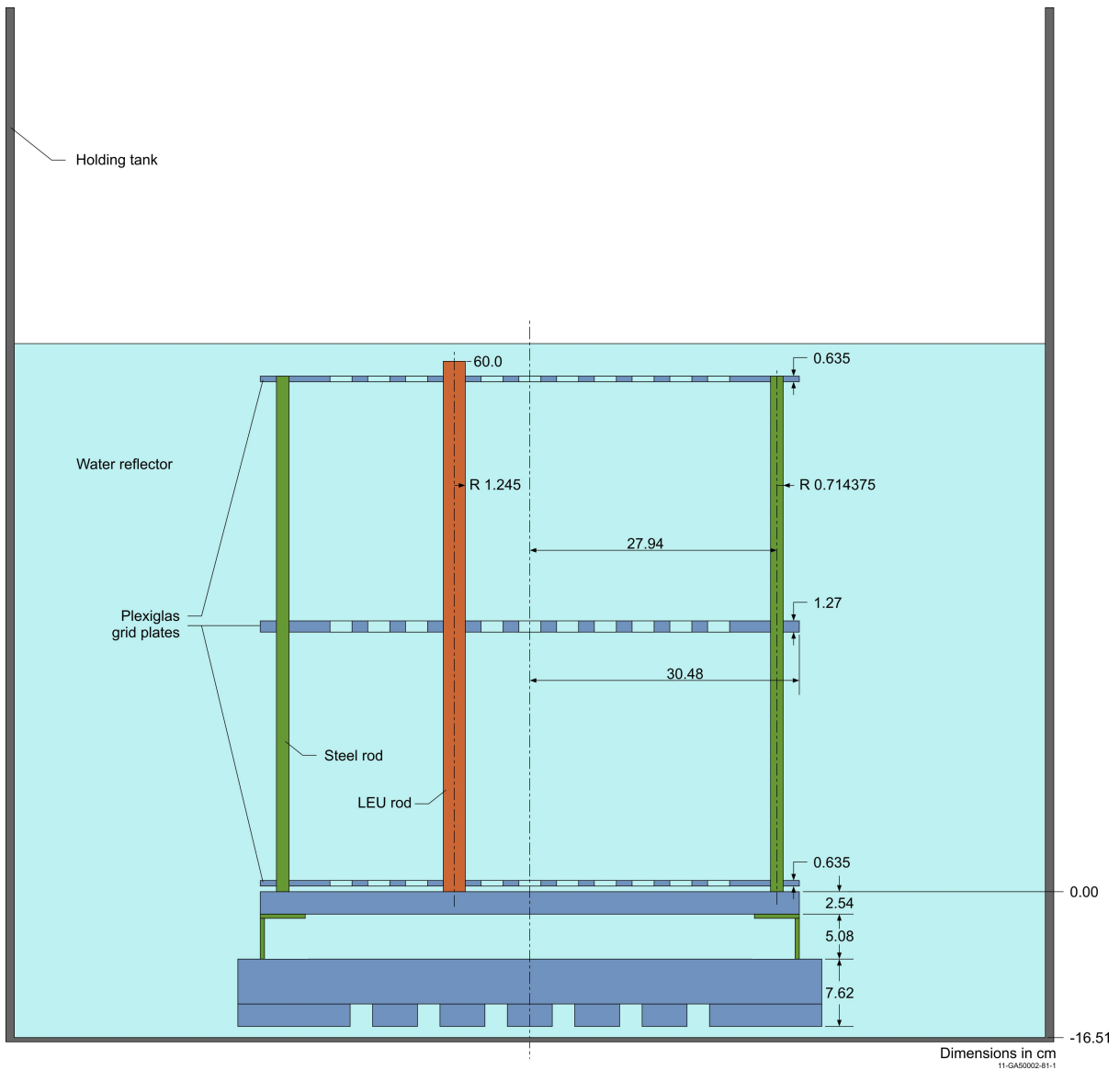


Figure 2.2. An example experimental assembly for a co-axially-stacked lattice (not to scale). In the co-axial lattices, the fuel rod height is 60 cm..



describing the arrays is found in Table 2.2 with additional measurement data in Table 1.3. In the 60-cm height cases, the arrangement of fuel rods consisted of a coaxial stack of two 30-cm rods.

Table 2.2. Experimental Lattice Specifications for the Evaluated Experiments.

Lattice Spacing		Lattice Height (cm)	Total Number of Rods	Date of Experiment
Surface (cm)	Center (cm)			
1.78	4.27	30	50	1/5/1967
		60	34 ( $\times 2$ ) 35 ( $\times 2$ )	1/9/1967
2.23	4.27	30	45 46	1/10/1967
		60	31 ( $\times 2$ ) 32 ( $\times 2$ )	
2.73	5.22	30	49 48	2/21/1967
		60	31 ( $\times 2$ ) 32 ( $\times 2$ )	2/22/1967
3.53	6.02	30	73 72	2/22/1967
		60	39 ( $\times 2$ ) 38 ( $\times 2$ )	2/23/1967

Sketches were provided (Appendix B) of the different arrays' configurations in the logbook. A collection of the arrangements is provided in Figures 2.3 and 2.4.

#### 2.1.2.6 EXPERIMENTAL DATA

Notations throughout the logbook [3] provide period measurements for each experimental configuration. In some cases, the configuration is listed as "subcritical" or "just critical." In the cases where an arrangement was critical a water height measurement was included. This information was tabulated in the letter from E. B. Johnson to G. E. Whitesides dated February 16, 1968 (Appendix B). The letter also includes extrapolated reactivity corresponding to a fully submerged lattice (i.e., if the top reflector were infinite) for each configuration. These values are not used in this report. The  $\beta_{\text{eff}}$  used to calculate the reported reactivity worth was not given. The reactivity and critical water height are presented in

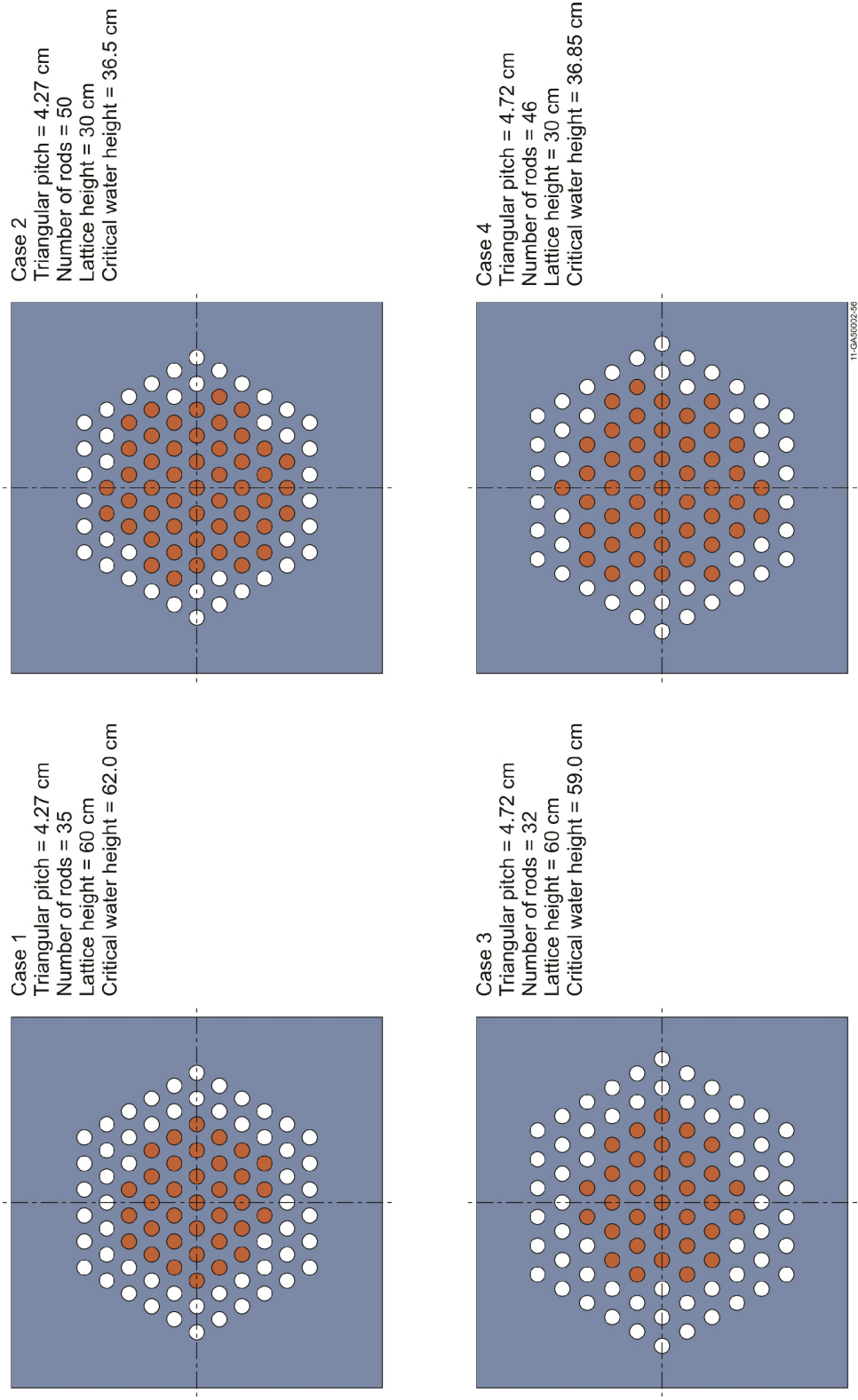


Figure 2.3. Experimental Lattice Arrangements for Cases 1 through 4.

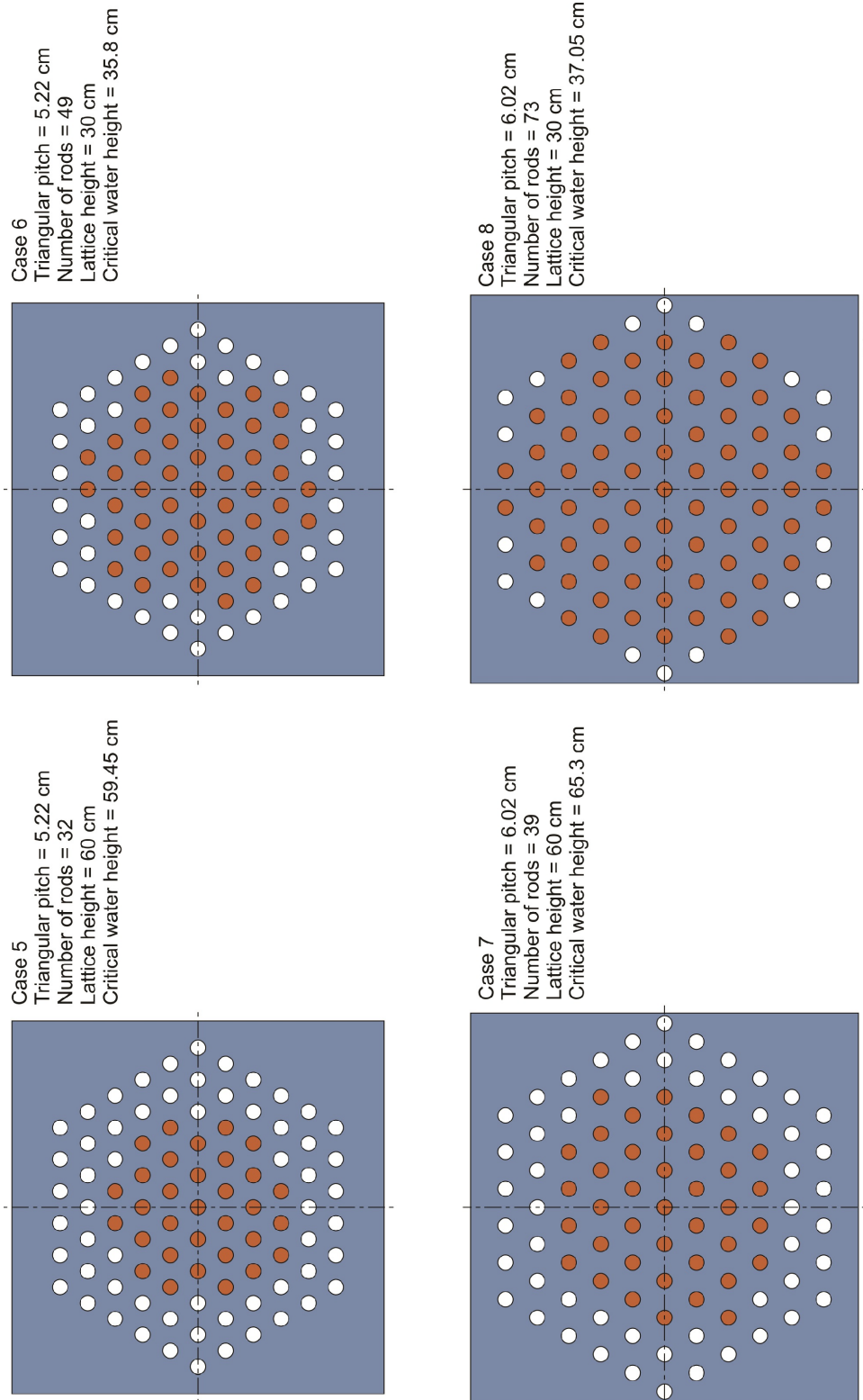


Figure 2.4. Experimental Lattice Arrangements for Cases 5 through 8.

Table 2.3. Only in the cases where a configuration is described as “just critical” is the critical water height included. In two cases, the water height is slightly less than the height of the fuel rods.

A sixteenth experiment is described in the logbook, but not included in the summary table. This configuration was presumably rejected by the experimenter because of the substantial difference between the top of the rods and the critical water height. A subsequent configuration was examined and recorded, effectively replacing the prior experiment. The 60-cm height arrangements consisted of a co-axial stack of two 30-cm rods. Table 2.3 is a summary of the recorded experimental data.

Table 2.3. Recorded Experimental Data from the Experimental Logbooks.

Lattice Type (Type)	Center-to-Center Lattice Spacing (cm)	Total Number of Rods	Reactivity of Fully Reflected Lattice ( $\rho$ )	“Just Critical” Water Height (cm)
Triangular (30 cm)	4.27	50	$\approx 0.21$	36.5
Triangular (60cm)		34 ( $\times 2$ )	Subcritical	—
		34 ( $\times 2$ )	$\approx 0.37$	62.00
Triangular (30 cm)	4.72	45	Subcritical	—
		46	$\approx 0.18$	36.85
Triangular (60cm)		31 ( $\times 2$ )	Subcritical	—
		32 ( $\times 2$ )	1.02	59.0
Triangular (30 cm)	5.22	49	$\approx 0.33$	35.8
		48	Subcritical	—
Triangular (60cm)		31 ( $\times 2$ )	Subcritical	—
		32 ( $\times 2$ )	$\approx 0.92$	59.45
		33 ( $\times 2$ )	—	54.0
Triangular (30 cm)	6.02	73	$\approx 0.16$	37.05
		72	-0.029	—
Triangular (60cm)		39 ( $\times 2$ )	0.096	65.3
		38 ( $\times 2$ )	Subcritical	—

## 2.1.3 DESCRIPTION OF MATERIAL DATA

### 2.1.3.1 LEU RODS

Logbook data show that the measured enrichment was between 4.92 wt% and 4.97 wt% ([6], p.141). This conflicts with the published article (Ref. 1), which describes uranium with 4.89 wt%  $^{235}\text{U}$ . However, in the letter from E. B. Johnson to C. Ho, (Appendix G of [4]), the experimenter indicated that the correct enrichment is  $4.95 \pm 0.05$  wt%  $^{235}\text{U}$ , and included instructions to disregard the previously published enrichment. Also in the letter, the experimenter provided calculations of approximate atom densities of the  $^{235}\text{U}$  and  $^{238}\text{U}$  composition of the LEU rods. No other information is given regarding the method by which these atom densities were obtained. The experimenter's reported atom densities are shown in Table 2.4.

Table 2.4. Reported Material Atom Densities.

Isotope	Atom Density (atom $\cdot$ barn $^{-1}$ $\cdot$ cm $^{-1}$ )
$^{235}\text{U}$	$2.40347 \times 10^{-3}$
$^{238}\text{U}$	$4.50884 \times 10^{-2}$

Included with the assay measurements in the logbook are purity measurements [6]. The results of these analyses are shown in Table 2.5. No information is provided about the type of analysis performed or any associated measurement uncertainties. The measurements are dated 6/19/1969.

Table 2.5. Reported Enrichment Analysis Results of Uranium Metal Rods Used as Fuel.

Rod Diameter (inches)	Purity (g $\cdot$ gU $^{-1}$ )	Assay (wt% $^{235}\text{U}$ )
0.094	0.999774	4.93
0.30	0.999781	4.97
0.50	0.999507	4.95
0.75	0.999768	4.97
1.0	0.999993	4.92
Average	0.999765	4.95

Mass data for  $^{235}\text{U}$  were recorded and tabulated by the experimenter (Appendix B). The data are shown in Table 2.6. The total mass and enrichment of the uranium rods were provided to the experimenter from the supplier. Individual rod mass data were inferred, not measured, from the supplied data. No measurement uncertainties or information about the measurement method were provided.

Table 2.6. Reported Mass Data for Fuel Rods Used in the Experimental Configurations.

Lattice Type (Type)	Center-to-Center Lattice Spacing (cm)	Number of Rods	Mass of $^{235}\text{U}$ (kg)
Triangular (30 cm)	4.27	50	6.772
Triangular (60cm)		34 ( $\times 2$ )	9.210
		35 ( $\times 2$ )	9.481
Triangular (30 cm)	4.72	45	6.095
		46	6.231
Triangular (60cm)		31 ( $\times 2$ )	8.398
		32 ( $\times 2$ )	8.669
Triangular (30 cm)	5.22	49	6.637
		48	6.502
Triangular (60cm)		31 ( $\times 2$ )	8.398
		32 ( $\times 2$ )	8.669
Triangular (30 cm)	6.02	73	9.888
		72	9.752
Triangular (60cm)		39 ( $\times 2$ )	10.565
		38 ( $\times 2$ )	10.294

### 2.1.3.2 SUPPORT STRUCTURE

No material composition data was provided by the experimenter for any of the Plexiglas or steel pieces used in the experiment. In a memo provided to J. C. Puit from E. B. Johnson on February 15, 1968, the experimenter states that the rod support was provided with perforated plates of Plexiglas with a reference density of  $1.18 \text{ g}\cdot\text{cm}^{-3}$  (Appendix B).

### 2.1.3.3 REFLECTOR

The reflector is light water, at a temperature range of 21.5 to 24.5 °C. The corresponding density range is 0.997995 to 0.997048  $\text{g}\cdot\text{cm}^{-3}$  [7]. Table 2.7 shows the water temperature and water height for the critical arrangements. Two temperature measurements were included for each configuration, but no data is provided about the placement or use of the temperature detectors.

Table 2.7. Reflector Properties for the Critical Arrangements Used in the Experiments.

Lattice Type (height)	Center-to-Center Lattice Spacing (cm)	Total Number of Rods	Water Temperature (°C)	“Just Critical” Water Height (cm)
Triangular (30 cm)	4.27	50	24.5	36.5
Triangular (60 cm)			24.5	
Triangular (30 cm)	4.72	35 ( $\times 2$ )	24.3	62.00
Triangular (60 cm)			24.3	
Triangular (30 cm)	5.22	46	24.0	36.85
Triangular (60 cm)			24.0	
Triangular (30 cm)	5.22	32 ( $\times 2$ )	24.0	59.0
Triangular (60 cm)			24.2	
Triangular (30 cm)	6.02	49	22.5	35.8
Triangular (60 cm)			22.7	
Triangular (30 cm)	6.02	32 ( $\times 2$ )	22.0	59.45
Triangular (60 cm)			22.5	
Triangular (30 cm)	6.02	73	22.7	37.05
Triangular (60 cm)			22.7	
Triangular (30 cm)	6.02	39 ( $\times 2$ )	21.5	65.3
Triangular (60 cm)			22.5	

#### 2.1.3.4 HOLDING TANK

No information is reported on the material properties of the tank used in this experiment.

#### 2.1.4 TEMPERATURE

Experimental temperatures are recorded in Table 2.7.

#### 2.1.5 SUPPLEMENTAL EXPERIMENTAL MEASUREMENTS

No additional measurements were performed.

## 2.2 EVALUATION OF THE EXPERIMENTAL DATA

Monte Carlo N-Particle (MCNP) version 5-1.51 calculations were utilized to estimate the biases and uncertainties associated with the experimental results in this evaluation. MCNP is a general-purpose, continuous-energy, generalized-geometry, time-dependent, coupled n-particle Monte Carlo transport code [8]. The Evaluated Neutron Data File library, ENDF/B-VII.0 [9] neutron cross section data were utilized in this benchmark. The 1- $\sigma$  Monte Carlo statistical uncertainty for the calculations was less than or equal to  $\pm 0.00010$ . For this report, an uncertainty is considered negligible if  $^{\circ}k_i$  is less than 0.00010. The individual parameter uncertainties, even those less than this threshold, are shown in their respective sections. Tables 2.34 and 2.35 serves as a summary table for the total uncertainty and shows the values used in the computation of overall uncertainty. The total uncertainty for these experiments is considered acceptable.

Unless otherwise mentioned, the standard uncertainty,  $\Delta k_i$ , was calculated by the difference between the upper and lower perturbation limits divided by the number of standard deviations, as shown below:

$$\Delta k_i = \frac{\mu_i}{\delta x_i} (k_{\text{upper}} - k_{\text{lower}}) \quad (2.1)$$

where  $\mu_i$  is the standard uncertainty in the parameter being perturbed and  $\delta x_i$  is the value of the perturbation. For values reported with an upper and lower limit perturbation, the  $\Delta k$  reported in the corresponding table is the average of the upper and lower perturbations. The reported scaling factor then corresponds to the number of single-direction standard deviations by which the value was perturbed.

Eight of the fifteen cases reported in the logbook were evaluated. These cases correspond to the eight critical configurations, one for each pitch and each height (30 cm and 60 cm). All of the evaluated cases are acceptable benchmark experiments. The remaining sub-critical configurations were not evaluated. Table 2.8 lists the configurations for each case. Drawings for each of the configurations are shown in Figures 2.3 and 2.4. The rod configurations match the configurations shown in the logbook for each experiment.



Table 2.8. Case Identifiers and Critical Configurations Under Evaluation.

Case	Pitch	Height
1	4.27 cm	60 cm
2		30 cm
3	4.72 cm	60 cm
4		30 cm
5	5.22 cm	60 cm
6		30 cm
7	6.02 cm	60 cm
8		30 cm

## 2.2.1 LOW ENRICHED URANIUM ROD UNCERTAINTIES

### 2.2.1.1 LEU MASS

The experiment used rods with 4.948 wt%  $^{235}\text{U}$  enrichment. The calculated enrichment differs from published data (Reference 1) and is based on statements in the letter from E. B. Johnson to C. Ho, June 28, 1976,(Appendix G of [4]). as well as measured enrichment data from the logbook ([6], p.141). The purity and enrichment analysis are tabulated in Table 2.6. The metal used in this experiment was drawn from a batch of material used in a number of experiments in this series. The metal was cast into the proper size rods as required by the experimenter. Thus, it is appropriate to use the average value of the rod measurements from Table 2.6 to determine the proper enrichment and purity. The calculated average purity was  $99.9765 \pm 0.0172$  wt%, and the calculated average enrichment was  $4.948 \pm 0.020$  wt%

Using the experimenter's hand calculations (Appendix D) as a reference, the mass of uranium per rod is calculated. The experimenter indicates that a total mass of 224.363 kg as listed on the waybills was utilized to create 81 total rods. This gives a mean uranium mass per rod of 2.770 kg. The experimenter also includes what appears to be a direct measurement of 7 of the fabricated rods and gives a weight of 42.5 lb (19.318 kg). The hand calculation uses a conversion factor of 2.2 lb per kg. The correct metric weight of these 7 rods should be 19.278 kg, giving a mean value of 2.754 kg per rod. Given the limited mass data for the rods, the difference between the population mean of 2.770 kg per rod and the sample mean of 2.754 kg per rod, 15.96 g per rod, is assumed as a  $1-\sigma$  standard deviation. This falls within 1% of the population mean (15.99 g per rod). This gives a final calculated mass value of  $2769.91 \pm 15.96$

gU per rod. Using the calculated enrichment value of  $4.948 \pm 0.020$  wt%, the average mass of  $^{235}\text{U}$  per rod is calculated as  $137.055 \pm 0.791$  g $^{235}\text{U}$  per rod.

Table 2.9 is a summary of mass parameters and associated uncertainty. The mass uncertainty was evaluated for each case and the results are summarized in Table 2.10. For the 60-cm height cases, the deviation in mass was scaled by a factor of  $\sqrt{2}$  to reflect the use of two rods in the assembly. Volume was conserved for the mass perturbation.

Table 2.9. Summary of Mass Uncertainty for Experimental Fuel Rods.

Parameter	Mean Measured Value or Design Value	Uncertainty in Parameter	Type of Uncertainty	$\nu$ Degrees of Freedom	Number of Standard Deviations Associated with the Uncertainty	Standard Uncertainty ( $1\sigma$ )
Uranium Mass per Rod (g)	2769.91	15.96	A	—	1	15.96
$^{235}\text{U}$ mass per rod (g)	137.055	0.791	—	—	1	0.791

Table 2.10. Results for Perturbations in Uranium Fuel Rod Mass.

Case	Deviation ( $\pm 3\sigma$ )	$\rho k_{\text{eff}} \pm \rho k$	Scaling Factor	$\Delta k_{\text{eff}} \pm \rho k$
1	$\pm 67.71$ g	$0.00147 \pm 0.00007$	3	$0.00049 \pm 0.00002$
2	$\pm 47.88$ g	$0.00196 \pm 0.00006$		$0.00065 \pm 0.00002$
3	$\pm 67.71$ g	$0.00131 \pm 0.00006$		$0.00044 \pm 0.00002$
4	$\pm 47.88$ g	$0.00205 \pm 0.00006$		$0.00068 \pm 0.00002$
5	$\pm 67.71$ g	$0.00146 \pm 0.00006$		$0.00049 \pm 0.00002$
6	$\pm 47.88$ g	$0.00206 \pm 0.00006$		$0.00069 \pm 0.00002$
7	$\pm 67.71$ g	$0.00138 \pm 0.00006$		$0.00046 \pm 0.00002$
8	$\pm 47.88$ g	$0.00189 \pm 0.00006$		$0.00063 \pm 0.00002$

### 2.2.1.2 LEU DIMENSIONS

A sample of rods was measured to determine the average diameter, with three measurements being taken and averaged per rod. The measurements were recorded in the logbook [5]. The measured rod diameters are given in section 1.2.1. The average and standard deviation of these averages are calculated as  $0.982 \pm 0.007$  in.

The rod length has been given as  $30.00 \pm 0.01$  cm (Appendix B), the reported uncertainty of which is interpreted to be a machining tolerance. A standard deviation of 0.006 cm (Type B) was calculated from this measurement. Appendix H describes the uncertainty as  $\pm 0.01$  in. This discrepancy is noted, but the effect is trivial and therefore is neglected. For the cases where two rods are stacked to form a 60 cm height array, the standard deviation is calculated as 0.008 cm. Table 2.11 is a summary of dimensional parameters and associated uncertainty. It shows the nominal values and uncertainty for the fuel rod length and diameter.

Table 2.11. Summary of Dimensional Uncertainty for Uranium Fuel Rods.

Parameter	Mean Measured Value or Design Value	Uncertainty in Parameter	Type of Uncertainty	$\nu$ Degrees of Freedom	Number of Standard Deviations Associated with the Uncertainty	Standard Uncertainty ( $1\sigma$ )
Rod Length (cm)	30.00	0.01	B	$\infty$	$\sqrt{3}$	0.006
Rod Length (cm)	60.00	—	—	—	1	0.008
Rod Diameter (cm)	2.495	0.017	A	4	1	0.017

The uncertainty associated with each dimensional parameter was evaluated for each case. The results are shown in Tables 2.12 and 2.13. Each parameter was perturbed independently with mass conserved for the radius and height perturbations. It is assumed for these calculations that the mass and radius uncertainties are uncorrelated. However, in reality, some degree of correlation exists. Insufficient data exists to fully examine the degree of correlation, but it can be assumed that these reported data may present a small overestimation in the total uncertainty.

### 2.2.1.3 LEU SPATIAL VARIATION

The size of the holes used to support the rods was 1-1/64 in (2.580 cm). The pitch for each case was varied by  $\pm 0.12$  cm from the nominal pitch listed in Table 2.8. This is based on the assumption that the pitch would be “off” simultaneously for all the rods, either bigger or smaller. For each case, the resulting perturbation was then scaled by  $\sqrt{N}$ , where N is the number of rods. The results are shown below. The standard uncertainty is assumed as 1/64 in (0.04 cm), based on the design specifications in

Table 2.12. Fuel Rod Radius Perturbation Results.

Case	Deviation ( $\pm 3\sigma$ )	${}^{\circ}k_{\text{eff}} \pm {}^{\circ}k$	Scaling Factor	$\Delta k_{\text{eff}} \pm {}^{\circ}k$
1		$-0.00437 \pm 0.00006$		$-0.00146 \pm 0.00002$
2		$-0.00445 \pm 0.00006$		$-0.00148 \pm 0.00002$
3		$-0.00130 \pm 0.00006$		$-0.00043 \pm 0.00002$
4	$\pm 0.026 \text{ cm}$	$-0.00122 \pm 0.00006$	3	$-0.00041 \pm 0.00002$
5		$0.00157 \pm 0.00006$		$0.00052 \pm 0.00002$
6		$0.00151 \pm 0.00006$		$0.00050 \pm 0.00002$
7		$0.00485 \pm 0.00006$		$0.00162 \pm 0.00002$
8		$0.00488 \pm 0.00006$		$0.00163 \pm 0.00002$

Table 2.13. Fuel Height Perturbation Results.

Case	Deviation ( $\pm 3\sigma$ )	${}^{\circ}k_{\text{eff}} \pm {}^{\circ}k$	Scaling Factor	$\Delta k_{\text{eff}} \pm {}^{\circ}k$
1	$\pm 0.008 \text{ cm}$	$0.00004 \pm 0.00006$		Neg.
2	$\pm 0.006 \text{ cm}$	$0.00004 \pm 0.00006$		Neg.
3	$\pm 0.008 \text{ cm}$	$0.00003 \pm 0.00006$		Neg.
4	$\pm 0.006 \text{ cm}$	$-0.00009 \pm 0.00006$	3	$-0.00003 \pm 0.00002$
5	$\pm 0.008 \text{ cm}$	$-0.00010 \pm 0.00006$		$-0.00003 \pm 0.00002$
6	$\pm 0.006 \text{ cm}$	$0.00005 \pm 0.00006$		Neg.
7	$\pm 0.008 \text{ cm}$	$-0.00002 \pm 0.00006$		Neg.
8	$\pm 0.006 \text{ cm}$	$0.00007 \pm 0.00006$		Neg.

the grid plate design sketch. The evaluated uncertainty associated with the fuel rod pitch is shown in Table 2.14.

#### 2.2.1.4 LEU ISOTOPIC CONTENT

The LEU used in this experimental series was most likely manufactured using the Fernald process prior to being shipped to Oak Ridge National Lab. Pre- and post-casting analyses were performed, but no detailed uranium isotope analysis is available. Based on knowledge of the process, it is likely that no  ${}^{236}\text{U}$  and only small amounts of  ${}^{234}\text{U}$  were present in the metal. The atom density for  ${}^{234}\text{U}$  was calculated using the same enrichment ratio as for  ${}^{235}\text{U}$ . An example calculation is shown in Equation 2.2. The balance was taken as  ${}^{238}\text{U}$  to match both enrichment and uranium density. Table 2.15 shows the evaluated isotopic composition of the uranium metal.

Table 2.14. Lattice Pitch Perturbation Results.

Case	Deviation ( $\pm 3\sigma$ )	$^{\circ}k_{\text{eff}} \pm ^{\circ}k$	Scaling Factor	$\Delta k_{\text{eff}} \pm ^{\circ}k$
1		$0.00660 \pm 0.00007$	$3\sqrt{35}$	$0.00037 \pm 0.00002$
2		$0.00462 \pm 0.00007$	$3\sqrt{50}$	$0.00022 \pm 0.00002$
3		$0.00212 \pm 0.00006$	$3\sqrt{32}$	$0.00012 \pm 0.00002$
4	$\pm 0.12$ cm	$0.00061 \pm 0.00006$	$3\sqrt{46}$	$0.00003 \pm 0.00002$
5		$-0.00198 \pm 0.00006$	$3\sqrt{32}$	$-0.00012 \pm 0.00002$
6		$-0.00327 \pm 0.00006$	$3\sqrt{49}$	$-0.00016 \pm \text{Neg.}$
7		$-0.00633 \pm 0.00006$	$3\sqrt{39}$	$-0.00034 \pm \text{Neg.}$
8		$-0.00776 \pm 0.00006$	$3\sqrt{73}$	$-0.00030 \pm \text{Neg.}$

The calculated enrichment, based on recorded measurements, was 4.948 wt%  $^{235}\text{U}$  with a standard uncertainty of 0.020 wt%. The evaluated uncertainty associated with the enrichment is shown in Table 2.16.

$$\text{wt}\% \text{ } ^{234}\text{U} = \text{wt}\% \text{ } ^{234}\text{U}_{\text{nat.}} \times \left( \frac{E^{235}}{^{234}\text{U}_{\text{nat.}}} \right) \quad (2.2)$$

Table 2.15. Nominal Uranium Fuel Rod Composition.

Isotope	Wt% Uranium	Uncertainty (wt%)
$^{234}\text{U}$	0.038	0.0002
$^{235}\text{U}$	4.948	0.020
$^{236}\text{U}$	Neg.	Neg.
$^{238}\text{U}$	95.014	0.020

### 2.2.1.5 LEU IMPURITIES

The average total impurity concentration in the LEU was determined to be 0.0235 wt.%. The specific impurity isotopes were determined using mass spectrograph measurements of the rods. The results from the mass spectrograph show a number of elements listed as “less than” some quantity. Based on correspondence with a spectrographer<sup>1</sup>, a “less than” quantity indicates that the element could not be measured with any confidence. The impurities that have detectable presence in the samples are shown

<sup>1</sup>Email correspondence between David Keebler, Oak Ridge National Laboratory and Joseph Christensen, 3/29/11

Table 2.16. Fuel Enrichment Perturbation Results.

Case	Deviation ( $\pm 3\sigma$ )	${}^0k_{\text{eff}} \pm {}^0k$	Scaling Factor	$\Delta k_{\text{eff}} \pm {}^0k$
1		$0.00155 \pm 0.00006$		$0.00052 \pm 0.00002$
2		$0.00154 \pm 0.00006$		$0.00051 \pm 0.00002$
3		$0.00153 \pm 0.00006$		$0.00051 \pm 0.00002$
4	$\pm 0.060 \text{ wt}\%$	$0.00155 \pm 0.00006$	3	$0.00052 \pm 0.00002$
5		$0.00161 \pm 0.00006$		$0.00054 \pm 0.00002$
6		$0.00161 \pm 0.00006$		$0.00054 \pm 0.00002$
7		$0.00161 \pm 0.00006$		$0.00054 \pm 0.00002$
8		$0.00167 \pm 0.00006$		$0.00056 \pm 0.00002$

Table 2.17. U-234 Content Perturbation Results.

Case	Deviation ( $\pm 3\sigma$ )	${}^0k_{\text{eff}} \pm {}^0k$	Scaling Factor	$\Delta k_{\text{eff}} \pm {}^0k$
1		$-0.00003 \pm 0.00006$		Neg.
2		$-0.00011 \pm 0.00006$		$-0.00004 \pm 0.00002$
3		$-0.00005 \pm 0.00006$		Neg.
4	$\pm 0.0006 \text{ wt}\%$	$-0.00012 \pm 0.00006$	3	$-0.00004 \pm 0.00002$
5		$-0.00012 \pm 0.00006$		$-0.00004 \pm 0.00002$
6		$-0.00009 \pm 0.00006$		$-0.00003 \pm 0.00002$
7		$0.00014 \pm 0.00006$		$0.00005 \pm 0.00002$
8		$-0.00001 \pm 0.00006$		Neg.

in Table 2.11. The average concentration of each element was used to evaluate the data. In two cases, lead and niobium, one or more samples indicated a “less than” value in the analysis. For these cases, a  $-1\sigma$  value of the minimum detectable quantity was used to calculate the average concentration because it is likely that some of the element is present, but below the detectable level. The  $1\sigma$  value was determined assuming a triangular distribution between the minimum detectable value and zero. The value used for the average is shown in Table 2.18.

The difference in impurity concentration between the gross measurement and the spectrographic measurements is accounted for by the probable inclusion of small quantities of light elements, specifically oxygen and nitrogen. The detailed analysis included assumed values of 25 ppm oxygen and 9.8 ppm nitrogen. The assumed uncertainty in the total impurity concentration is determined by calculating the average standard deviation in the spectrographic analysis (35.71 ppm) and scaling it upwards to match the overall impurity concentration. This gives a standard uncertainty ( $1\sigma$ ) of 41.9 ppm (0.00419 wt%)

the impurity concentration was perturbed from 0.0379 wt% to 0.0091 wt%. The concentration of each impurity was perturbed simultaneously, without changing the ratio between individual elements. The perturbation results are shown in Table 2.19.

Table 2.18. Fuel Impurity Concentrations.

Element (ppm)	Sample 684558	Sample 684557	Sample 684556	Sample 684555	Sample 684554	Average	Standard Deviation
Aluminum	12	12	6	10	10	10	2.45
Boron	0.1	0.2	0.2	0.3	0.2	0.2	0.07
Copper	4	4	3	40	4	11	16.22
Iron	25	25	20	40	15	25	9.35
Manganese	10	10	6	8	6	8	2.00
Niobium	(6.827)	(6.827)	(6.827)	(6.827)	10	7.46	1.42
Nickel	15	12	10	10	8	11	2.65
Lead	1	1	(0.6827)	3	2	1.54	0.96
Silicon	125	110	125	175	95	126	30.08
Total	198.9	181.0	177.7	293.1	150.2	200.2	35.71

Table 2.19. Fuel Impurity Content Perturbation Results.

Case	Deviation ( $\pm 3\sigma$ )	$^{\circ}k_{\text{eff}} \pm ^{\circ}k$	Scaling Factor	$\Delta k_{\text{eff}} \pm ^{\circ}k$
1		$0.00005 \pm 0.00006$		Neg.
2		$0.00002 \pm 0.00006$		Neg.
3		$-0.00002 \pm 0.00006$		Neg.
4	$\pm 0.0144$ wt.%	$-0.00007 \pm 0.00006$	3.43	Neg.
5		$-0.00007 \pm 0.00006$		Neg.
6		$0.00006 \pm 0.00006$		Neg.
7		$0.00012 \pm 0.00006$		$0.00003 \pm 0.00002$
8		$-0.00025 \pm 0.00006$		$-0.00007 \pm 0.00002$

## 2.2.2 SUPPORT STRUCTURE

### 2.2.2.1 SUPPORT STRUCTURE DIMENSIONS

The support plates holding the fuel rods were Plexiglas sheets. For the 4.27, 4.72, and 5.22 cm pitches, the sheets were 60.96 cm (24 in) square. The 6.02 cm pitch sheets were 63.5 cm (25 in) square.

For the 30-cm fuel height configurations, the bottom sheet was 0.635 cm (0.25 in) thick and placed near the bottom of the rods. The top sheet was 1.27 cm (0.5 in) thick and at about 29 cm in height. The 60-cm height cases used a 1.27 cm (0.5 in) piece at the center-line to support the coaxial stack of rods, as well as the 0.635 cm (0.25 in) piece at a height of about 58 cm. The support plates were held in position by carbon steel bolts 1.42875 cm (9/16 in) in diameter, placed in the corners of the support plates at 2.54 cm (1 in) square for all but Cases 7 and 8. For these cases, the bolts were 3.81 cm (1.5 in) from the corners, due to the larger lattice plates in these cases. The position of the lattice plates was maintained by carbon steel wing nuts at the top and bottom of the plates.

Supporting the assembly from below was a table consisting of a 1 in (2.54 cm) thick piece of Plexiglas on top of a stainless steel support, 2 in (5.08 cm) high and 2 in (5.08 cm) wide. The steel support was constructed of 3/16 in (0.47625 cm) thick stainless steel shaped into an angle. Under the steel support, another Plexiglas table was added, 3 in (7.62 cm) thick with drilled holes and slats to allow water drainage from the assembly. The bottom table was constructed of three 1 in (2.54 cm) thick pieces glued together to form the assembly (Appendix E).

The modern nominal thickness of a 0.25 in thick Plexiglas plate is 0.236 in (0.60 cm). The tolerance range for this nominal thickness is 0.186 to 0.266 in<sup>2</sup> (0.47 to 0.68 cm). Similarly, for a 0.5 in thick sheet, the nominal thickness is 0.472 in (1.20 cm) with a tolerance of 0.397 to 0.507 in (1.01 to 1.29 cm); and for a 1 in thick sheet, 0.944 in (2.40 cm) with a tolerance of 0.833 to 0.993 in (2.12 to 2.52 cm). It is assumed that these values are similar to those that were used in the experiment. As a consequence, it is likely that the reported 0.25 in, et cetera, values that were reported in the experiment configurations are actually slightly different from reality. The modern thickness tolerances were used to calculate the uncertainty in the Plexiglas thickness. These tolerance bounds are asymmetric and not a large contributor to the total uncertainty; therefore, the Type B standard uncertainty is calculated using the upper and lower tolerance bounds. The uncertainty calculations are summarized in Table 2.20.

To better quantify any separate effects, the thickness of the lattice plates and the thickness of the support table were perturbed separately. For the 3 in table at the bottom of the assembly, the individual 1 in Plexiglas uncertainties were combined to give a thickness uncertainty of 0.080 in. The results of the perturbations are shown below. The nominal thickness was not modified in this analysis to match the expected modern values, only the uncertainties were used.

The thickness tolerance for 3/16 in stainless steel is  $\pm 0.007$  in (0.018 cm). The thickness of the stainless steel support was perturbed  $\pm 0.021$  in (0.053 cm). This perturbation applies to both the vertical and horizontal sections of the support. The results of the perturbation are shown in Table 2.23.

<sup>2</sup>Plexiglas® G Acrylic Sheet Technical Data Sheet, Altuglas International



Table 2.20. Plexiglas Sheet Dimensional Uncertainty.

Thickness (in)	Nominal Thickness (in)	Tolerance (in)	$\nu$ Degrees of Freedom	Number of Standard Deviations Associated with the Uncertainty	Standard Uncertainty ( $1\sigma$ ) (in)
0.25	0.236	0.186-0.266			0.023
0.5	0.472	0.397-0.507	$\infty$	$\sqrt{3}$	0.032
1	0.944	0.833-0.993			0.046

Table 2.21. Plexiglas Lattice Plate Thickness Perturbation Results.

Case	Deviation ( $\pm 3\sigma$ )	${}^{\circ}k_{\text{eff}} \pm {}^{\circ}k$	Scaling Factor	$\Delta k_{\text{eff}} \pm {}^{\circ}k$
1		$0.00001 \pm 0.00006$		Neg.
2		$0.00006 \pm 0.00006$		Neg.
3		$0.00004 \pm 0.00006$		Neg.
4	$\pm 0.069$ in. (1/4 in.)	$0.00017 \pm 0.00006$	3	$0.00006 \pm 0.00002$
5	$\pm 0.096$ in. (1/2 in.)	$-0.00001 \pm 0.00006$		Neg.
6		$0.00012 \pm 0.00006$		$0.00004 \pm 0.00002$
7		$0.00001 \pm 0.00006$		Neg.
8		$0.00027 \pm 0.00006$		$0.00009 \pm 0.00002$

### 2.2.2.2 PLEXIGLAS DENSITY

Plexiglas has a nominal material density of  $1.19 \text{ g}\cdot\text{cm}^{-3}$ . The range of density for Plexiglas is  $1.17\text{-}1.20 \text{ g}\cdot\text{cm}^{-3}$  [10]. This corresponds with a standard uncertainty (Type B) of  $0.0087 \text{ g}\cdot\text{cm}^{-3}$ . Perturbations were performed using  $1.1639\text{-}1.2161 \text{ g}\cdot\text{cm}^{-3}$  as a  $\pm 3\sigma$  perturbation. The results are shown in Table 2.24 and 2.25 show that variations in Plexiglas density are negligible. The experimenter reported a value of  $1.18 \text{ g}\cdot\text{cm}^{-3}$ , as mentioned in Section 1.3.2; however this value appears to be referenced as a nominal value and not an actual measurement. The difference between the reported nominal density and the density utilized in this evaluation is negligible.

### 2.2.2.3 PLEXIGLAS COMPOSITION

Typically, Plexiglas is greater than 99.9% pure, but may contain minor impurities introduced during the polymerization process or by intentional addition. No indication exists that these experiments were

Table 2.22. Plexiglas Table Thickness Perturbation Results.

Case	Deviation ( $\pm 3\sigma$ )	${}^{\circ}k_{\text{eff}} \pm {}^{\circ}k$	Scaling Factor	$\Delta k_{\text{eff}} \pm {}^{\circ}k$
1		$0.00023 \pm 0.00006$		$0.00008 \pm 0.00002$
2		$0.00031 \pm 0.00006$		$0.00010 \pm 0.00002$
3		$-0.00012 \pm 0.00006$		$-0.00004 \pm 0.00002$
4	$\pm 0.239$ in. (3 in.)	$0.00024 \pm 0.00006$	3	$0.00008 \pm 0.00002$
5	$\pm 0.138$ in. (1 in.)	$-0.00004 \pm 0.00006$		Neg.
6		$0.00015 \pm 0.00006$		$0.00005 \pm 0.00002$
7		$0.00009 \pm 0.00006$		$0.00003 \pm 0.00002$
8		$0.00034 \pm 0.00006$		$0.00011 \pm 0.00002$

Table 2.23. Stainless Steel Support Thickness Perturbation Results.

Case	Deviation ( $\pm 3\sigma$ )	${}^{\circ}k_{\text{eff}} \pm {}^{\circ}k$	Scaling Factor	$\Delta k_{\text{eff}} \pm {}^{\circ}k$
1		$0.00009 \pm 0.00006$		$0.00003 \pm 0.00002$
2		$0.00004 \pm 0.00006$		Neg.
3		$-0.00010 \pm 0.00006$		$-0.00003 \pm 0.00002$
4	$\pm 0.021$ in.	$<0.00001 \pm 0.00006$	3	Neg.
5		$-0.00013 \pm 0.00006$		$-0.00004 \pm 0.00002$
6		$-0.00005 \pm 0.00006$		Neg.
7		$-0.00006 \pm 0.00006$		Neg.
8		$-0.00006 \pm 0.00006$		Neg.

performed with any additives in the Plexiglas. A senior technical engineer from Altuglas International, a Plexiglas manufacturer, was consulted and provided some information for use in determining Plexiglas composition.<sup>3</sup> Plexiglas manufactured around the time of the experiments would have been produced using one of two different chemical processes, but the primary component (greater than 90%) of the composition in either process is polymethyl methacrylate (PMMA), which has the chemical composition  $(C_5O_2H_8)_n$ . Therefore, this chemical composition was used to calculate the atom densities of Plexiglas used in the experiment. Table 2.26 shows the nominal atom density of Plexiglas.

To provide a bounding uncertainty on the effect of impurities in the Plexiglas, a 1 ppm natural boron impurity was introduced. The results of the perturbation are shown in Table 2.27. In one case, the effect was slightly positive. The result is slightly outside the statistical uncertainty of the models, and may be due to the proximity of the upper lattice plate with the water's surface. This individual uncertainty did

<sup>3</sup>Personal communication between Robert Cheritano, Altuglas International and Joseph Christensen, August 2010.

Table 2.24. Plexiglas Lattice Plate Density Perturbation Results.

Case	Deviation ( $\pm 3\sigma$ )	${}^{\circ}k_{\text{eff}} \pm {}^{\circ}k$	Scaling Factor	$\Delta k_{\text{eff}} \pm {}^{\circ}k$
1		$0.00010 \pm 0.00006$		$0.00003 \pm 0.00002$
2		$0.00027 \pm 0.00006$		$0.00009 \pm 0.00002$
3		$0.00004 \pm 0.00006$		Neg.
4	$\pm 0.0261 \text{ g}\cdot\text{cm}^{-3}$	$0.00007 \pm 0.00006$	3	Neg.
5		$0.00004 \pm 0.00006$		Neg.
6		$-0.00009 \pm 0.00006$		$-0.00003 \pm 0.00002$
7		$-0.00001 \pm 0.00006$		Neg.
8		$0.00012 \pm 0.00006$		$0.00004 \pm 0.00002$

Table 2.25. Plexiglas Table Density Perturbation Results.

Case	Deviation ( $\pm 3\sigma$ )	${}^{\circ}k_{\text{eff}} \pm {}^{\circ}k$	Scaling Factor	$\Delta k_{\text{eff}} \pm {}^{\circ}k$
1		$0.00013 \pm 0.00006$		$0.00004 \pm 0.00002$
2		$0.00005 \pm 0.00006$		Neg.
3		$<0.00001 \pm 0.00006$		Neg.
4	$\pm 0.0261 \text{ g}\cdot\text{cm}^{-3}$	$0.00015 \pm 0.00006$	3	$0.00005 \pm 0.00002$
5		$0.00007 \pm 0.00006$		Neg.
6		$0.00005 \pm 0.00006$		Neg.
7		$0.00015 \pm 0.00006$		$0.00005 \pm 0.00002$
8		$0.00005 \pm 0.00006$		Neg.

not significantly contribute to the total uncertainty.

#### 2.2.2.4 PLEXIGLAS SPATIAL VARIATION

The nominal lattice plate heights were 0.25 in (0.635 cm) and approximately 28 cm for the 30-cm height rods, or 58 cm for the 60-cm height rods. The height of the lattice plates was varied in 5-cm increments. The 30-cm models had bottom lattice plate heights of 0 (reference), 5, 10, 15, and 20 cm. The 60-cm models had the same bottom lattice plate heights plus 25 cm, as well as top lattice plate heights of 35, 40, 45, and 50-cm. The results are shown below. Using the maximum differential  $k_{\text{eff}}$  as a bounding uncertainty with uniform probability distribution, each case is assigned an uncertainty associated with lattice plate height.

Table 2.26. Nominal PMMA Atom Densities.

Element	Atom Density (atoms·b <sup>-1</sup> ·cm <sup>-1</sup> )
Hydrogen	$5.7264 \times 10^{-2}$
Oxygen	$1.4316 \times 10^{-2}$
Carbon	$3.5790 \times 10^{-2}$
Total	$1.0737 \times 10^{-1}$

Table 2.27. Plexiglas Impurity Uncertainty Results.

Case	Boron Impurity	$^{\circ}k_{\text{eff}} \pm ^{\circ}k$
1		Neg.
2		Neg.
3		Neg.
4	+1 ppm boron inclusion	$-0.00011 \pm 0.00006$
5		$0.00015 \pm 0.00006$
6		Neg.
7		$-0.00011 \pm 0.00006$
8		Neg.

### 2.2.2.5 STAINLESS STEEL DENSITY AND COMPOSITION

The stainless steel support is assumed to be type 304 Stainless Steel<sup>4</sup> with the same composition as the holding tank (Sect. 2.4.1). The density of stainless steel is 8.03 g·cm<sup>-3</sup>. No uncertainties were assessed for the steel support composition or density because the bias for removing it was determined to be insignificant.

## 2.2.3 REFLECTOR

### 2.2.3.1 REFLECTOR DENSITY

The reflector in these experiments was light water. The experimental temperature was recorded, with two readings for each. It is assumed that the two readings were taken simultaneously from independent instruments. No data is provided on the type or specifications of the temperature readings. The reference models were run using a simple average of the two readings shown in Table 2.7. The largest differential between the readings occurs in Case 7 (1°C). Using this and the significant figures in the measurements

<sup>4</sup>AK Steel, 304/304L Stainless Steel Product Data Sheet, 2007

Table 2.28. Lattice Plate Height Bounding Uncertainty Results.

Case	Bounding Lattice Plate Height	$^{\circ}\text{k}_{\text{eff}} \pm ^{\circ}\text{k}$
1	Upper Lattice Plate at 50 cm	$0.00012 \pm 0.00004$
2	Lower Lattice Plate at 10 cm	$-0.00035 \pm 0.00004$
3	Lower Lattice Plate at 15 cm	$-0.00005 \pm 0.00004$
4	Lower Lattice Plate at 15 cm	$-0.00025 \pm 0.00004$
5	Upper Lattice Plate at 50 cm	$0.00014 \pm 0.00004$
6	Lower Lattice Plate at 15 cm	$-0.00008 \pm 0.00004$
7	Lower Lattice Plate at 15 cm	$0.00010 \pm 0.00004$
8	Lower Lattice Plate at 15 cm	$0.00021 \pm 0.00004$

as references, the temperature readings are assumed to be bounded by  $\pm 1^{\circ}\text{C}$ , giving a bounding standard uncertainty (Type B) in the temperature readings of  $0.577^{\circ}\text{C}$ . Perturbations were evaluated at  $18^{\circ}\text{C}$  and  $28^{\circ}\text{C}$ . The densities used were  $0.99860 \text{ g}\cdot\text{cm}^{-3}$  ( $18^{\circ}\text{C}$ ) and  $0.99624 \text{ g}\cdot\text{cm}^{-3}$  ( $28^{\circ}\text{C}$ ). The results are shown in Table 2.29.

Table 2.29. Temperature Perturbation Results.

Case	Deviation ( $\pm 3\sigma$ )	$^{\circ}\text{k}_{\text{eff}} \pm ^{\circ}\text{k}$	Scaling Factor	$\Delta\text{k}_{\text{eff}} \pm ^{\circ}\text{k}$
1		$-0.00052 \pm 0.00006$		$-0.00003 \pm <0.00001$
2		$-0.00060 \pm 0.00006$		$-0.00003 \pm <0.00001$
3		$-0.00060 \pm 0.00006$		$-0.00003 \pm <0.00001$
4	18 $^{\circ}\text{C}$ to 28 $^{\circ}\text{C}$	$-0.00058 \pm 0.00006$	17.33	$-0.00003 \pm <0.00001$
5		$-0.00028 \pm 0.00006$		$-0.00002 \pm <0.00001$
6		$-0.00017 \pm 0.00006$		$-0.00001 \pm <0.00001$
7		$0.00022 \pm 0.00006$		$0.00001 \pm <0.00001$
8		$0.00026 \pm 0.00006$		$0.00002 \pm <0.00001$

### 2.2.3.2 REFLECTOR IMPURITIES

The logbook contains data with an analysis of the water contained in the reflector tank [3]. The analysis shows a uranium concentration of 0.6 ppm ( $\mu\text{gU}\cdot\text{gU}^{-1}$ ). It is not certain when the cited water analysis was performed. It may have been performed prior to the experiments (following experiments with HFIR fuel elements) in which case the uranium contaminant may have been highly enriched. There is likely no certain information regarding uranium contamination in the water, and no information

regarding other possible contaminants. No uncertainties were determined for this analysis because the bias for removing it was determined to be negligible.

### 2.2.3.3 REFLECTOR DIMENSIONS

The reflector between the bottom of the fuel rods and the bottom of the tank was 16.51 cm (6.5 in), which meets the experimenter's description of being at least 15 cm thick. This corresponds with the dimensions reflected in Figure 1, although no direct measurement correlations can be made. The radial reflector is reported as at least 15 cm on all sides, and is approximated as a cylindrical tank with a nominal 58.3 cm radius, such that the closest point of approach (to the corner of the lattice plate) is 15.2 cm. The analysis was performed using a cylindrical tank prior to discovery that the tank was in fact rectangular. This difference has a negligible effect because removal of the tank shows a negligible bias and the cylindrical tank is smaller than the rectangular tank. The top reflector was the control parameter, and varied with each experiment.

The bottom reflector uncertainty is bounded by the height of the table assembly, 6 in (15.24 cm) minimum. This is considered a maximum uncertainty because a thicker bottom reflector has no significant effect. The radial reflector was perturbed  $\pm 3$  cm with an assumed standard uncertainty of 1 cm. The results are shown in Tables 2.30 and 2.31.

Table 2.30. Bottom Reflector Perturbation Results.

Case	Deviation	$\%k_{\text{eff}} \pm \%k$
1		Neg.
2		$-0.00011 \pm 0.00006$
3		Neg.
4	-1.27 cm	$-0.00007 \pm 0.00006$
5		$0.00007 \pm 0.00006$
6		$0.00008 \pm 0.00006$
7		$-0.00011 \pm 0.00006$
8		$-0.00012 \pm 0.00006$

The water height above the rods was used as a control parameter. No data is provided regarding measurement uncertainty and there is some ambiguity in the accuracy of the mirrored scale used to record water height because of the difference in significant figures recorded for the different cases. Because of this, a standard uncertainty of 0.1 cm was assumed based on the more conservative significant figures of the height measurement. The water height was perturbed, with the results shown in Table 2.32.

Table 2.31. Side Reflector Perturbation Results.

Case	Deviation ( $\pm 3\sigma$ )	${}^{\circ}k_{\text{eff}} \pm {}^{\circ}k$	Scaling Factor	$\Delta k_{\text{eff}} \pm {}^{\circ}k$
1		$-0.00002 \pm 0.00006$		Neg.
2		$<0.00001 \pm 0.00006$		Neg.
3		$-0.00001 \pm 0.00006$		Neg.
4	$\pm 3$ cm	$0.00001 \pm 0.00006$	3	Neg.
5		$0.00006 \pm 0.00006$		Neg.
6		$-0.00004 \pm 0.00006$		Neg.
7		$0.00002 \pm 0.00006$		Neg.
8		$-0.00008 \pm 0.00006$		Neg.

Table 2.32. Water Height Perturbation Results.

Case	Deviation ( $\pm 3\sigma$ )	${}^{\circ}k_{\text{eff}} \pm {}^{\circ}k$	Scaling Factor	$\Delta k_{\text{eff}} \pm {}^{\circ}k$
1	61.85-62.15 cm	$0.00009 \pm 0.00007$		$0.00006 \pm 0.00004$
2	36.35-36.65 cm	$0.00005 \pm 0.00006$		Neg.
3	58.85-59.15 cm	$0.00024 \pm 0.00006$		$0.00016 \pm 0.00004$
4	36.70-37.00 cm	$0.00016 \pm 0.00006$	1.5	$0.00011 \pm 0.00004$
5	59.30-59.60 cm	$0.00013 \pm 0.00006$		$0.00009 \pm 0.00004$
6	35.65-35.95 cm	$0.00018 \pm 0.00006$		$0.00012 \pm 0.00004$
7	65.15-65.45 cm	$0.00006 \pm 0.00006$		Neg.
8	36.90-37.20 cm	$0.00011 \pm 0.00006$		$0.00007 \pm 0.00004$

## 2.2.4 HOLDING TANK

### 2.2.4.1 TANK COMPOSITION

An examination of Figure 2.1 shows that the holding tank was either stainless steel or comprised of carbon steel with stainless steel lining. The tank is assumed to be Type 304 stainless steel (Appendix C). The density of stainless steel is  $8.03 \text{ g}\cdot\text{cm}^{-3}$ . No uncertainties were assessed for the tank composition because the bias for removing it was determined to be negligible. The composition of Type 304 stainless steel is shown in Table 2.33.

Table 2.33. Type 304 Stainless Steel Composition.

Element	Typical Range (wt%)	Nominal wt%
Carbon	0.08 (max)	0.04
Manganese	2.00 (max)	1.00
Phosphorous	0.045 (max)	0.0225
Sulfur	0.030 (max)	0.015
Silicon	0.75 (max)	0.375
Chromium	18.00-20.00	19.00
Nickel	8.00-12.00	10.00
Nitrogen	0.10 (max)	0.05
Iron	Balance	Balance

#### 2.2.4.2 TANK DIMENSIONS

The holding tank is modeled as a cylinder with a 116.6 cm (45.9 in) inner diameter, and is 0.9525 cm (0.375 in) thick at the sides and on the bottom. The dimensions for the tank in the model are smaller than the actual tank. No uncertainties were assessed for the tank dimensions because the bias for removing it was determined to be negligible.

#### 2.2.5 ROOM RETURN

Systems with large reflectors, such as is used in this experiment, are assumed to have a negligible room return effect. Therefore, this uncertainty was not evaluated, and assumed to be negligible.

#### 2.2.6 TEMPERATURE EFFECTS

##### 2.2.6.1 REFLECTOR TEMPERATURE

All the experiments were performed at room temperature. Reflector temperature effects are quantified in Section 2.2.3.1 as reflector density effects. No other significant variations in temperature occurred during the experiments.

#### 2.2.7 TOTAL EXPERIMENTAL UNCERTAINTY

The total uncertainty for the experiment was calculated by combining all the individual uncertainties discussed in this section as the square root of the sum of the squares. The summarized total uncertainties



for each case are presented in Tables 2.34 and 2.35. For the purpose of calculating total uncertainty, an uncertainty is considered negligible (Neg.) if the evaluated  $\Delta k$  is less than 0.00010.

## 2.3 BENCHMARK SPECIFICATIONS

A primary goal in development of a benchmark model is to simplify the input specifications as much as possible without changing  $k_{\text{eff}}$  with any statistical significance. Results of the simplification sensitivity studies are detailed below, as well as a comparison of detailed models with the simplified, benchmark model  $k_{\text{eff}}$  values.

### 2.3.1 DESCRIPTION OF MODEL

The benchmark model consists of LEU rods with no impurities in pure water. The rods are arranged identically to the critical arrangements used by the experimenter for each of the eight cases. The rods are held in the axial center of a water cylinder, 116.6 cm in diameter, with the bottom of the rods 16.51 cm above the bottom of the cylinder. The height of the cylinder is measured from the bottom of the rods and varies by case, which represents the critical water height for each experiment.

#### 2.3.1.1 BIAS ASSESSMENT

A summary of individually assessed biases is provided in Table 3.1. A summation of the individual biases is provided, however, the true simplification bias is obtained by comparison of detailed models with the simplified benchmark models. The difference between the summation of the individual biases and the computation of a total bias can be explained by possible correlation of effects and statistical uncertainty in the computation of the biases. Discussions of the individual biases are found later in this section. Any individual bias less than 0.00010 is considered negligible, and the statistical uncertainty for all of the individual biases is  $\pm 0.00009$ .

**2.3.1.1.1 Holding Tank** Removal of the holding tank (discussed in more detail in Section 2.4) shows no statistical significance, as shown in Table 2.38.

**2.3.1.1.2 Support Lattice Structure** Replacement of the lattice plates, bolts, and Plexiglas table with water shows little to no statistical significance, as shown in Table 2.39.

**2.3.1.1.3 Water Density** The water moderator/reflector was modeled at 25°C. The effect was modeled using changes in the water density only, with no changes in the nuclear cross-sections. The

resultant biases for each case are shown in Table 2.40. There is no significant bias. Temperature effects on cross section data are assumed to be negligible.

**2.3.1.1.4 LEU Impurities** Fuel impurities were removed. The resultant biases are shown in Table 2.41. There is no significant bias.

## 2.3.2 MODEL DIMENSIONS

### 2.3.2.1 LEU RODS

The LEU metal rods are modeled as either 30 cm or 60 cm in length, according to the experimental arrangement, and 2.495 cm in diameter.

### 2.3.2.2 MODERATOR/REFLECTOR

The moderator and reflector are modeled as light water with no impurities. The reflector is a cylinder with the base 16.51 cm below the bottom of the fuel rods with a radius of 58.3 cm. The height of the cylinder extends from the bottom of the fuel rods to the height specified in each experiment case.

### 2.3.2.3 ASSEMBLY DESCRIPTION

The assembly consists of low-enriched uranium rods in pure water. Eight cases are evaluated, corresponding to the eight critical configurations used by the experimenter. The lattice arrangement for each evaluated case matches the experimental arrangement for each case. Figure 4 shows the arrangement of the rods for each case.

## 2.3.3 DESCRIPTION OF MATERIAL DATA

### 2.3.3.1 LEU METAL

The LEU metal was modeled using calculated atom densities of uranium isotopes with no impurities. The atom densities are given in Table 2.43. The uranium metal mass density is  $18.889 \text{ g}\cdot\text{cm}^{-3}$  and then reduced for the removal of impurities by multiplying by a purity factor of 0.999765, giving a benchmark uranium density of  $18.885 \text{ g}\cdot\text{cm}^{-3}$ . The  $^{235}\text{U}$  enrichment is 4.948 wt%.

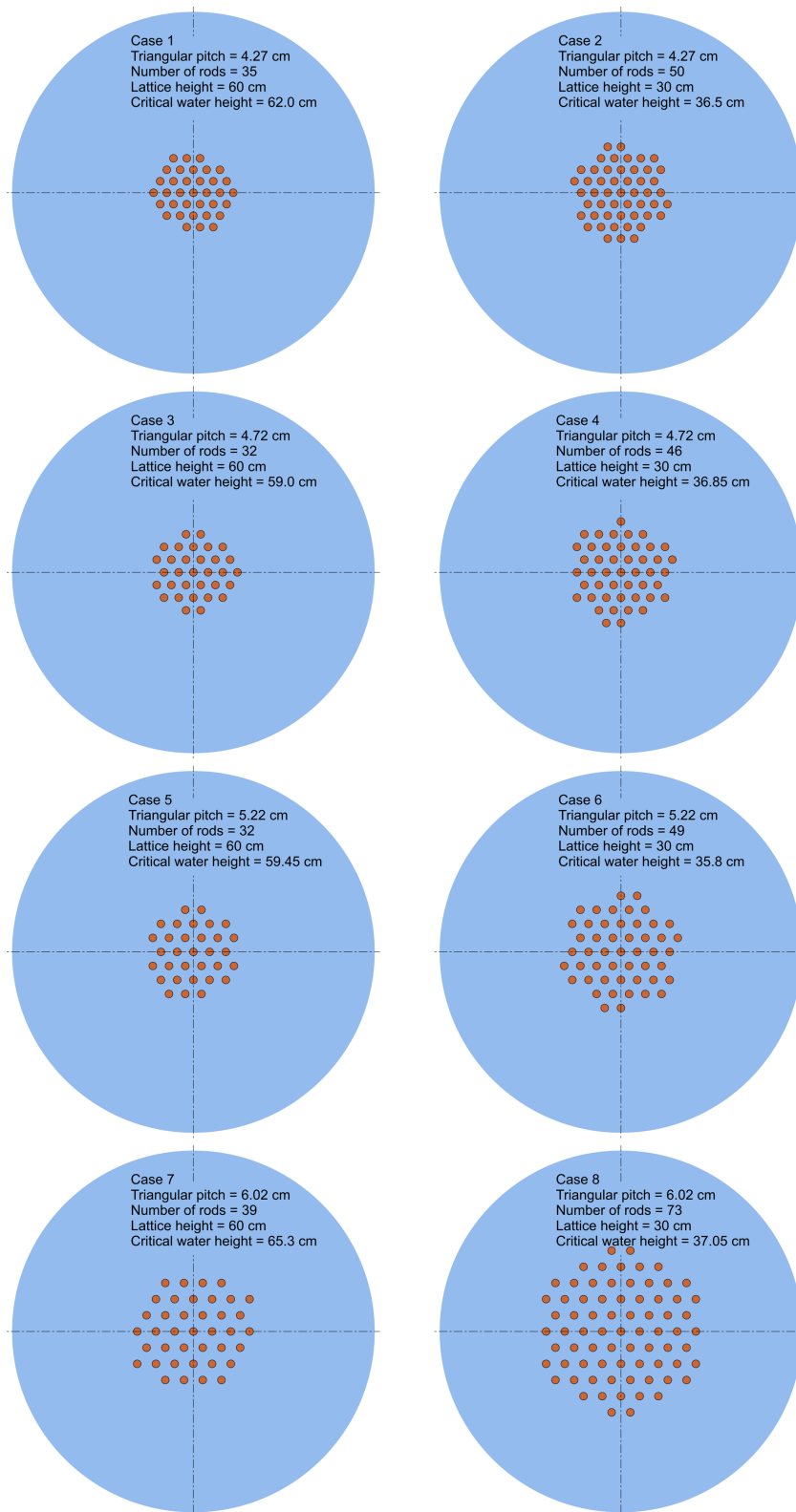


Figure 2.5. Simplified model lattice arrangements for all of the benchmark model cases. The fuel rods are shown in the lattice arrangement which resulted in the experimenter's critical assembly in each case..

### 2.3.3.2 MODERATOR AND REFLECTOR

The light water moderator and reflector are modeled at a reference temperature, 25°C. The density of the reflector at this temperature is 0.997048 g·cm<sup>-3</sup>. The material composition of the reflector is shown in Table 2.44.

### 2.3.4 BENCHMARK TEMPERATURE DATA

The benchmark models are at room temperature (298 K).

### 2.3.5 EXPERIMENTAL AND BENCHMARK MODEL $k_{\text{EFF}}$

The experimental and benchmark model eigenvalues are shown in Table 2.45. The experimental  $k_{\text{eff}}$  values were obtained for critical configurations where  $k_{\text{eff}} = 1.0000$ . The total simplification bias summarized in Section 2.3.1.1 was applied to the experimental  $k_{\text{eff}}$  to obtain the benchmark experiment  $k_{\text{eff}}$  value for each configuration. Experimental uncertainties were summarized in Section 2.7; the uncertainty in the simplification bias ( $\pm 0.00009$ ) does not contribute significantly to the total benchmark uncertainty.

## 2.4 RESULTS OF SAMPLE CALCULATIONS

The benchmark model was evaluated using MCNP5 version 1.51 with the ENDF/B-VII.0 library. Each case was evaluated with 750 total cycles, with 50 skipped cycles, resulting in 700 active cycles, with each cycle using 100,000 particles. Results are shown in Table 2.46. The model also was evaluated using KENO-VI with ENDF/B-VII.0 continuous-energy cross sections. Each case was evaluated with 1,550 total cycles, skipping the first 50 cycles, with 10,000 particles per cycle. Results are shown in Table 2.47.

Table 2.34. Total Experimental Uncertainty,  $\Delta k_{\text{eff}}$ , Cases 1 through 4.

Description	Case 1	Case 2	Case 3	Case 4
LEU Mass	0.00049	0.00065	0.00044	0.00068
Fuel Rod Radius	0.00146	0.00148	0.00043	0.00041
Fuel Rod Length	Neg.	Neg.	Neg.	Neg.
LEU Spatial Variations (Pitch)	0.00037	0.00022	0.00012	Neg.
LEU Enrichment	0.00052	0.00051	0.00051	0.00052
U-234 Content	Neg.	Neg.	Neg.	Neg.
LEU Impurity Content	Neg.	Neg.	Neg.	Neg.
Lattice Plate Thickness	Neg.	Neg.	Neg.	Neg.
Table Thickness	Neg.	0.00010	Neg.	Neg.
Stainless Steel Thickness	Neg.	Neg.	Neg.	Neg.
Lattice Plate Density	Neg.	Neg.	Neg.	Neg.
Table Density	Neg.	Neg.	Neg.	Neg.
1 ppm Boron	Neg.	Neg.	Neg.	0.00011
Lattice Plate Height	0.00012	0.00035	Neg.	0.00025
Reflector Temperature	Neg.	Neg.	Neg.	Neg.
Bottom Reflector Height	Neg.	0.00011	Neg.	Neg.
Reflector Radius	Neg.	Neg.	Neg.	Neg.
Water Height	Neg.	Neg.	0.00016	0.00011
Reflector Impurities	Neg.	Neg.	Neg.	Neg.
Room Return	Neg.	Neg.	Neg.	Neg.
Total	0.00167	0.00175	0.00082	0.00099

Table 2.35. Total Experimental Uncertainty,  $\Delta k_{\text{eff}}$ , Cases 5 through 8.

Description	Case 5	Case 6	Case 7	Case 8
LEU Mass	0.00049	0.00069	0.00046	0.00063
Fuel Rod Radius	0.00052	0.00050	0.00162	0.00163
Fuel Rod Length	Neg.	Neg.	Neg.	Neg.
LEU Spatial Variations (Pitch)	-0.00012	-0.00016	-0.00034	-0.00030
LEU Enrichment	0.00054	0.00054	0.00054	0.00056
U-234 Content	Neg.	Neg.	Neg.	Neg.
LEU Impurity Content	Neg.	Neg.	Neg.	Neg.
Lattice Plate Thickness	Neg.	Neg.	Neg.	Neg.
Table Thickness	Neg.	Neg.	Neg.	0.00011
Stainless Steel Thickness	Neg.	Neg.	Neg.	Neg.
Lattice Plate Density	Neg.	Neg.	Neg.	Neg.
Table Density	Neg.	Neg.	Neg.	Neg.
1 ppm Boron	0.00015	Neg.	-0.00011	Neg.
Lattice Plate Height	0.00012	Neg.	0.00010	0.00021
Reflector Temperature	Neg.	Neg.	Neg.	Neg.
Bottom Reflector Height	Neg.	Neg.	-0.00011	-0.00012
Reflector Radius	Neg.	Neg.	Neg.	Neg.
Water Height	Neg.	0.00012	Neg.	Neg.
Reflector Impurities	Neg.	Neg.	Neg.	Neg.
Room Return	Neg.	Neg.	Neg.	Neg.
Total	0.00093	0.00103	0.00181	0.00187

Table 2.36. Bias Summary for Cases 1 Through 4.

Description	Case 1	Case 2	Case 3	Case 4
Tank Removed	+0.00014	Neg.	Neg.	Neg.
Carbon Steel Bolts Removed	+0.00016	Neg.	Neg.	Neg.
Plexiglas Lattice Plates Removed	+0.00023	-0.00018	Neg.	-0.00060
Plexiglas Table Removed	-0.00042	-0.00183	-0.00035	-0.00203
Steel Support Removed	+0.00021	Neg.	+0.00010	Neg.
Water Density Bias	Neg.	Neg.	+0.00015	Neg.
LEU Impurity Removal Bias	+0.00015	0.00024	Neg.	Neg.
Total Bias (Summation)	+0.00047	-0.00177	+0.00003	-0.00263
Simplified Model Bias	-0.00022	-0.00221	-0.00065	-0.00275
(Simplified - Summation)	-0.00069	-0.00044	-0.00068	-0.00012

Table 2.37. Bias Summary for Cases 5 Through 8.

Description	Case 5	Case 6	Case 7	Case 8
Tank Removed	-0.00020	+0.00012	+0.00016	Neg.
Carbon Steel Bolts Removed	Neg.	+0.00012	-0.00013	+0.00023
Plexiglas Lattice Plates Removed	-0.00096	-0.00089	-0.00117	-0.00126
Plexiglas Table Removed	-0.00075	-0.00188	-0.00037	-0.00214
Steel Support Removed	Neg.	Neg.	Neg.	+0.00019
Water Density Bias	-0.00033	Neg.	+0.00023	Neg.
LEU Impurity Removal Bias	-0.00014	+0.00025	+0.00018	Neg.
Total Bias (Summation)	-0.00238	-0.00228	-0.00110	-0.00298
Simplified Model Bias	-0.00140	-0.00295	-0.00161	-0.00320
(Simplified - Summation)	0.00098	-0.00067	-0.00051	-0.00022

Table 2.38. Holding Tank Removal Bias.

Case	Holding Tank Removal Bias
1	+0.00014
2	+0.00005
3	-0.00005
4	+0.00007
5	-0.00020
6	+0.00012
7	+0.00016
8	<0.00001



Table 2.39. Support Assembly Removal Biases.

Case	Bolts Removed	Lattice Plates Removed	Table Removed	Steel Supports Removed
1	+0.00016	+0.00023	-0.00042	+0.00021
2	-0.00004	-0.00018	-0.00183	+0.00007
3	+0.00002	+0.00001	-0.00035	+0.00010
4	-0.00003	-0.00060	-0.00203	-0.00002
5	<0.00001	-0.00096	-0.00075	-0.00004
6	+0.00012	-0.00089	-0.00188	+0.00001
7	-0.00013	-0.00117	-0.00037	-0.00009
8	+0.00023	-0.00126	-0.00214	+0.00019

Table 2.40. Reflector Temperature Bias.

Case	Reflector Temperature Bias
1	+0.00009
2	+0.00003
3	+0.00015
4	-0.00007
5	-0.00033
6	-0.00001
7	+0.00023
8	+0.00009

Table 2.41. Fuel Impurity Removal Bias.

Case	Bias
1	+0.00021
2	+0.00024
3	+0.00013
4	-0.00002
5	-0.00014
6	+0.00025
7	+0.00018
8	+0.00008

Table 2.42. Summary of Benchmark Experimental Parameters.

Case	Pitch (cm)	Height (cm)	Number of Rods	Top Reflector Height (cm)
1	4.27	60	35	62.00
2		30	50	36.50
3	4.72	60	32	59.00
4		30	46	36.85
5	5.22	60	32	59.45
6		30	49	35.80
7	6.02	60	39	65.30
8		30	73	37.05

Table 2.43. Benchmark Model Fuel Atom Densities.

Isotope	Isotopic Composition (wt%)	Atom Density (atoms·barn <sup>-1</sup> ·cm <sup>-1</sup> )
<sup>234</sup> U	0.038	$1.8465 \times 10^{-5}$
<sup>235</sup> U	4.948	$2.3941 \times 10^{-3}$
<sup>238</sup> U	95.014	$4.5391 \times 10^{-2}$

Table 2.44. Benchmark Model Reflector Atom Density.

Element	Atom Density (atoms·barn <sup>-1</sup> ·cm <sup>-1</sup> )
Hydrogen	$6.6658 \times 10^{-2}$
Oxygen	$3.3329 \times 10^{-2}$
Total	$9.9988 \times 10^{-2}$

Table 2.45. Experimental and Benchmark Model Multiplication Factors ( $k_{\text{eff}}$ ).

Case	Experimental $k_{\text{eff}} \pm 1\sigma$	Simplification Bias	Benchmark $k_{\text{eff}} \pm 1\sigma$
1	$1.0000 \pm 0.0017$	$-0.0002 \pm <0.0001$	$0.9998 \pm 0.0017$
2	$1.0000 \pm 0.0018$	$-0.0022 \pm <0.0001$	$0.9978 \pm 0.0018$
3	$1.0000 \pm 0.0018$	$-0.0007 \pm <0.0001$	$0.9993 \pm 0.0009$
4	$1.0000 \pm 0.0010$	$-0.0028 \pm <0.0001$	$0.9972 \pm 0.0010$
5	$1.0000 \pm 0.0009$	$-0.0014 \pm <0.0001$	$0.9983 \pm 0.0010$
6	$1.0000 \pm 0.0010$	$-0.0030 \pm <0.0001$	$0.9970 \pm 0.0010$
7	$1.0000 \pm 0.0018$	$-0.0016 \pm <0.0001$	$0.9984 \pm 0.0018$
8	$1.0000 \pm 0.0019$	$-0.0032 \pm <0.0001$	$0.9968 \pm 0.0019$

Table 2.46. Sample Calculation Results using MCNP5 with the ENDF/B-VII.0 Nuclear Data Library.

Case	Benchmark $k_{\text{eff}} \pm 1\sigma$	MCNP5 $k_{\text{eff}} \pm 1\sigma$	(C-E)/E (%)
1	$0.9998 \pm 0.0017$	$0.9990 \pm 0.0001$	-0.08
1	$0.9978 \pm 0.0018$	$0.9966 \pm 0.0001$	-0.12
1	$0.9993 \pm 0.0019$	$0.9988 \pm 0.0001$	-0.06
1	$0.9972 \pm 0.0010$	$0.9963 \pm 0.0001$	-0.09
1	$0.9983 \pm 0.0010$	$0.9983 \pm 0.0001$	-0.03
1	$0.9970 \pm 0.0010$	$0.9965 \pm 0.0001$	-0.06
1	$0.9984 \pm 0.0018$	$0.9972 \pm 0.0001$	-0.12
1	$0.9968 \pm 0.0019$	$0.9953 \pm 0.0001$	-0.16

Table 2.47. Sample Calculation Results using KENO-VI with the ENDF/B-VII.0 Nuclear Data Library.

Case	Benchmark $k_{\text{eff}} \pm 1\sigma$	KENO-VI $k_{\text{eff}} \pm 1\sigma$	(C-E)/E (%)
1	$0.9998 \pm 0.0017$	$0.9994 \pm 0.0001$	-0.04
2	$0.9978 \pm 0.0018$	$0.9968 \pm 0.0001$	-0.10
3	$0.9993 \pm 0.0019$	$0.9993 \pm 0.0001$	0.00
4	$0.9972 \pm 0.0010$	$0.9971 \pm 0.0001$	-0.01
5	$0.9983 \pm 0.0010$	$0.9991 \pm 0.0001$	+0.08
6	$0.9970 \pm 0.0010$	$0.9968 \pm 0.0001$	-0.02
7	$0.9984 \pm 0.0018$	$0.9974 \pm 0.0001$	-0.10
8	$0.9968 \pm 0.0019$	$0.9959 \pm 0.0001$	-0.09

[Results provided by Dr. John D. Bess of Idaho National Laboratory]

## REFERENCES

- [1] Joseph A. Christensen. “Triangular Lattices of 2.49 cm Diameter LEU (4.948) Rods in Water”. In: *International Handbook of Evaluated Criticality Safety Benchmark Experiments*. LEU-MET-THERM-004. Paris: OECD Nuclear Energy Agency, 2020.
- [2] Elizabeth B. Johnson. “Critical Lattices of U(4.89) Metal Rods in Water”. In: *Transactions of the American Nuclear Society* 10 (1967), p. 190.
- [3] Unknown. *Book 104R, U 4.9 Rods # 2 Log*. Scanned by Sheila Finch, RSICC/Oak Ridge National Lab, September 13, 1999. Oak Ridge Critical Experiments Facility, 2021. URL: <https://ncsp.llnl.gov/sites/ncsp/files/2021-05/book104r.pdf>.
- [4] Kermit A. Bunde and Richard D. McKnight. *The U9 benchmark assembly: a cylindrical assembly of U metal (9%  $^{235}\text{U}$ ) with a thick depleted-uranium reflector*. In: *International Handbook of Evaluated Criticality Safety Benchmark Experiments*. [DVD]. Tech. rep. IEU-MET-FAST-010. Nuclear Energy Agency, 2019.
- [5] Unknown. *Book 103R, HTRE U(4.2)F<sub>6</sub> U(4.89) Rods*. Scanned by Sheila Finch, RSICC/Oak Ridge National Lab, September 13, 1999. Oak Ridge Critical Experiments Facility, 2021. URL: <https://ncsp.llnl.gov/sites/ncsp/files/2021-05/book103r.pdf>.
- [6] Unknown. *Book 101R, U(4.9) Rods #2*. Scanned by Sheila Finch, RSICC/Oak Ridge National Lab, September 13, 1999. Oak Ridge Critical Experiments Facility, 2021. URL: <https://ncsp.llnl.gov/sites/ncsp/files/2021-05/book103r.pdf>.
- [7] *CRC Handbook of Chemistry and Physics*. 75th ed. Cleveland, OH: CRC Press, 1995.
- [8] F.B. Brown et al. *MCNP Version 5*. Technical Report LA-UR-02-3935. Los Alamos National Laboratory, 2002.
- [9] M.B. Chadwick et al. “ENDF/B-VII.0: Next Generation Evaluated Nuclear Data Library for Nuclear Science and Technology”. In: *Nuclear Data Sheets* 107.12 (2006). Evaluated Nuclear Data File ENDF/B-VII.0, pp. 2931–3060. ISSN: 0090-3752. DOI: <https://doi.org/10.1016/j.nds.2006.11.001>. URL: <https://www.sciencedirect.com/science/article/pii/S0090375206000871>.
- [10] R.G. McConn Jr. et al. *Compendium of Material Composition Data for Radiation Transport Modeling*. Tech. rep. PNNL-15870. Pacific Northwest National Laboratory, 2006.

# CHAPTER 3: PARAMETRIC STUDY OF MINIMUM CRITICAL VOLUME FOR HIGH-ASSAY LOW-ENRICHED URANIUM (20%) IN SPHERICAL GEOMETRY AGAINST PARTICLE SIZE

**Joseph A. Christensen and R. A. Borrelli. “Parametric Study of Minimum Critical Volume for High-Assay Low-Enriched Uranium (20%) in Spherical Geometry Against Particle Size”. In: *Nuclear Science and Engineering* 196.1 (2022), pp. 98–108. DOI: 10.1080/00295639.2021.1940066. eprint: <https://doi.org/10.1080/00295639.2021.1940066>. URL: <https://doi.org/10.1080/00295639.2021.1940066>**

## 3.1 ABSTRACT

Algorithms used to generate Monte Carlo input decks and to analyze the output over a range of uranium mass, water volume, and particle size in a regular lattice are described. The algorithms produce input decks for both homogeneous and heterogeneous, regular-lattice systems of twenty percent enriched uranium metal and water and then analyze the results to determine the minimum critical mass over a range of input mass and particle size. The output is presented and analyzed for a twenty percent enriched uranium metal and water system and comparisons to existing technical reports and safety guides are discussed. Two particular existing recommendations are tested and compared with new results – the boundary between a homogeneous system and a heterogeneous system, and the recommended margins of safety which can be applied to account for the effects of heterogeneity.

## 3.2 INTRODUCTION

It is of interest to expand the examination of the effects of heterogeneity on uranium with twenty percent enrichment by weight. The typical preferred hierarchy for developing subcritical limits for nuclear criticality safety applications is (1) use of experimentally-determined values, (2) use of calculated values which are validated by direct comparison to experimental measurements, and (3) use of calculated values which are validated by statistical comparison to experiments. For many applications involving

the use of HALEU, there are no experimental data which can be used to directly develop subcritical limits, and the available benchmark data at this enrichment are limited. Consequently, development of subcritical limits relies on the use of literature and direct calculation using statistically-evaluated validation. This approach has an additional restriction — the current literature available to nuclear criticality safety professionals relies on technical reports developed using dated techniques and broad interpolations between low enrichment (five weight percent) and high enrichment (twenty weight percent) which sometimes produce conflicting results.

This work is an examination of a new methodology by which subcritical limits can be systematically-derived to supplement and improve the volume of data currently available in handbooks. It is an examination specifically for the minimum critical spherical volume for twenty-percent enriched uranium in both homogeneous and heterogeneous metal-water mixtures. This examination is intended to help nuclear criticality safety professionals in the determination of safe geometry parameters for the handling of HALEU by providing a method by which ranges of input parameters can be more fully evaluated and understood.

### 3.2.1 GOALS

The goals of this work are threefold:

1. Describe a methodology by which the minimum critical volume of uranium-water systems may be systematically examined in both homogeneous and heterogeneous systems. The methodology automates the process of input deck generation for use in Monte Carlo neutron transport codes to improve the efficiency of evaluations.
2. Using the described methodology, examine the effect of uranium mass and particle size on the minimum critical volume of uranium-water systems of twenty percent enriched uranium. This examination is intended to identify the minimum critical volume for a heterogeneous and homogeneous systems and to compare the two systems with respect to percent relative change.
3. Compare the results of the examination to previous results presented in technical literature and propose recommendations. Several assumptions present in current literature regarding particle size and the difference in critical volume between homogeneous and heterogeneous systems are tested and compared to the results derived using the described algorithms.

### 3.3 BACKGROUND

#### 3.3.1 PARTICLE SIZE IN HETEROGENEOUS SYSTEMS

It is generally understood that the critical mass and volume for a heterogeneous system of fissile material in a moderator matrix is lower than that of a similar homogeneous system. In order to effectively determine which values are applicable to a particular system, it is necessary to first define the boundary between the two. Some guidance exists in technical literature – the Los Alamos National Laboratory nuclear criticality safety guide (Ref. [2]) gives a lower limit on particle size for the determination of the difference between a “homogeneous” and a “heterogeneous” system of uranium and water as “127 microns (i.e. not capable of being passed through a 120-mesh screen)” when computing the minimum critical mass, and it is clear from the context of this safety guide that the intended use of this criterion is for low-enriched uranium (less than six weight percent). This same argument is also presented in the U.S. Nuclear Regulatory Commission nuclear safety guide [3] without significant difference. The references cited to produce this criterion (Refs. [4] and [5]) provide little in the way of how it was developed, however. K-1550 [4] gives a specific condition for uranium enriched to 0.95% as having one dimension less than or equal to 0.02 inch (508 microns), and no similar conditions exist in [5]. It is possible that the value of 127 microns was selected for convenience as a fraction (one-fourth, precisely) of the 508 microns developed in K-1550, rather than on a technical examination of the effect of particle size in a uranium-water mixture. This work provides a method by which this criterion can be further examined to determine if there is, in fact, a lower limit on the particle size at which the difference between a heterogeneous and a homogeneous system exists and whether or not the recommendation provided in the guides is adequate for nuclear criticality safety applications.

#### 3.3.2 MINIMUM CRITICAL VOLUME IN HETEROGENEOUS SYSTEMS

A similar argument regarding heterogeneity is presented in Anomalies of Nuclear Criticality [6], which states that the heterogeneous uranium-water system produces the smallest critical mass below six weight percent enrichment and the homogeneous system produces the smallest mass above this value, which is the same position established in LA-12808 [2]. Anomalies provides additional information on the effect on the minimum critical volume of uranium-water mixtures. It states that, while the minimum critical mass above six weight percent enrichment is constrained by the homogeneous case, the minimum critical volume is constrained by the heterogeneous case up to approximately thirty-four weight percent. The report presents the results of calculations which demonstrate this phenomenon, but does not include a

discussion of the methodology by which the data were obtained. Personal communications with the editor suggested that the data were likely generated using the EGGNIT code [7] using a heterogeneous pin model and flux-weighted conversion to a homogeneous model. Figure 3.1 shows the calculated minimum critical spherical volume results for homogeneous and heterogeneous systems and for unmoderated metal systems as a function of uranium enrichment. The figure also gives a proposed subcritical limit curve which exists as some fraction of the calculated minimum volume. The fraction of the minimum critical volume is not given, but some guidance on how such a limit can be obtained is available in European criticality safety guides [8] [9]. In the French handbook, the recommended safety factor on volume is 75 percent of the critical volume if heterogeneity is possible, or 85 percent of the critical volume if it is not. The German criticality safety guide [9] recommends a safety factor of 80 percent of critical volume for homogeneous volumes greater than 5 liters and 75 percent of critical volume for homogeneous systems less than five liters and for heterogeneous systems. It is of interest in this work to determine the magnitude of the difference in minimum critical volume between the homogeneous and heterogeneous mixtures of uranium and water at twenty weight percent. Determination of the difference will provide clarity regarding the "possible subcritical limit curve" described in Anomalies and shown in Figure 3.1 and will test whether or not the recommended safety factors are adequate at this enrichment.

### 3.4 METHODOLOGY

Using a pair of algorithms, a data set was generated and analyzed to evaluate the difference in critical spherical volume of uranium-water systems. Using Microsoft Visual Basic for Applications (VBA), the first algorithm generates input decks for the Monte Carlo neutron transport code MCNP for both homogeneous and heterogeneous systems, which are solved to find  $k_{\text{eff}}$ . The user input parameters are uranium mass, uranium enrichment, water volume, and particle size.

Homogeneous models are generated by straightforward computation of system volume and material atomic density. The system volume is the sum of the input water volume and the volume of uranium as the quotient of the input mass divided by the uranium density. The material composition for each material, uranium and water, was computed by determining the total number of atoms for each nuclide from the mass and dividing by the volume of the system with conversion to appropriate units for MCNP input ( $\text{b}^{-1}\cdot\text{cm}^{-1}$ ). Input parameters used in the computation of material properties and system volume are shown in Table 3.1. The fuel region radius is computed from the sphere volume in the typical way, and the reflector radius for the homogeneous cases is computed by adding constant 30 cm to the fuel region radius.



Table 3.1. Input parameters used in the determination of material specifications for modeling [10].

Isotope	Atomic Mass (grams per mole)
$^1\text{H}$	1.007975
$^{16}\text{O}$	15.9949
$^{235}\text{U}$	235.0439301
$^{238}\text{U}$	238.0507884

Material	Density (grams per liter)
Uranium Metal	18.95 (Ref. [11])
Water (25 °C, 1 ATM)	0.99705 (Ref. [12])

For the heterogeneous cases, a regular square lattice of uranium particles surrounded by interstitial water is created to replace the homogeneous material composition in the central sphere. The algorithm computes the number of uranium particles in the system by dividing the uranium mass by the volume of the particles, which is computed from the input particle diameter. Then, the total system volume is divided by the number of particles to determine the size of the cuboid lattice cell needed to contain the particle. The size of the lattice cell is then computed as shown in equation 3.1. The lattice parameter is used to generate the repeated square lattice of individual cells with a uranium metal particle of the specified diameter in the center of each cell. The lattice is then used to fill the fissile sphere using the same computed radius as the homogeneous case. A cross sectional view of the model is shown as Figure 3.2.

$$x = \sqrt[3]{\left(1 + \frac{V_{water}}{V_{uranium}}\right) \left(\frac{4}{3}\pi r^3\right)} \quad (3.1)$$

where:

$x$	lattice edge length (cm)
$V_{water}$	uranium volume (liters)
$V_{uranium}$	water volume (liters)
$r$	particle radius (cm)

The second algorithm uses  $k_{\text{eff}}$  as the independent variable to generate a third-order linear polynomial fit to the volume results and solves for the root of the polynomial between the upper and lower

analysis bounds to find the critical volume ( $k_{\text{eff}}=1$ ). The critical volumes are plotted over ranges of mass and particle size to determine the minimum volume for each parameter.

For this work, all evaluations were performed at twenty weight percent enrichment using a method that simulates fresh fuel without consideration of burnup. The impact of fuel depletion and buildup of fission products if this work were expanded to include used nuclear fuel would tend to increase the critical volume in two ways: (1) the availability of fissile  $^{235}\text{U}$  would decrease as its mass was depleted, and (2) fission product absorbers which accumulate in nuclear fuel as it is consumed would reduce  $k_{\text{eff}}$  by removing neutrons from the system which otherwise might cause fission to occur.

Mass was evaluated between six and twenty-five kilograms and water volume was evaluated from seven to eleven liters and particle sizes from 10 to 10,000 microns ( $1 \times 10^{-6}$  m). The ranges of these parameters were selected to canvass the range in which the minimum critical volume would be found for both homogeneous and heterogeneous systems. A 30-cm reflector was used in all cases. The atomic weight ( $A_{\text{EU}}$ ) of enriched uranium was calculated for the enrichment without consideration of contributions from  $^{234}\text{U}$  or  $^{236}\text{U}$ , using equation 3.2. This approach produces conservative results in that the estimation of  $k_{\text{eff}}$  is higher in two ways: (1) the atomic weight of the uranium is higher by omission of  $^{234}\text{U}$  which gives higher atom densities in the input, and (2) the absorption of neutrons by non-fissile isotopes of uranium ( $^{234}\text{U}$  and  $^{236}\text{U}$ ) is not accounted for in the model. Similarly, the minor isotopes of hydrogen ( $^2\text{H}$  and  $^3\text{H}$ ) and oxygen ( $^{17}\text{O}$  and  $^{18}\text{O}$ ) were omitted due to their low abundance and negligible contribution to the calculation of  $k_{\text{eff}}$ .

$$A_{EU} = \frac{1}{\frac{0.20}{A_{235U}} + \frac{0.80}{A_{238U}}} \quad (3.2)$$

The second algorithm is implemented using the open-source mathematics program GNU Octave. It uses the Monte Carlo output  $k_{\text{eff}}$  as the independent variable to generate a third-order linear polynomial fit (the `polyfit` function) to the volume and solves for the root (the `roots` function) of the polynomial between the upper and lower analysis bounds to find the volume at which the system is precisely critical ( $k_{\text{eff}}=1$ ). The process is repeated for each value of mass and for each particle size. After the critical volume is determined for each mass and particle size, the data are tabulated and plotted and the minimum critical volume for each mass is identified. The difference in critical volume is expressed as percent relative change ( $\text{RC}_{\text{ht,hm}}$ ) between the heterogeneous cases and the homogeneous cases as the reference values, which is calculated using equation 3.3.

$$RC_{ht,hm} = \frac{V_{heterogeneous}^{min} - V_{homogeneous}^{min}}{V_{homogeneous}^{min}} \times 100 \quad (3.3)$$

### 3.4.1 MONTE CARLO SOFTWARE

Monte Carlo n-Particle (MCNP), version 5-1.60 was used to compute  $k_{\text{eff}}$  in this work. The MCNP model uses 10,000 particle histories per cycle and 5,500 cycles with the first 50 cycles discarded. The selection of this quantity of particle histories was made to minimize the statistical error ( $\sigma_{k_{\text{eff}}}$ ) produced by the code itself because error propagation through the fitting and root-finding algorithm was not conducted. Future work in this area will use larger particle histories per cycle to reduce the number of active cycles, consistent with recommendations. The range of  $\sigma_{k_{\text{eff}}}$  in the Monte Carlo results is 0.00012 to 0.00044. Consequently, there is some amount of error in the computed minimum volumes but it is considered negligible for this work. The cross sections used in this work are taken from the ENDF/B-VIII.0 nuclear data library [13]. All cross sections used in this work were from the continuous energy series of room temperature (293.6K) cross sections in the data library (.80c). Verification of the code on the computer systems used was performed using the developer-provided verification tools.

### 3.4.2 VALIDATION

The WHISPER utility is distributed with later versions of MCNP. It uses benchmark critical experiments, nuclear data sensitivities from MCNP, and nuclear covariance data to set a baseline upper subcritical limit [14] based on computed bias and bias uncertainty for use in validation activities involving computational methods. The WHISPER utility was used on two test cases and produced a range of recommended upper subcritical limits. The test cases were heterogeneous models near the predicted minimum critical volume (19 kilograms / 8.563 liters) with a 4000  $\mu\text{m}$  particle size.

## 3.5 RESULTS

### 3.5.1 MINIMUM PARTICLE SIZE

Figures 3.3 and 3.4 show the effect of particle size on calculated critical volume over the evaluated range of uranium mass. For each mass value, the same behavior in critical volume is observed as particle size is increased. Starting from the homogeneous cases (0- $\mu\text{m}$ ), the critical volume decreases to a minimum and then increases. At low mass, the sensitivity of the critical volume to the particle size is significant, and as mass is increased, the sensitivity of volume to particle size diminishes substantially.

The smallest particle size, 400  $\mu\text{m}$ , occurs in the system with the smallest mass, noting that systems with 5 kilograms of uranium were not critical in either the homogeneous or heterogeneous cases. The inability to find a critical system at 5 kilograms is consistent with expectations. At this mass and enrichment, only 1000 grams of  $^{235}\text{U}$  are present in the system, which is very close to the absolute minimum critical mass for a uranium water-system at 100 percent enrichment; contributions from  $^{238}\text{U}$  as a neutron absorber explain the difference. The particle size at which each minimum critical volume was determined is shown in Table 3.2. As the mass increases, the size of the particles which produce the minimum critical volume also increases.

Table 3.2. Homogeneous and minimum heterogeneous volume versus uranium mass for uranium enriched to twenty percent by weight.

Uranium Mass (grams)	Homogeneous Volume (liters)	Minimum Heterogeneous Volume (liters)	Relative Change (%)	Particle Size ( $\mu\text{m}$ )
6000	12.546	11.856	-5.5	400
7000	11.096	10.440	-5.9	500
8000	10.424	9.731	-6.6	900
9000	10.052	9.328	-7.2	900
10000	9.857	9.085	-7.8	1500
11000	9.711	8.892	-8.4	1500
12000	9.644	8.798	-8.8	2000
13000	9.620	8.709	-9.5	2000
14000	9.620	8.658	-10.0	2000
15000	9.614	8.595	-10.6	2500
16000	9.648	8.587	-11.0	2500
17000	9.682	8.578	-11.4	3000
18000	9.728	8.584	-11.8	3000
19000	9.770	8.563	-12.4	4000
20000	9.816	8.567	-12.7	4000
21000	9.886	8.593	-13.1	5000
22000	9.935	8.601	-13.4	5000
23000	9.995	8.603	-13.9	5000
24000	10.074	8.631	-14.3	5000
25000	10.120	8.668	-14.4	6000

### 3.5.2 MINIMUM CRITICAL VOLUME

Figure 3.5 shows the minimum critical volume for the heterogeneous cases and the homogeneous minimum critical volume as a basis for comparison. The results are tabulated in Table 3.2 with the percent relative change. Comparison with the computed critical volumes in Figure 3.1 shows good agreement, given the natural constraints when comparing against legacy documents. Within the analysis bounds of this work (6 to 25 kilograms of uranium), the maximum observed relative change between the heterogeneous and homogeneous cases was 14.4%. As can be seen in Figure 3.5, the minimum homogeneous volume decreases between 6 and 15 kilograms, where a local minimum is reached, and above 15 kilograms, the minimum critical volume increases. The minimum critical volume for the heterogeneous cases does not have an easily discernible local minimum in the same region. The trend appears to stagnate for uranium masses above 15 kilograms with only a slight increase in the final data point in the range. It is possible that extension of the mass range would clarify more precisely the response of critical volume to changes in mass.

### 3.5.3 VALIDATION USING WHISPER

Two input cases were tested using the WHISPER utility. The cases were the heterogeneous models which used 19000 grams of uranium, 4000  $\mu\text{m}$  particle size, and 8000 (Case 1) and 9000 (Case 2)  $\text{cm}^3$  of water. These cases are near what appears to be a local minimum of the heterogeneous cases, although as stated previously, selection of the true local minimum in this region is difficult.

The results produced by WHISPER are shown in Table 3.3, and histograms showing the range of correlation coefficients to various benchmarks are shown as Figures 3.6 and 3.7. As shown in Table 3.3, the recommended upper subcritical limits are 0.98616 and 0.96495, respectively. These data highlight a number of considerations: (1) despite the relative proximity of the test cases with respect to input values, significantly different predicted upper subcritical limits were obtained, (2) the response of the utility to relatively minor changes in the selected model can produce significantly different output, and (3) the predicted upper subcritical limits are relatively lower than would be expected for a uranium-water system.

The histograms, Figures 3.6 and 3.7, depict the range of correlation coefficients used by the utility to recommend the subcritical limit. For the Case 1, the correlation coefficients show a generally normal distribution and fewer contributing benchmarks. Case 2 shows a bimodal distribution in the correlations and a larger number of contributing benchmarks with slightly lower correlations. Because the WHISPER

Table 3.3. WHISPER Output Results for Test Case 1.

Case	Calculation Margin	Data Uncertainty ( $1\sigma$ )	Baseline USL	$k_{\text{calc}} > \text{USL}$
Case 1	0.00779	0.00040	0.98616	0.02541
Case 2	0.02905	0.00038	0.96495	0.06868
Case	Bias and Bias Uncertainty	Nuclear Data Uncertainty Margin	Software/method Margin	Non-coverage Penalty
Case 1	$0.00504 \pm 0.00275$	0.00040	0.00500	0.00000
Case 2	$0.00811 \pm 0.02094$	0.00038	0.00500	0.00000

utility uses the extreme value theorem in its computation of subcritical limit, the lack of normality in the distribution of correlation coefficients does not have an impact on the output [15], so the distribution of correlation coefficients is merely an interesting observation. It is clear, however, that the lower correlation coefficients and the correspondingly lower recommended upper subcritical limits for Case 2 indicates that additional benchmark or experimental data could be valuable for this range of enrichment.

Recognizing that the recommended upper subcritical limits demonstrate inconsistency even for models which are close in proximity to the minimum critical volume, it is important to recognize the need for more precise validation of the results presented in this work. This demonstration of inconsistency between just two test cases with proximate input variables primarily indicates that any validation attempt for work of this kind must be exhaustive before being applied to practical criticality safety problems. Additionally, it must be emphasized that a validation which relies entirely on homogeneous cases may not be sufficient for determination of the subcritical limit for heterogeneous cases, especially after recognizing that even outwardly similar heterogeneous cases can product non-trivial differences in the computed subcritical limit.

Follow-on work is planned to evaluate methods by which an effective validation approach may be developed using the WHISPER utility over the entire range of input variables. Following an effective validation, the appropriate subcritical limit should be generated and substituted for  $k_{\text{eff}} = 1$  in the volume prediction algorithm to produce minimum critical volume results which may be used for nuclear criticality safety applications.

## 3.6 DISCUSSION

The goals established for this work were met. The methodology for a systemic evaluation of the minimum subcritical volume for both homogeneous and heterogeneous systems produced results which were both consistent with existing literature and useful for the evaluation of critical volume at the subject enrichment. The effects of mass and particle size on minimum critical volume were examined and compared to existing safety guides with promising results.

### 3.6.1 COMPARISON WITH EXISTING SAFETY GUIDES

The effect of particle size on the critical volume of a heterogeneous system of uranium particles in water is consistent with existing guides as discussed in Section 3.3.1. The recommended boundary condition between a heterogeneous system and a homogeneous system,  $127\ \mu\text{m}$ , is adequate for twenty percent enriched uranium as demonstrated by the results of this work. As seen in Section 3.5.1, the smallest particle size at which a minimum critical volume was encountered was  $400\ \mu\text{m}$ , which is consistent with the experimental results described in [4], which evaluate uranium rods in water with a diameter of  $508\ \mu\text{m}$ .

Regarding the appropriate safety factor for use in heterogeneous systems, it appears that the available European guidance is adequate, at least in the range of this evaluation. Using the percent relative change (Table 3.2), it can be seen that the recommended safety factors discussed in section 3.3.2 are conservative relative to the results seen in this work. The maximum percent relative change between the homogeneous and heterogeneous systems evaluated in this work was 14.4%. Application of a twenty-five percent reduction in homogeneous critical volume appears to bound the effects of potential heterogeneity at this enrichment. Generally these arbitrary safety factors are not recommended for use without extensive consideration of all potential process upsets which might result in heterogeneity. They are, however, useful as a starting point and a basis for comparison to computed results. Explicit evaluation of the effects of heterogeneity in any particular application should be performed as part of the determination of criticality safety limits.

### 3.6.2 NUCLEAR CRITICALITY SAFETY APPLICATIONS

The methodology described in this work could be used in practical nuclear criticality safety problems which require the determination of a subcritical limit for volume. The methodology described can easily be applied to other systems of fissile material and moderator or to different ranges of enrichment,

mass, or moderator volume. Direct application to problems associated with a facility safety basis would require slight modifications and increased validation of the computational system. Modifications to the curve-fitting algorithm would be necessary to replace  $k_{\text{eff}}=1$  with an appropriate value which includes an approved subcritical margin and computational bias as determined during validation of the computer system as discussed in section 3.4.2 or by traditional validation methods.

Alternatively, application of a safety factor similar to those discussed in section 3.3.2 could be appropriate in addition to the computed relative change between the homogeneous and heterogeneous systems if there were adequate experimental data available for a particular material composition and enrichment. For example, because the maximum relative change in volume between the homogeneous and heterogeneous systems analyzed in this work was determined to be 14.4%, a safety factor which reduces the computed heterogeneous volume by twenty percent, or even fifteen percent, of the homogeneous volume might be appropriate. This approach represents a modest improvement over the recommended safety factors in section 3.3.2 and has a more secure basis. Again, reliance on arbitrary safety factors for systems which contain the potential for heterogeneity is not generally recommended and should only be used under circumstances where the safety factor has been extensively evaluated.

It is very important to note that, because the algorithm relies on polynomial linear interpolation, the minimum volumes computed in this methodology cannot be extrapolated beyond the bounds of the analysis. Additional work is needed to ensure that the behaviors observed in the results of this work regarding particle size and minimum critical volume extend to higher masses and particle size.

### 3.7 FUTURE WORK

In order to build upon the existing body of work in this area, several advancements are planned:

1. Continue development of the model-generating algorithm
  - (a) Include additional material compositions such as uranium oxides. This step would allow more widespread use of the algorithms for practical problems.
  - (b) Formalize the algorithms and code into more robust computing languages: Python, Java, or R. This would be necessary to improve the version control and security of the code if it is to be used by a widespread audience.
2. Formalization of the algorithms used in this work as stand-alone code packages which could eventually be used to supplement existing nuclear criticality safety codes and tools. Continued testing



and validation of the algorithm against experimental results are necessary to allow the use of this algorithm for safety-basis applications in the industry.

3. Expand the use of the WHISPER utility to better understand the effects of variation in the models on the validation results. Because only two test cases were evaluated in this work, and those test cases revealed significant questions, continued examination of the evaluated systems and their relationships to the benchmarks used by WHISPER is warranted.
4. Perform a traditional validation of this uranium-water system and compare to an expanded WHISPER validation. Formalized validation of this work would allow it be more easily incorporated into practical criticality safety applications, and a comparison between the traditional validation approach and newer validation algorithms would be valuable for the continued development of those tools.
5. Extend the range of evaluation to higher mass systems. The existing algorithm has this capability. Evaluation of higher-mass systems, documentation of the results, and comparison to legacy guidance would be a useful first step in replacing dated references and safety guides with more modern methods and results.

### 3.8 SUMMARY REMARKS

This work demonstrates that it is possible to use algorithmically-generated models to predict the minimum critical volume for systems of uranium and water in both heterogeneous and homogeneous systems. It confirms the previously-reported maximum value of particle size which may be considered homogeneous [2] ( $127 \mu\text{m}$ ) in that the critical volume for systems of particles below that value is higher than for systems above it. In this work, the smallest particle size which produced a minimum critical volume over the range of evaluation was  $400 \mu\text{m}$ , which is approximately equivalent to the  $508 \mu\text{m}$  heterogeneous metal rod system which forms the basis for the  $127 \mu\text{m}$  recommendation. Furthermore, this work produced results which are effectively equivalent to the work presented in Anomalies [6] with respect to the difference in minimum critical mass between a heterogeneous and homogeneous system, despite the differences in calculational methods. Consequently, the recommendations to use a safety margin derived as a fractional value of the homogeneous critical mass is judged to be an acceptable method, and the proposed safety margins present in the European nuclear criticality safety guides [8] [9] are very likely to be adequate for uranium at twenty percent enrichment.

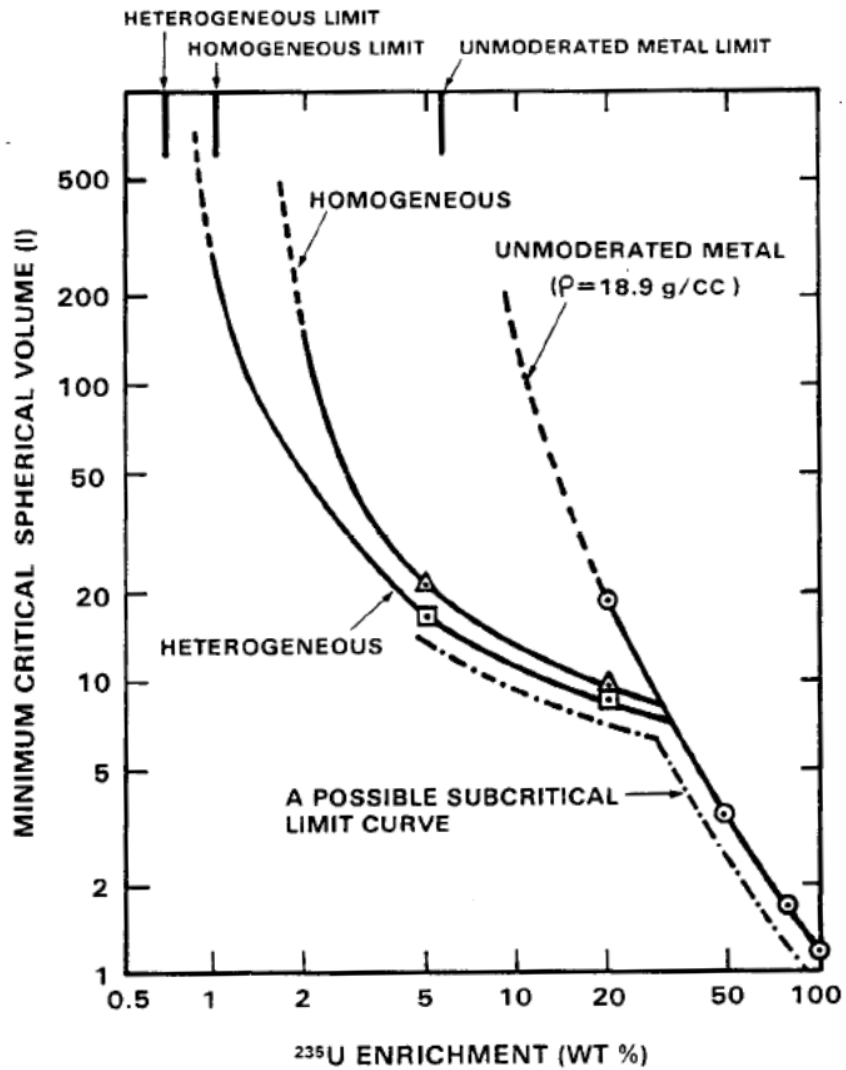


Figure 3.1. Calculated minimum critical volume for homogeneous, heterogeneous, and single-unit uranium-water systems and a proposed subcritical limit curve. This figure is a reprint of Figure 11 from reference [6].

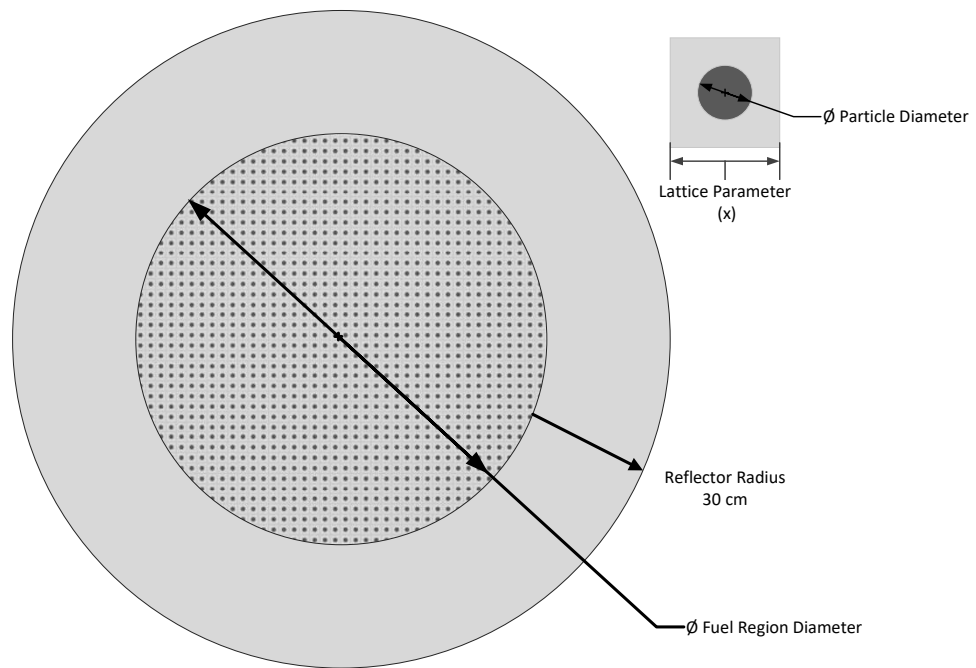


Figure 3.2. Cross-sectional view of the modeled heterogeneous lattice. Depicted are the fuel lattice region, close-up view of an individual lattice cell, and the reflector region.

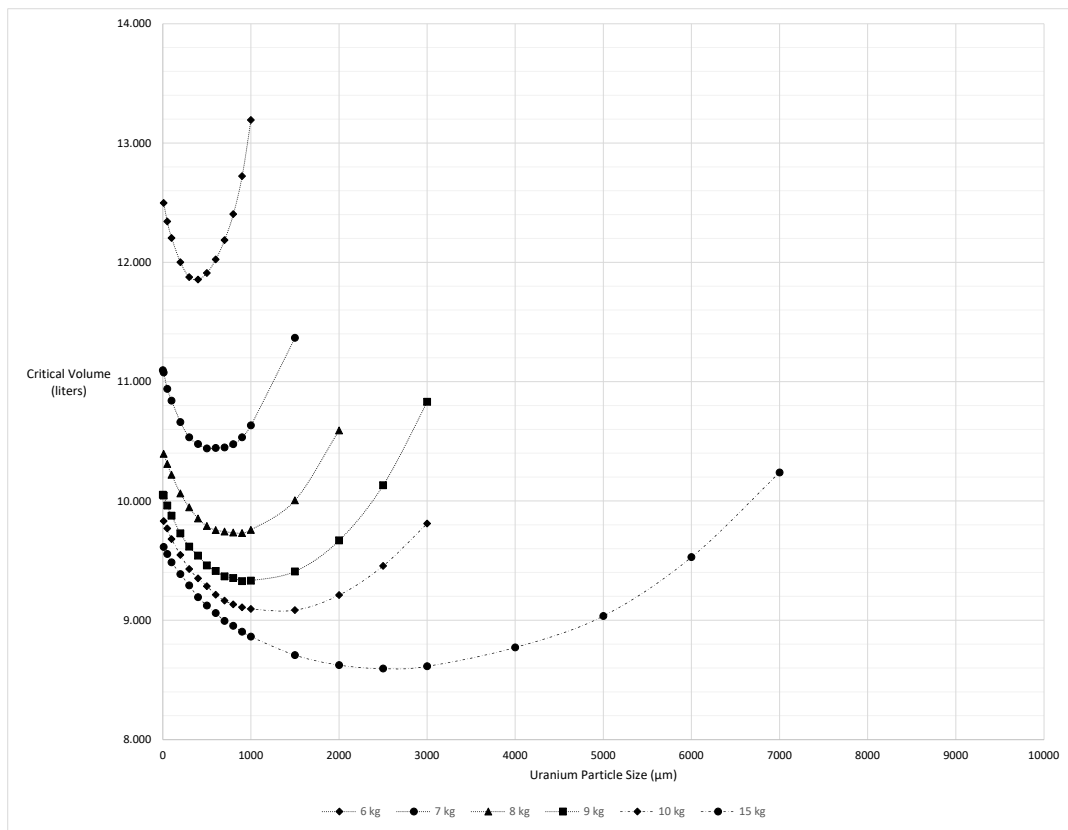


Figure 3.3. Critical volume plotted as a function of uranium particle size. Each line represents a fixed uranium mass from six kilograms to fifteen kilograms, evaluated at different particle size. Sensitivity of critical volume to particle size is dramatically more pronounced at lower mass.

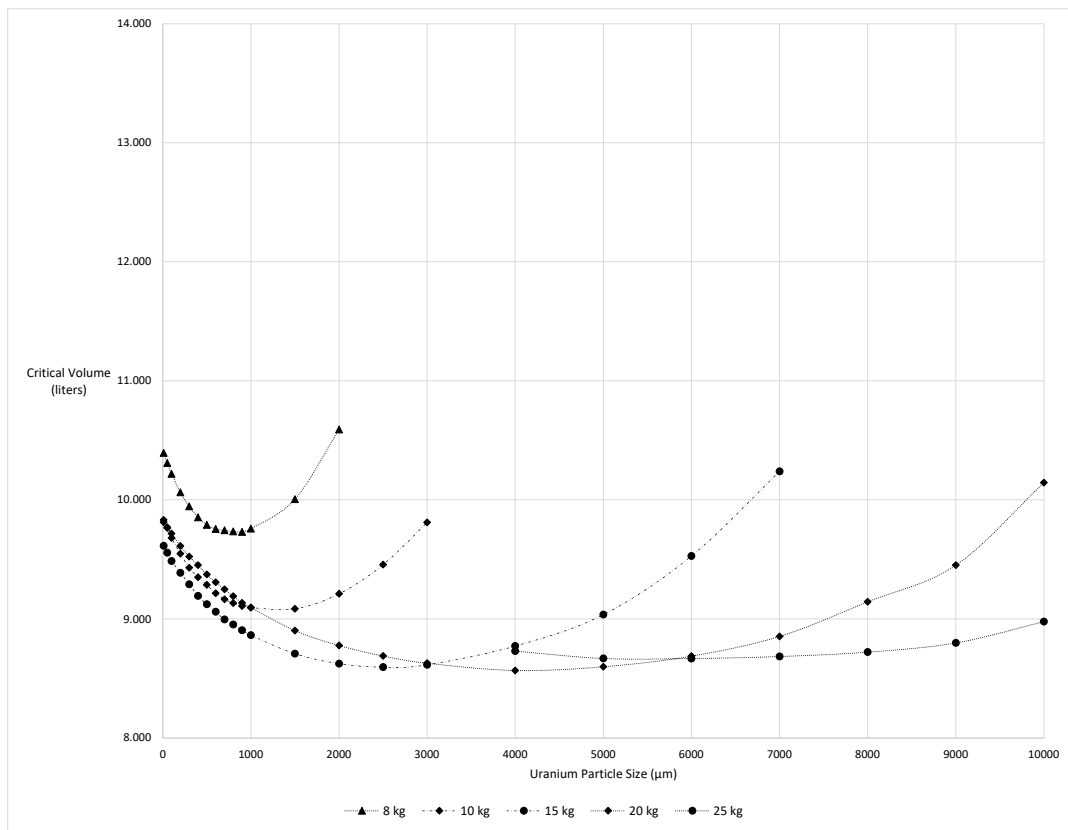


Figure 3.4. Critical volume plotted as a function of uranium particle size. Each line represents a fixed uranium mass from 8 kilograms to twenty-five kilograms evaluated at particle size. As mass increases, the sensitivity of critical volume to particle size diminishes.

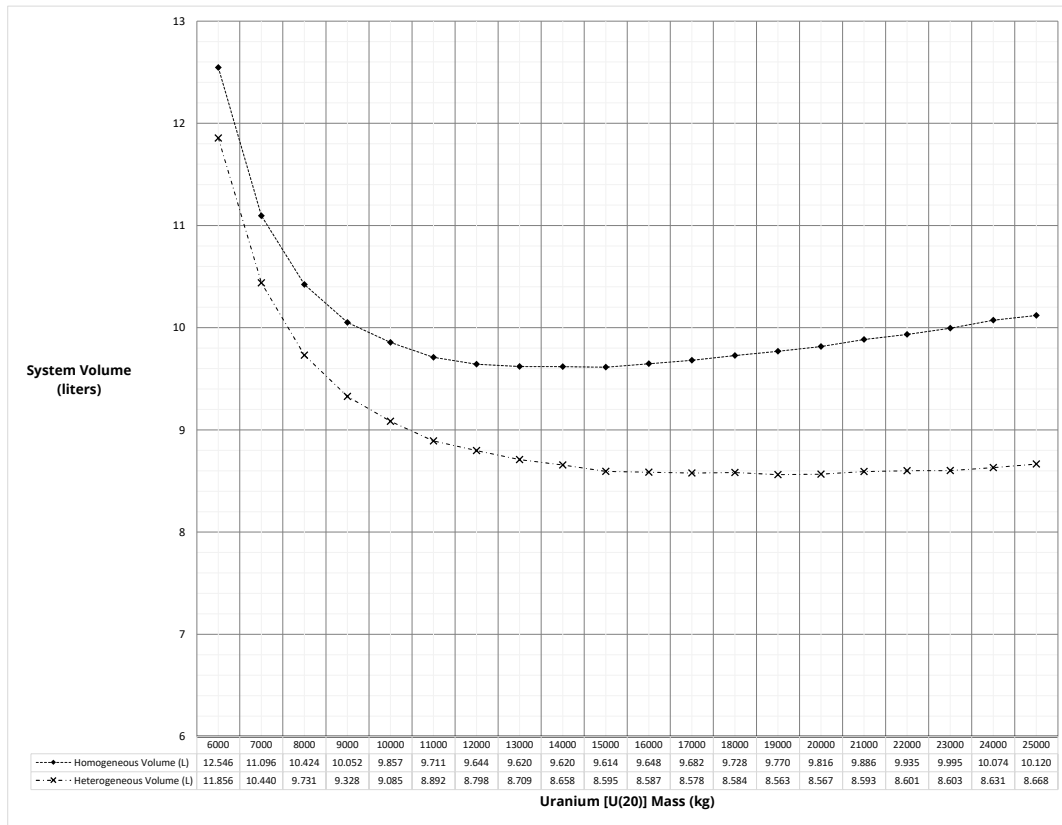


Figure 3.5. Homogeneous critical volume and the minimum heterogeneous critical volume versus uranium mass. As mass is increased, the homogeneous cases reach a minimum volume of approximately 9.6 liters at about 15 kilograms before increasing with increased mass. The heterogeneous cases exhibit only a slight increasing trend above 19 kilograms which may not be statistically significant.

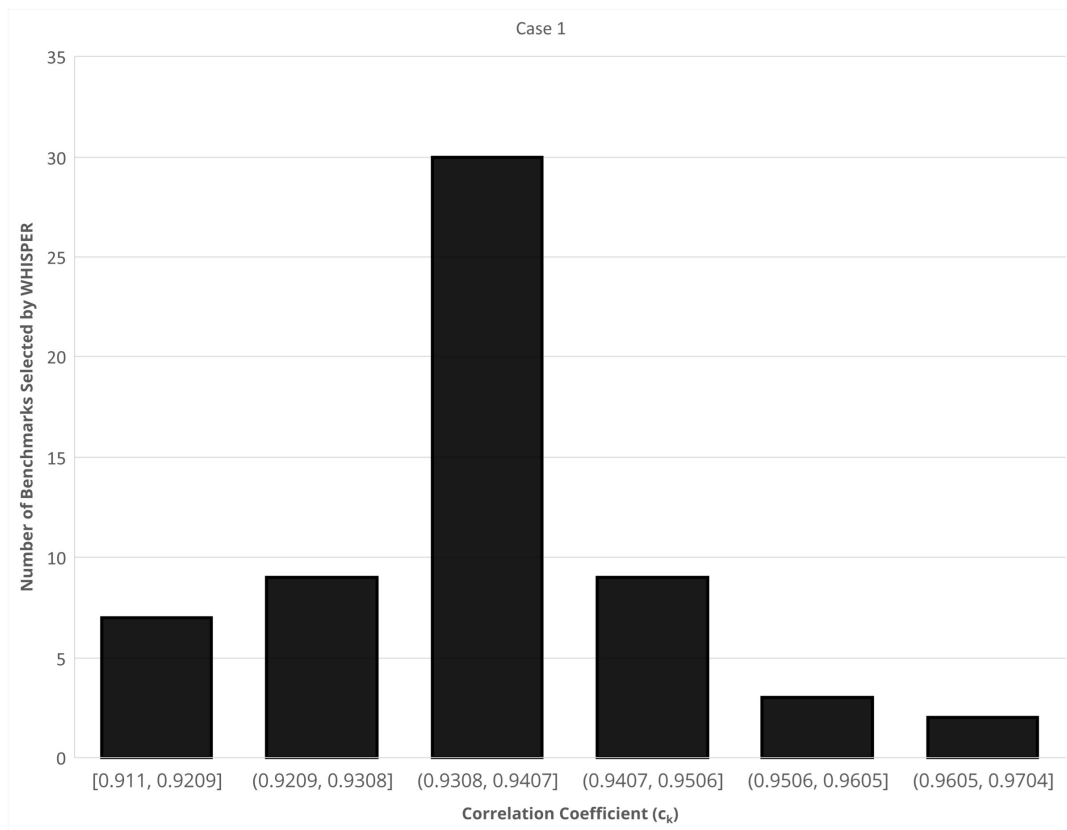


Figure 3.6. A histogram depicting the range of correlation coefficients selected by the WHISPER utility program for Case 1 of the selected MCNP models. This test case produces a near-normal distribution of benchmark correlation coefficients and a correspondingly higher recommended upper subcritical limit.

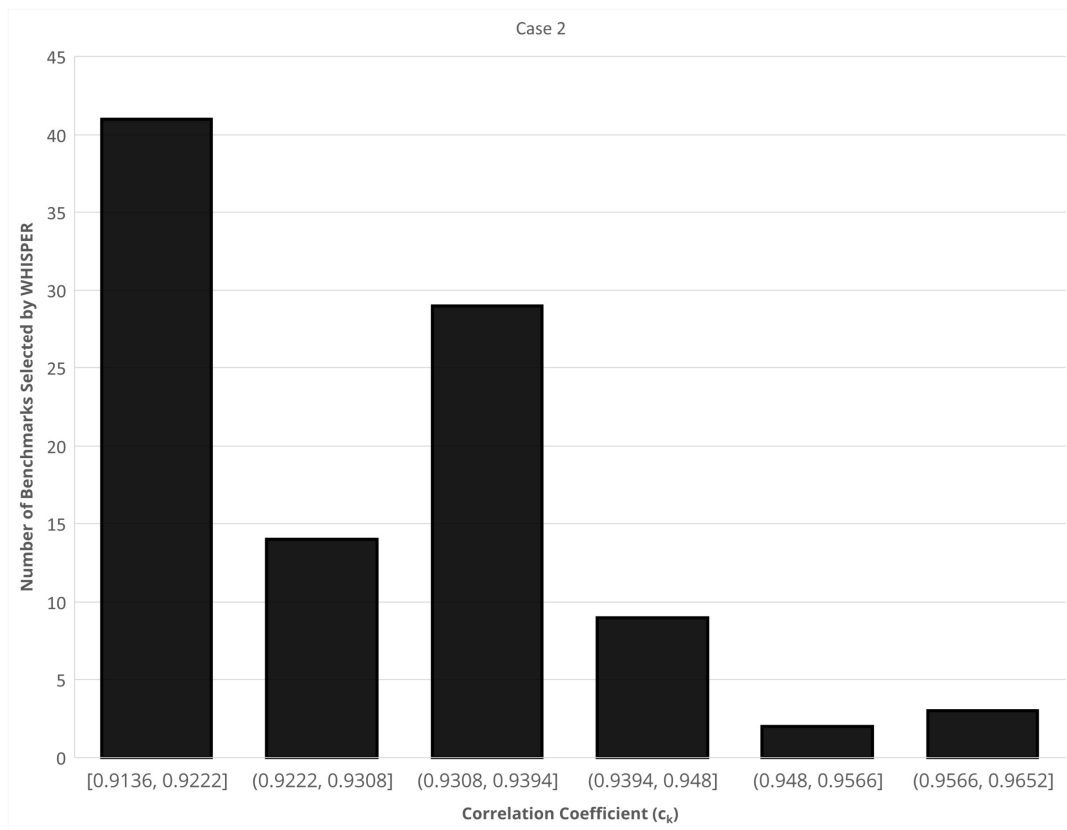


Figure 3.7. A histogram depicting the range of correlation coefficients selected by the WHISPER utility program for Case 2 of the selected MCNP models. This test case produces a bi-modal distribution of benchmark correlation coefficients and a lower recommended upper subcritical limit.



## REFERENCES

- [1] Joseph A. Christensen and R. A. Borrelli. “Parametric Study of Minimum Critical Volume for High-Assay Low-Enriched Uranium (20%) in Spherical Geometry Against Particle Size”. In: *Nuclear Science and Engineering* 196.1 (2022), pp. 98–108. DOI: 10.1080/00295639.2021.1940066. eprint: <https://doi.org/10.1080/00295639.2021.1940066>. URL: <https://doi.org/10.1080/00295639.2021.1940066>.
- [2] Norman L. Pruvost, Hugh C. Paxton, eds. *Nuclear Criticality Safety Guide*. Technical Report LA-12808. Los Alamos, NM: Los Alamos National Laboratory, Sept. 1996.
- [3] J.T. Thomas ed. *Nuclear Safety Guide*. Tech. rep. NUREG/CR-0095. U.S. Nuclear Regulatory Commission, 1978.
- [4] C.E. Newlon. *The Effect of Uranium Density on the Safe U-235 Enrichment Criterion*. Technical Report K-1550. Oak Ridge, TN: Oak Ridge Gaseous Diffusion Plant, Oct. 1962.
- [5] E.D. Clayton et al. “Basis for Subcritical Limits in Proposed Criticality Safety Standard for Mixed Oxides”. In: *Nuclear Technology* 1.35 (1977), pp. 97–111.
- [6] Clayton, E.D. *Anomalies of Nuclear Criticality*. Tech. rep. PNNL-19176. Pacific Northwest Laboratory, 2010.
- [7] C.R. Richey. *EGGNIT: A Multigroup Cross Section Code*. Tech. rep. BNWL-1203. Battelle Memorial Institute Pacific Northwest Laboratories, 1969.
- [8] Commissariat à l’Energie Atomique. *Guide De Criticité*. Tech. rep. CEA-R3114. CEA, 1967.
- [9] Gesellschaft für Anlagen-und Reaktorsicherheit (GRS) gGmbH. *Handbuch zur Kritikalität*. Tech. rep. GRS-379. Gesellschaft für Anlagen-und Reaktorsicherheit, 2015.
- [10] *Atomic Weights and Isotopic Compositions with Relative Atomic Masses*. <https://www.nist.gov/pml/atomic-weights-and-isotopic-compositions-relative-atomic-masses>. Accessed: 2020-01-30.
- [11] *Composition of Uranium*. <https://physics.nist.gov/cgi-bin/Star/compos.pl?matno=092>. Accessed: 2020-01-30.
- [12] *Thermophysical Properties of Fluid Systems*. <https://webbook.nist.gov/chemistry/fluid/>. Accessed: 2020-01-30.
- [13] D.A. Brown et al. “ENDF/B-VIII.0: The 8th major release of the nuclear reaction data library with CIELO-project cross sections, new standards and thermal scattering data”. In: *Nucl. Data Sheets* 148.1 (2018).

- [14] Brian C. Kiedrowski et al. “Whisper: Sensitivity/Uncertainty-Based Computational Methods and Software for Determining Baseline Upper Subcritical Limits”. In: *Nuc. Sci. Eng.* (Sept. 2015). LA-UR-14-26558.
- [15] Brian C. Kiedrowski. *Methodology for Sensitivity and Uncertainty-Based Criticality Safety Validation*. Tech. rep. LA-UR-14-23202. Los Alamos National Laboratory, 2014.

# CHAPTER 4: NUCLEAR CRITICALITY SAFETY ASPECTS FOR THE FUTURE OF HALEU: EVALUATING HETEROGENEITY IN INTERMEDIATE-ENRICHMENT URANIUM USING CRITICAL BENCHMARK EXPERIMENTS

Joseph A. Christensen and R. A. Borrelli. “Nuclear Criticality Safety Aspects for the Future of HALEU: Evaluating Heterogeneity in Intermediate-Enrichment Uranium Using Critical Benchmark Experiments”. In: *Nuclear Science and Engineering* 195.3 (2021), pp. 300–309. DOI: 10.1080/00295639.2020.1819143. eprint: <https://doi.org/10.1080/00295639.2020.1819143>. URL: <https://doi.org/10.1080/00295639.2020.1819143>

## 4.1 ABSTRACT

In order to support the development and deployment of uranium fuels with enrichment beyond five percent, additional criticality safety methodologies are needed to prevent the possibility of criticality accidents. Specifically, improved methodologies for computer code validation using evaluated critical experiments, particularly for dissolver-systems, need to be developed. Potential candidate evaluations and methodologies are presented to evaluate the effect of heterogeneity for intermediate-enrichment uranium systems.

## 4.2 INTRODUCTION

The effect of heterogeneity in systems which use uranium enriched to what are considered “intermediate” values, that is greater than five to ninety-three weight percent is not well understood (Ref. [2]). It is known that available critical data in this range is sparse, and new experiments in this range are conducted seldomly or not at all. This work is a survey of evaluated benchmark experiments from the *International Handbook of Evaluated Criticality Safety Benchmark Experiments* (Ref. [3]) which have appropriate characteristics to be studied in detail to examine the effects of heterogeneity in the intermediate uranium enrichment range.

### 4.2.1 MOTIVATION

It is clear that the nuclear fuels industry intends to begin manufacture and handling of uranium fuels with enrichment up to, or possibly greater than, twenty weight percent. These fuels are known today as “high-assay, low-enriched uranium,” or HALEU. This type of fuel is anticipated to be used in the current fleet of advanced and micro-reactors which are under development and expected to be deployed by the mid-twenty-first century. By one estimate, there are more than six hundred metric tons of HALEU which might be needed to deploy these reactors to the market (Ref. [4]).

Some work has been done in an attempt to evaluate the industry readiness for the manufacture and deployment of HALEU fuels, and one of the primary challenges is the availability of criticality safety benchmark information, which is needed to ensure that computer models are properly validated for use with HALEU fuels (Ref. [5]). The potential consequences of adapting manufacturing and handling processes to fuels of this type without proper precautions and understanding can clearly be demonstrated by one of the world’s most notable and recent nuclear criticality accidents, which occurred at the JCO Fuel Fabrication Plant in Tokai-Mura, Japan (Ref. [6]).

### 4.2.2 GOALS

This work is an attempt to survey existing intermediate-enrichment benchmark evaluations and identify candidates which can be used to more fully evaluate the effects of heterogeneity in the subject enrichment range. This work is the first step in addressing two high-level questions: (1) can existing evaluated benchmarks be used to effectively determine the difference in system multiplication (expressed as  $\Delta k_{\text{eff}}$ ) between a system which contains heterogeneous fuel geometry and a system which does not? and (2) can a distinction between micro-heterogeneity and macro-heterogeneity be determined and generalized using evaluated benchmarks? In order to address these larger questions on the effects of heterogeneity in intermediate-enrichment systems, this work establishes selection criteria and appropriate bases which are used to selected candidate benchmarks for future work. Several criteria are established to support these goals:

1. Establish and explain selection criteria for the identification of candidate benchmark evaluations,
2. Identify and describe the selected benchmarks, and
3. Propose modifications to the evaluated benchmark models which will aid in the evaluation of the effects of heterogeneity.

While modifications of existing benchmarks will give insight into the effect of heterogeneity for each evaluated case, it is likely that the “most-reactive” geometry system cannot be identified using these data alone. However, it is expected that an aggregated look at the effects of heterogeneity over a range of system parameters (enrichment, in this work) from multiple benchmark experiments will provide useful insights which can then be used to create more generalized rules for the treatment of heterogeneity in nuclear criticality safety applications. Successful completion of this work and the follow-on work proposed in section 4.7 will provide such a generalized set of selection criteria and rules which can be used by practitioners of nuclear criticality safety to effectively and appropriately adapt critical experiment data to systems which may contain an unknown character and degree of heterogeneity to establish safe subcritical limits.

### 4.3 BACKGROUND

#### 4.3.1 THE CRITICALITY ACCIDENT AT THE JCO FUEL FABRICATION FACILITY

The details of the criticality accident at the JCO fuel fabrication facility in Tokai-Mura, Japan in 1999 are described in *A Review of Criticality Accidents* (Ref. [6].) At the summary level, a criticality accident took place due to a series of procedural violations by operators which allowed a critical mass of 18.8 weight percent enriched fuel solution into an unfavorable geometry container. The operators’ procedural violations involved the use of unauthorized portable equipment: a bucket and flasks, to bypass the installed favorable-geometry dissolver and storage vessel and a large, non-favorable-geometry mixing vessel to reduce the process time necessary to process a batch of solid uranium oxide into liquid uranyl nitrate solution (See Fig. 4.1). Under the conditions to which the operators had become accustomed, working with five percent enriched uranium, these procedural deviations were “safe” in that they were not sufficient to cause a criticality accident, although they were completely outside the analyzed safety basis. Introduction of higher-enrichment fuel resulted in an accident due to these procedural deviations, killing two operators and exposing a third to dangerous levels of radiation.

A remarkable fact about this accident is that the facility itself had been licensed and authorized to handle fissile material with an enrichment up to twenty percent, and appropriately-designed engineered controls and procedures had been developed to accommodate the higher enrichment. Nonetheless, a long-term decline in oversight and nuclear safety culture in the facility coupled with the concept that a criticality accident had been made “not credible” through the use of passive design controls were sufficient in defeating the prescribed and licensed controls for the facility and directly contributed to the accident.

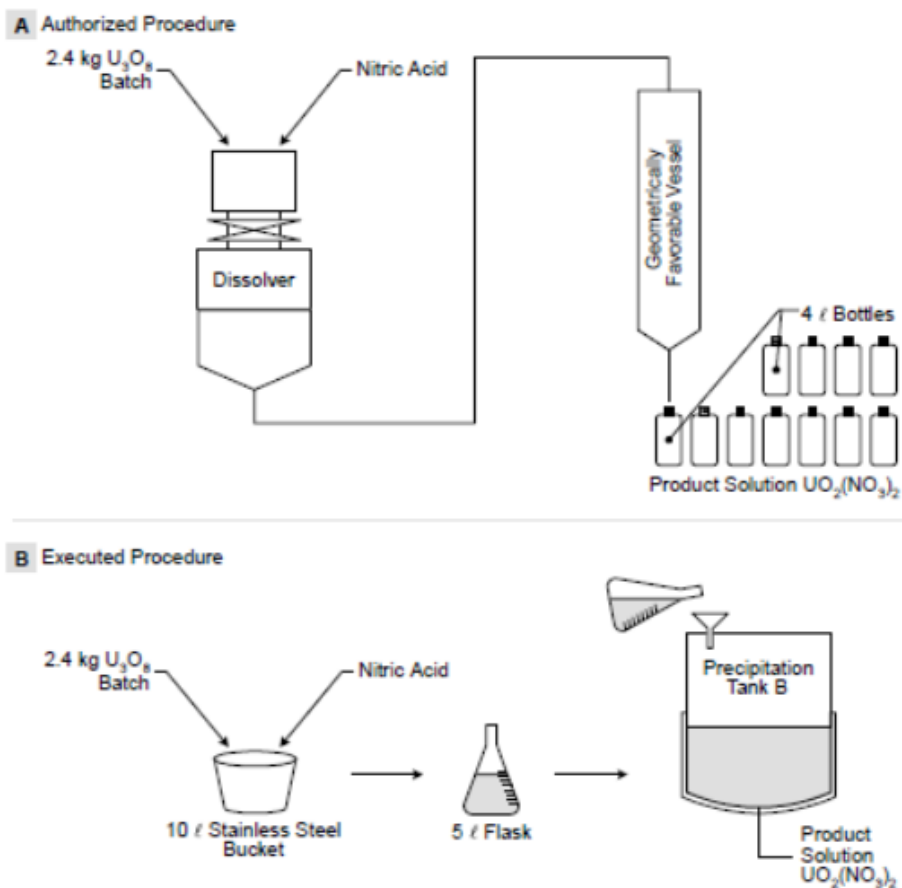


Figure 4.1. A simplified diagram depicting the procedural deviations which led to the Tokai-Mura criticality accident. This figure is a reprint of Figure 34 from (Ref. [6]).

The overall familiarity with nuclear criticality safety at all levels in the operating company was severely inadequate and contributed significantly to the precursors which led to this accident.

Similar precursor conditions to the Tokai-Mura criticality accident exist for the development and deployment of HALEU: (1) most of the industry in the United States is centered around the production and handling of five percent enriched fuel for power reactors, so the existing criticality safety infrastructure may be insufficient for higher enrichment, (2) the development and deployment of HALEU fuels has significant time pressure and economic consideration which tend to challenge the prioritization of safety, and (3) familiarity by facility operators and criticality safety staff with the implications of higher-enrichment fuel material may be insufficient to adequately gauge the challenges introduced by higher-enrichment fissile material. As a consequence to the existence of these precursors, it is entirely possible that fuel enrichment, manufacturing, storage, handling, and utilization facilities have conditions

which could result in criticality accidents due to the introduction of higher assay fuels. The development of techniques which can be used by nuclear criticality safety staff in these facilities to accommodate intermediate-enrichment fuels is therefore imperative. This work is a first step in the development of techniques which can help close the gap in available knowledge.

#### 4.3.2 CHALLENGES ASSOCIATED WITH HALEU

Two proposed methods production of HALEU have been suggested (Ref. [4]). Both of these methods involve the dissolution of highly-enriched uranium into a liquid where it is combined with low-enriched or depleted uranium to create HALEU which is then extracted from the liquid back to a solid which can then be fabricated into fuel. From a criticality safety perspective, this sort of process creates a unique challenge, know colloquially as the “dissolver paradox” (Ref. [2]). In this sort of process, the intermediate state, where solid fissile material co-exists with dissolved fissile material in solution has the potential to be more reactive than either of the two end states: solid fissile material submerged in liquid, or dissolved fissile material in solution. Most critical experiments use either solid fuel or liquid fuel; very few experiments are documented where the two are combined. Consequently, the availability of critical experiment data which describes the dissolver system is limited, and therefore the potential to fully validate criticality safety codes and models is also limited.

The combination of the nature of these type of dissolver systems with sparse critical data leads to a conclusion that the production and handling of HALEU fuels can lead to significant criticality safety risks if not adequately evaluated. A review of current literature does not reveal peer-reviewed information on methodologies or strategies for nuclear criticality safety specific to HALEU. Most of the existing criticality safety information contained in guides or technical reports which have historically focused on ensuring safety for low-enriched uranium for reactor fuel manufacturing or highly-enriched uranium for defense applications. Aside from identifying specific anomalies associated with intermediate enrichment (Ref. [2]), existing criticality safety guides rely on the interpolation between low enrichment and high enrichment to establish a criticality safety basis for intermediate enrichment material (Ref. [7]).

One specific aspect of the challenges associated with HALEU in criticality safety is how to properly evaluate the effect of heterogeneity. It is widely understood that solid fissile material with interspersed moderator will generally produce a more reactive (higher multiplication) system than an equivalent mass or volume of homogeneous fuel-moderator mixture. What is not well-characterized, however, is the magnitude of the effect in the intermediate enrichment range. Because the existing guidance relies on a wide interpolation in experimental data between high and low enrichment, the actual behavior of

heterogeneous systems in this range should be investigated in order to provide a basis for criticality safety evaluations of HALEU dissolver systems.

The typical strategies for evaluation of heterogeneity for nuclear criticality safety are to (1) use experimental data from equivalent experiments and apply a margin of safety to one or more geometric parameters, or (2) model the heterogeneous system and calculate the multiplication by direct or statistical methods. Each of these current methods has its own set of shortcomings. The challenges associated with use of experimental data and the application of margin of safety is easily summarized as: “not enough data” and are discussed in section 4.3.3. Of course, the second option is available, but it can be limited by (1) a lack of sufficient computing resources, because modeling heterogeneous systems can be extremely time-consuming; (2) insufficient information regarding the distribution of fuel in the heterogeneous system, which relates back to the problem with using experimental data; and (3) insufficient validation data for the modeling methods used. This work does not directly address challenges associated with validation of computational methods.

### 4.3.3 EVALUATIONS OF INTERMEDIATE-ENRICHMENT CRITICAL DATA

Prior attempts to identify and evaluate the critical parameters of intermediate-enrichment uranium have been met primarily with a lack of available experimental data from which to start (Ref. [2]). Attempts have been made to interpolate the effects of heterogeneity through the intermediate range based on data from low and high enrichment, but these attempts have had mixed results. For example, comparison of an interpolation made as part of a compilation of critical volume data (Fig. 4.2) with similar analytical results from the *Anomalies* technical report (Fig. 4.3) shows that the set of data in this region is clearly incomplete. The analytical results in *Anomalies* give a clear discontinuity in the critical volumes which is not present in the interpolation of critical volume. It is precisely this lack of consistency in the analysis approach and the lack of available critical data which gives rise to a need for improved analysis methods and more experimental data. This comparison of handbook data also tends to cast doubt on the ability to select appropriate margins of safety for nuclear criticality safety limits derived from homogeneous experimental data, because the magnitude of the effects of heterogeneity are not well characterized.

Unfortunately, critical experiments are extremely difficult to conduct in the current state of the nuclear industry due to a lack of the facilities and necessary resources. The financial and regulatory hurdles associated with the construction and operation of a new nuclear facility in the United States are significant, as evidenced by the failure of several major nuclear construction projects in the last decade.



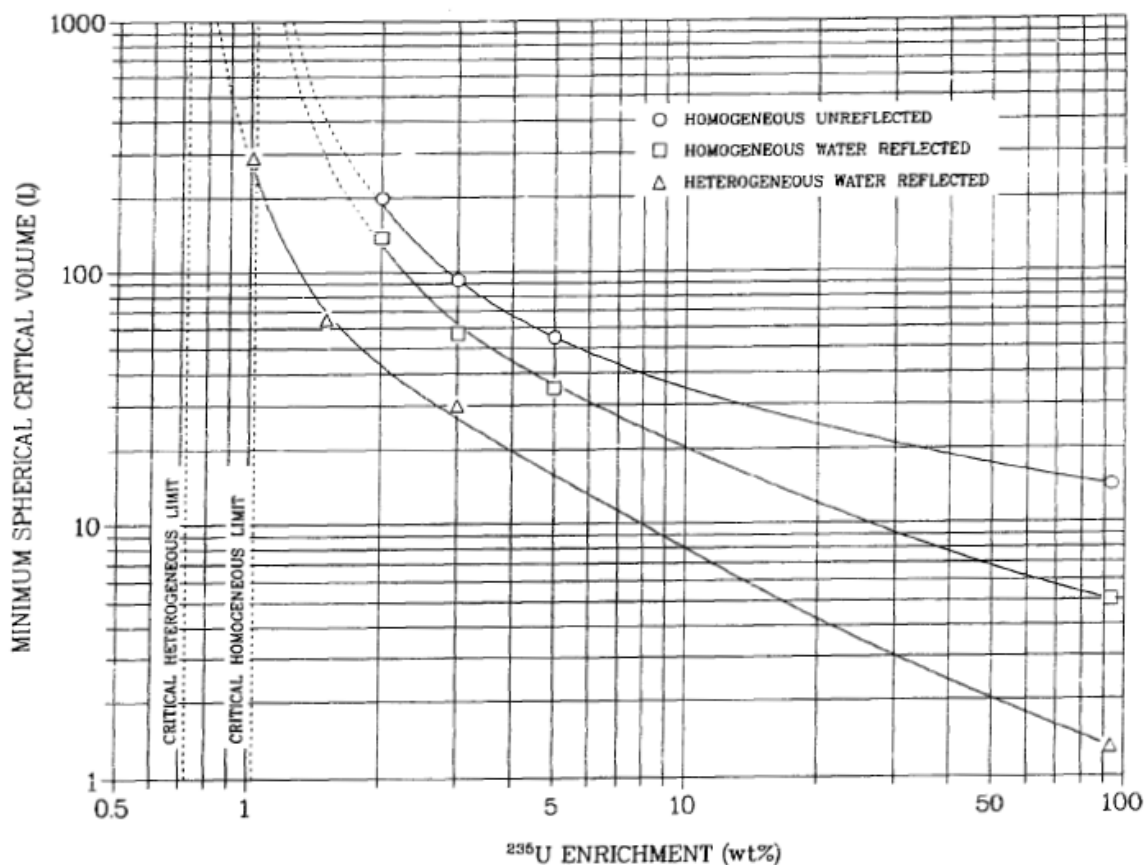


Figure 4.2. Minimum spherical critical volume versus uranium enrichment. There is a significant extrapolation between the data points at low enrichment (five percent and less) and high enrichment (ninety-three percent). This figure is a reprint of Figure 23 from (Ref. [7]).

When coupled with the general anti-nuclear public bias (Ref. [8]), the potential for a new nuclear facility with an experimental mission seems highly unlikely. Existing critical experiments facilities are aging and generally reserved for government-related research (defense and space), although some capability exists to request experiments through Department of Energy programs. As an alternative to new critical experiments, it is possible that improved analysis methods can be devised which can support the growing needs associated with deployment of intermediate-enrichment uranium using available existing data.

The best source of data from which to start an improved analysis method is the *International Handbook of Evaluated Criticality Safety Benchmark Experiments* (Ref. [3]). This resource contains evaluated benchmark experiments which can serve as an effective baseline from which to study the effects of heterogeneity on intermediate-enrichment uranium systems. Identification and analysis of these evaluated benchmarks can provide additional data from which criticality safety professionals can derive improved safety limits associated with intermediate-enrichment uranium without the additional resources associ-

ated with new critical experiments.

#### 4.4 SELECTION OF APPROPRIATE INTERMEDIATE-ENRICHMENT BENCHMARKS

As a starting point for the evaluation of heterogeneity in intermediate enrichment uranium, a number of selection criteria for candidate benchmarks have been developed:

1. Enrichment in the appropriate enrichment range, in this case nine to forty percent enrichment;
2. Appropriate geometry which can be used to introduce heterogeneity if the benchmark model is homogeneous, or vice versa - to homogenize a heterogeneous benchmark model;
3. Fuel compositions and mixtures which are compatible with comparison to other systems within the scope of this work; and
4. Benchmarks which contain evaluations of heterogeneity as part of the evaluation report.

The first criterion requires the least explanation. Based on the previous work in *Anomalies* (Ref. [2]), there is a clear discontinuity in the critical volume of intermediate enrichment systems at approximately thirty-four percent (Fig. 4.3). It is therefore desirable to identify candidate benchmark evaluations which can provide upper and lower bounds on this point. Therefore, benchmarks with enrichment between ten and forty percent are selected for this preliminary study. The second criterion is necessary to preclude overly-complex or overly-simple benchmarks from being included. Because the planned work to introduce or remove heterogeneity involves modifications to the evaluated system geometry, very complex or very simple benchmarks which require extensive modifications might introduce excessive or unintended bias. Complex benchmark models which require extensive modifications toward homogeneity could stray too far from the original critical experiment to remain sufficiently valid in the results. Conversely, overly simple experiments would require excessive justification to introduce useful quantities of heterogeneity. The third criterion allows integration of this work and other planned work with low-enrichment evaluations. It also works to exclude extremely esoteric fuel compositions which are unlikely to be useful for a generalized methodology. The fourth criterion is important in that some benchmark evaluations include work to establish the effects of heterogeneity as part of the evaluation. These evaluation reports will be valuable in determining the direction and efficacy of the final methodology as it is developed.

## 4.5 RESULTS

The *Database for the International Handbook of Evaluated Criticality Safety Benchmark Experiments* (DICE) is a relational database containing data extracted from the handbook coupled with a user interface which enables interrogation of the database along a variety of parameters (Ref. [9]). For this work, DICE was used to examine the database for available candidate benchmarks using the search parameters explained in section 4.4. Out of hundreds of possible choices, twelve evaluated benchmark reports were selected for further examination as part of this and future work. These evaluated benchmark reports are identified using an alphanumeric identifier in three categories: (1) the fuel material, (2) the composition of the fuel, and (3) the neutron energy spectrum in the critical system. For example, “IEU-MET-FAST” represents an intermediate-enrichment metal system with a fast neutron energy spectrum. A complete listing of the available categories of experiments is listed in the handbook (Ref. [3]). The selected benchmark evaluations and associated explanations are provided.

### 4.5.1 ZERO POWER PHYSICS REACTOR (ZPPR) EXPERIMENTS

Several of the IEU-MET-FAST series benchmarks were selected for this work. Table 4.1 gives a summary of the range of enrichment for these experiments, some of which fall outside the range of the selection criteria; they were retained because they include a specific evaluation of transformation bias, which is defined as the difference in  $k_{\text{eff}}$  between the as-built heterogeneous model and the simplified homogeneous benchmark model. These benchmarks consist of a partially-homogeneous model of the zero-power physics reactor (ZPPR), which was operated at the Idaho National Laboratory over a period of more than thirty years. The experiments themselves consisted of drawers loaded with small plates of various fuel and moderating materials which were then loaded into a large split-table assembly which could be closed to achieve criticality.

Table 4.1. Benchmarks selected from the IEU-MET-FAST series.

Benchmark	Enrichment	Geometry	Fuel Composition	Evaluation? (y/n)
IEU-MET-FAST-010	9			Yes
IEU-MET-FAST-012	16			Yes
IEU-MET-FAST-013	11	Partially-homogeneous cylinder	uranium metal	Yes
IEU-MET-FAST-014	16 & 21			Yes
IEU-MET-FAST-015	47 at%			Yes
IEU-MET-FAST-016	12 at%			Yes

The evaluators for these experiments homogenized the contents of the drawers and determined a transformation bias, which is shown in Table 4.2 (Refs. [10], [11], [12], [13], [14], [15].)

Table 4.2. Transformation Bias from the IEU-MET-FAST series.

Benchmark	Enrichment	Transformation Bias
IEU-MET-FAST-010	9	$-0.0061 \pm 0.0005$
IEU-MET-FAST-013	11	$-0.0081 \pm 0.0021$
IEU-MET-FAST-016	12 at%	$-0.0046 \pm 0.0010$
IEU-MET-FAST-012	16	$-0.0011 \pm 0.0020$
IEU-MET-FAST-014	16	$-0.0074 \pm 0.0020$
IEU-MET-FAST-014	21	$-0.0098 \pm 0.0020$
IEU-MET-FAST-015	47 at%	$-0.0059 \pm 0.0010$

#### 4.5.2 CRITICAL ARRAYS OF POLYETHYLENE-MODERATED URANIUM FLUORIDE - POLY-TETRAFLUOROETHYLENE CUBES

Twenty-nine cases of an experimental series conducted on a split-table assembly at the Los Alamos National Laboratory shortly after the end of World War II are documented as IEU-COMP-THERM-001 (Ref. [16]) and IEU-COMP-MIXED-001 (Ref. [17]). There are two evaluation reports for this series because of the variations in the neutron energy spectrum in several of the cases. This particular experiment series is an excellent candidate for evaluation of heterogeneity for several reasons:

1. The experiment series itself contains several critical arrangements that were intended to specifically study heterogeneity, and the results of that particular study are reported in the literature (Ref. [18]) (Ref. [19]);
2. This experiment series can be used to introduce additional heterogeneity by examination of the particle density and distribution in the fuel blocks, or it can be used to remove existing heterogeneity by “smearing” the core and homogenizing the materials; and
3. The general parameters of this series fall within the selection criteria—intermediate enrichment, generally thermal spectrum, moderately complex geometry, et cetera.

#### 4.5.3 SINGLE CORES OF ENRICHED URANIUM OXIDE AND WAX MIXTURES

The report IEU-COMP-THERM-015 [20] describes and evaluates a series of experiments conducted at Aldermaston and Dounreay in the United Kingdom which used solid uranium oxide and wax cubes

arranged in a number of critical configurations. The enrichment for these experiments was approximately thirty percent. Several of the configurations were arranged specifically to evaluate the effect of heterogeneity. This evaluation series is important in that most of the benchmark models are homogenized as part of the evaluation and determination of the bias for that transformation is listed. Two cases, however, remain heterogeneous and can be homogenized for comparison with the previously-reported results. Additionally, one particular case could not be used as a benchmark model due to uncertainty with its characteristics. This case could be examined more closely to determine why its particular heterogeneity creates issues with the transformation. Finally, this evaluation report includes an appendix which describes the effects of uranium oxide particle size on the benchmark parameters; it describes a linear dependency of the effect of heterogeneity on the size of the particles in the fuel material. Extension of this examination can be included in future work.

#### 4.5.4 URANIUM TETRAFLUORIDE AND TEFLON BLOCKS AT VARIOUS ENRICHMENT

A series of twenty-three critical experiments using mixtures of uranium tetrafluoride and Teflon as blocks arranged on a split-table apparatus were performed at the Oak Ridge National Laboratory Critical Experiments Facility in the late 1950s. These arrangements used blocks containing uranium enriched to 37.5 and 0.2 weight percent which could be arranged in the experiment to produce a range of average enrichment. The range of enrichment spanned between 12.5 percent and 37.5 percent. The benchmark experiments were evaluated in IEU-COMP-MIXED-002 [21], IEU-COMP-MIXED-003 [22], and IEU-COMP-INTER-003 [23]. These benchmarks are useful primarily because of the ability to directly compare the effects of inserting or removing heterogeneity across the entire range of enrichment. This series also describes the manufacturing process by which the blocks were made. The process involves finely-ground fuel particles which are cold-pressed into the Teflon matrix material. The evaluation report does not provide any information on the size or distribution of the fuel grains, which creates an opportunity for further evaluation, based on similar reported particle size distributions [24].

## 4.6 DISCUSSION

As a survey of the selected benchmark evaluations, there are two primary sources of heterogeneity which can be examined. First, each of the selected experiments consists of solid fuel blocks or plates which are arranged intermittently with moderating non-fuel materials. The resultant configuration is therefore heterogeneous by definition. In some of the benchmark evaluations, some or all of the fuel and non-fuel portions of the assembly were combined into a single evaluated material definition which

is then treated as homogeneous throughout the fueled region of the assembly. The second source of heterogeneity is from the manufacture of the fuel itself. In several of the selected benchmarks, solid fuel particles were manufactured and combined using a binding agent (Teflon, paraffin, or wax) into a solid fuel block which is then used in the experiment. In these cases, only limited data are provided on the size or material properties of the actual solid fuel particles, and nearly uniformly, the fuel block is treated as a homogeneous material. Some of the benchmark evaluations include a discussion of the effect of this homogenization of the fuel material, but generally the information provided is limited.

Using this division of heterogeneity into a macro- (fuel/non-fuel arrangement) and a micro- (fuel particle size and distribution), a number of perturbations from the evaluated benchmark models can be performed to better quantify the effects of heterogeneity in these systems. It should be possible to then generalize the behavior across the range of intermediate enrichment in order to increase the resolution on system behavior in that range.

Understanding the macro-heterogeneity of these systems is useful to criticality safety engineers because it will improve the analysis of arrays of discrete fissile units, such as trays of solid fuel material, tanks containing fuel liquids, or other large-fissile units which have the potential to become moderated between the units. Similarly, understanding micro-heterogeneity will improve the analysis of systems which contain fine particles of fuel or precipitates which could occur during processing or process upsets.

The primary motivation behind these sort of perturbations is the determination of the effect or sensitivity to varying degrees of heterogeneity in these intermediate-enrichment systems. Performance of this analysis will give important insight into the behavior of systems within the subject enrichment range which can then be used to improve the understanding of the safe physical characteristics of these systems, such as limiting critical mass or volume relative to the degree of heterogeneity. Understanding this behavior is extremely important, as the expansion of the use of intermediate-enrichment uranium is expected to occur throughout the twenty-first century. In order to support such an expansion in scope, existing nuclear criticality safety rules and processes must be modified to ensure appropriate degrees of safety are applied to prevent potential criticality accidents, such as the Tokai-Mura accident, from occurring.

#### 4.7 FUTURE WORK

The future work resulting from this survey will be to process and resolve in detail the effects of heterogeneity in the selected systems:

1. Generate baseline models of the evaluated benchmark cases using a Monte Carlo evaluation code and current data library
  - (a) Resolve any differences discovered which may be the result of differences in the code system or data libraries
  - (b) Collect baseline  $k_{\text{eff}}$  information and uncertainty to be used for comparison with modified models
2. Modify the benchmark models by inserting or removing heterogeneity and collect new  $k_{\text{eff}}$  results for comparison
  - (a) For arrangements which use solid fuel particles, conduct examinations of the effects of micro-heterogeneity by replacing homogeneous fuel materials with regular lattices of particles throughout the size distribution discussed in LEU-COMP-THERM-033.
  - (b) Replace instances of macro-heterogeneity with homogeneous fuel-moderator mixtures
  - (c) For cases where the benchmark evaluation model has already been homogenized, replace the homogeneous regions with heterogeneous arrangements based on the description of the original experiment
3. Using the results from the model modifications, determine the effects of heterogeneity by computing the relative change between heterogeneous and homogeneous models
  - (a) Determine if there are discernible dependencies on enrichment, fuel-to-moderator ratio, et cetera
  - (b) Attempt to establish generalized rules regarding the effects of heterogeneity which can be supported with comparison to other systems outside the scope of this survey

Of particular interest in future work is the determination of any differences in the effects of micro-heterogeneity between a solid fuel particle embedded in a solid matrix, such as those discussed in LEU-COMP-THERM-033, and systems which consist of solid fuel particles suspended in a liquid moderator, such as the dissolver system. While these systems are generally similar from the standpoint of moderator-to-fuel ratio, there may be significant differences in the effects of heterogeneity due to fuel particle size, shape, or distribution.

## 4.8 SUMMARY REMARKS

The use of evaluated benchmark reports for studies which extend the field of available information to criticality safety professionals is an area which should be explored. As discussed previously, the need for extended data sets in the intermediate enrichment range is growing, but the availability of new critical data is not. Therefore, development of new methods to evaluate existing data is imperative.

This work is the beginning of an attempt to generalize the behavior of heterogeneity in intermediate-enrichment uranium systems. It is intended to establish a set of general rules which can be used to further evaluate critical parameters in these systems.



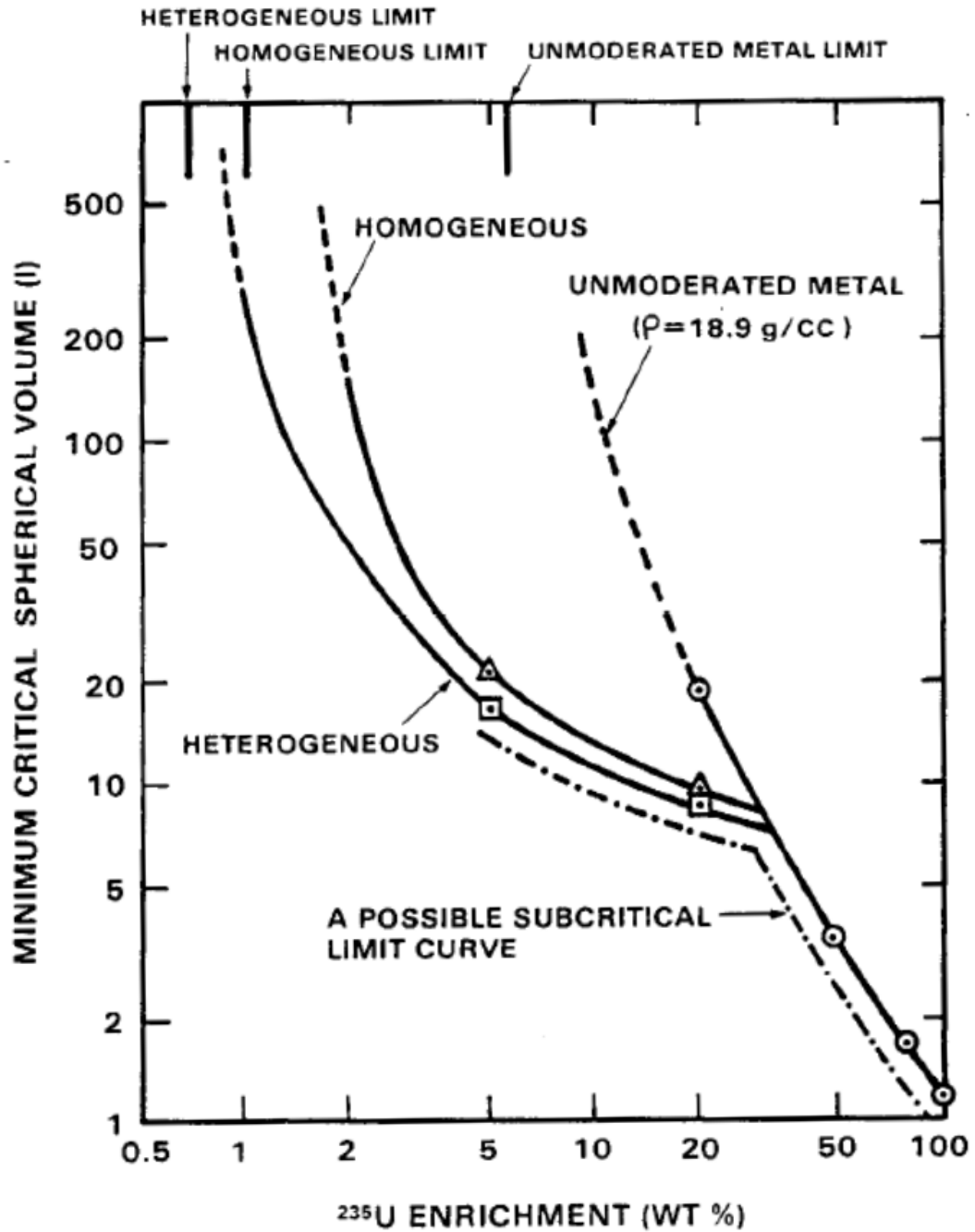


Figure 4.3. Calculated minimum critical volume versus uranium enrichment. Note the "elbow" discontinuity at approximately thirty-four percent enrichment. This figure is a reprint of Figure 11 from (Ref. [2]).

## REFERENCES

- [1] Joseph A. Christensen and R. A. Borrelli. “Nuclear Criticality Safety Aspects for the Future of HALEU: Evaluating Heterogeneity in Intermediate-Enrichment Uranium Using Critical Benchmark Experiments”. In: *Nuclear Science and Engineering* 195.3 (2021), pp. 300–309. DOI: 10.1080/00295639.2020.1819143. eprint: <https://doi.org/10.1080/00295639.2020.1819143>. URL: <https://doi.org/10.1080/00295639.2020.1819143>.
- [2] Clayton, E.D. *Anomalies of Nuclear Criticality*. Tech. rep. PNNL-19176. Pacific Northwest Laboratory, 2010.
- [3] Nuclear Energy Agency. *International Handbook of Evaluated Criticality Safety Benchmark Experiments. [DVD]*. Tech. rep. NEA-7328. Nuclear Energy Agency, 2019.
- [4] Office of Nuclear Energy. *What is High-Assay Low-Enriched Uranium (HALEU)*. US Department of Energy, Apr. 7, 2020. URL: <https://www.energy.gov/ne/articles/what-high-assay-low-enriched-uranium-haleu>.
- [5] Nuclear Energy Institute. *Addressing the Challenges with Establishing the Infrastructure for the front-end of the Fuel Cycle for Advanced Reactors*. White Paper. Washington, D.C.: Nuclear Energy Institute, 2018. URL: <https://www.nrc.gov/docs/ML1810/ML18103A250.pdf>.
- [6] Thomas P. McLaughlin et al. *A Review of Criticality Accidents*. Technical Report LA-13638. Los Alamos, NM: Los Alamos National Laboratory, May 2000.
- [7] H. C. Paxton and N. L. Pruvost. *Critical dimensions of systems containing  $^{235}\text{U}$ ,  $^{239}\text{Pu}$ , and  $^{233}\text{U}$* . Tech. rep. LA-10860-MS. Los Alamos National Laboratory, 1987.
- [8] A. Abdulla et al. “Limits to deployment of nuclear power for decarbonization: Insights from public opinion”. In: *Energy Policy* 129 (June 2019), pp. 1339–1346. DOI: <https://doi.org/10.1016/j.enpol.2019.03.039>.
- [9] Nuclear Energy Agency. *DICE: User’s Manual. [DVD]*. Tech. rep. NEA/NSC/DOC(95)03/II. Nuclear Energy Agency, 2019.
- [10] Kermit A. Bunde and Richard D. McKnight. *The U9 benchmark assembly: a cylindrical assembly of U metal (9%  $^{235}\text{U}$ ) with a thick depleted-uranium reflector*. In: *International Handbook of Evaluated Criticality Safety Benchmark Experiments. [DVD]*. Tech. rep. IEU-MET-FAST-010. Nuclear Energy Agency, 2019.

- [11] Amr Mohamed and Richard D. McKnight. *ZPR-3 assembly 41: a cylindrical assembly of U metal (16%  $^{235}\text{U}$ ), aluminum, and steel, reflected by depleted-uranium*. In: *International Handbook of Evaluated Criticality Safety Benchmark Experiments*. [DVD]. Tech. rep. IEU-MET-FAST-012. Nuclear Energy Agency, 2019.
- [12] Gerardo Aliberti et al. *ZPR-9 Assembly 1: a cylindrical assembly of U metal (93%  $^{235}\text{U}$ ) and depleted uranium with aluminum reflectors, IEU-MET-FAST-013*. In: *International Handbook of Evaluated Criticality Safety Benchmark Experiments*. [DVD]. Tech. rep. IEU-MET-FAST-013. Nuclear Energy Agency, 2019.
- [13] Robert W. Schaefer et al. *ZPR-9 Assemblies 2 and 3: cylindrical assemblies of U metal and tungsten with aluminum reflectors*. In: *International Handbook of Evaluated Criticality Safety Benchmark Experiments*. [DVD]. Tech. rep. IEU-MET-FAST-014. Nuclear Energy Agency, 2019.
- [14] Richard M. Lell. *ZPR-3 assembly 6F: a spherical assembly of highly-enriched uranium and depleted uranium with an average  $^{235}\text{U}$  enrichment of 47 atom %*. In: *International Handbook of Evaluated Criticality Safety Benchmark Experiments*. [DVD]. Tech. rep. IEU-MET-FAST-016. Nuclear Energy Agency, 2019.
- [15] Richard M. Lell. *ZPR-3 assembly 11: a cylindrical assembly of highly-enriched uranium and depleted uranium with an average  $^{235}\text{U}$  enrichment of 12 atom % and a depleted uranium reflector*. In: *International Handbook of Evaluated Criticality Safety Benchmark Experiments*. [DVD]. Tech. rep. IEU-MET-FAST-016. Nuclear Energy Agency, 2019.
- [16] Virginia F. Dean. *Critical arrays of polyethylene-moderated  $\text{U}(30)\text{F}_4$ -polytetrafluoroethylene one-inch cubes*. In: *International Handbook of Evaluated Criticality Safety Benchmark Experiments*. [DVD]. Tech. rep. IEU-COMP-THERM-001. Nuclear Energy Agency, 2019.
- [17] Virginia F. Dean. *Critical arrays of polyethylene-moderated  $\text{U}(30)\text{F}_4$ -polytetrafluoroethylene one-inch cubes*. In: *International Handbook of Evaluated Criticality Safety Benchmark Experiments*. [DVD]. Tech. rep. IEU-COMP-MIXED-001. Nuclear Energy Agency, 2019.
- [18] Clifford K. Beck, Dixon Callihan, and Raymond L. Murray. *Critical Mass Studies, Part I*. Tech. rep. A-4716. Los Alamos National Laboratory, 1947.
- [19] C. K. Beck, A. D. Callihan, and R. L. Murray. *Critical Mass Studies, Part II*. Tech. rep. K-126. Los Alamos National Laboratory, 1948.

- [20] James P. Dyrda, Nigel P. Tancock, and Matthew D. Eaton. *Single cores of 30.14%  $^{235}\text{U}$  enriched  $\text{UO}_2$ /wax mixtures—bare and with single reflector materials.* In: *International Handbook of Evaluated Criticality Safety Benchmark Experiments. [DVD]*. Tech. rep. IEU-COMP-THERM-015. Nuclear Energy Agency, 2019.
- [21] Karla R. Elam. *Unreflected  $\text{UF}_4$ - $\text{CF}_2$  blocks with uranium of 30, 25, 18.8, and 12.5%  $^{235}\text{U}$ .* In: *International Handbook of Evaluated Criticality Safety Benchmark Experiments. [DVD]*. Tech. rep. IEU-COMP-MIXED-002. Nuclear Energy Agency, 2019.
- [22] Karla R. Elam. *Unreflected  $\text{UF}_4$ - $\text{CF}_2$  blocks with 37.5%  $^{235}\text{U}$ .* In: *International Handbook of Evaluated Criticality Safety Benchmark Experiments. [DVD]*. Tech. rep. IEU-COMP-MIXED-003. Nuclear Energy Agency, 2019.
- [23] Karla R. Elam. *Unreflected  $\text{UF}_4$ - $\text{CF}_2$  blocks with 37.5%  $^{235}\text{U}$ .* In: *International Handbook of Evaluated Criticality Safety Benchmark Experiments. [DVD]*. Tech. rep. IEU-COMP-INTER-003. Nuclear Energy Agency, 2019.
- [24] Susumu Mitake. *Reflected and unreflected assemblies of 2 and 3%-enriched uranium fluoride in paraffin.* In: *International Handbook of Evaluated Criticality Safety Benchmark Experiments. [DVD]*. Tech. rep. LEU-COMP-THERM-033. Nuclear Energy Agency, 2019.

# CHAPTER 5: EVALUATIONS OF THE EFFECT OF HETEROGENEITY IN HALEU SYSTEMS USING MODIFIED CRITICAL BENCHMARKS

Joseph A. Christensen and R. A. Borrelli. “Evaluations of the Effect of Heterogeneity in HALEU Systems Using Modified Critical Benchmarks”. In: *Nuclear Science and Engineering* 196.11 (2022), pp. 1333–1348. DOI: 10.1080/00295639.2022.2087832. eprint: <https://doi.org/10.1080/00295639.2022.2087832>. URL: <https://doi.org/10.1080/00295639.2022.2087832>

## 5.1 ABSTRACT

This work uses evaluated criticality safety benchmarks to examine the effect of heterogeneity in HALEU systems. A subset of benchmarks selected based on their composition parameters is slightly modified to artificially introduce heterogeneity, and the difference in the effective multiplication factor between the homogeneous benchmark and the modified model is determined. The difference in multiplication factor is evaluated for correlations against both the moderator ratio and the enrichment of the benchmarks and the correlations are examined using established statistical methods. In several cases, statistically significant correlations are observed and discussed, and the lack of expected correlations is also discussed.

## 5.2 INTRODUCTION

As discussed in our previous work [2], it was explained that the study of heterogeneity in HALEU systems is of paramount importance for a number of applications. Work in this area has direct impact on the readiness of the US nuclear fuel industry to safely handle, manufacture, and transport advanced nuclear fuel with higher enrichments than those already in service. The nuclear criticality safety implications of a transition from “true” LEU fuels (five weight percent or less  $^{235}\text{U}$ ) to HALEU fuels are not trivial, as demonstrated by the JCO Tokai-Mura criticality accident in 1999. One significant shortcoming in the methods currently available for use in the evaluation of heterogeneity for nuclear criticality safety was discussed: the lack of available critical experiment data for uranium of the appropriate en-

richment. As a first-step to improving the methods available for the evaluation of heterogeneity, this work demonstrates a way to use existing critical benchmark data to improve the quality of the overall data set available to nuclear criticality safety practitioners.

In the previous work in this series, we identified candidate benchmark experiments for further analysis based on a number of factors which could be useful in the investigation of heterogeneity in intermediate-enrichment uranium (IEU) systems. Specifically, the benchmarks were selected based on (1) appropriate enrichment in the range of 9% to 40%, (2) appropriate geometry which could be used to induce heterogeneity, (3) comparable fuel and moderator compositions, and (4) existing comparisons of heterogeneity. Of the twelve benchmark series identified in that report, this work focuses on a subset of four: IEU-COMP-INTER-003, IEU-COMP-MIXED-002, IEU-COMP-THERM-001, and IEU-COMP-THERM-015. This subset contains benchmarks with characteristics useful for direct comparison between them and for the induction of heterogeneity to study the effects in a direct context.

### 5.2.1 MOTIVATION

The use of HALEU fuels is likely to expand in the twenty-first century as new, smaller, advanced design reactors enter into the conceptual and preliminary design phases across the globe. The adaptation of nuclear criticality safety guidance to accommodate such fuels is paramount to ensuring that fuel manufacturing and handling operations do not result in accidental nuclear criticality. One of the primary “known-unknowns” in this area is the effect of heterogeneity in multiplying systems of HALEU.

Based on some previous work [3], a relationship between the effect of heterogeneity and minimum critical volume was observed with regard to both the size of the particles in the multiplying system and the fuel-to-water ratio, which is also sometimes known as the ‘moderator ratio’. Generally, this ratio is easily expressed as an atomic ratio of fuel ( $^{235}\text{U}$ ) and the primary moderator element (hydrogen). This is a convenient parameter for use in comparison between moderated systems and is frequently available in the International Handbook of Evaluated Criticality Safety Benchmark Experiments [4] alongside the benchmark evaluation and development parameters. Accordingly, we selected this parameter as an initial focus to help investigate the effects of heterogeneity in the systems under evaluation. It is recognized that the systems in this work have moderator ratios which are generally considered ‘under-moderated’ in that they would achieve smaller mass or volume if the moderator ratio is increased and that there are other related parameters such as the average energy of neutrons causing fission (ANECF) which may be evaluated similarly and may provide different results; such an evaluation is included in our future work.

### 5.2.2 GOALS

1. Using evaluated critical benchmarks, determine whether or not a change in the fuel geometry from homogeneous to heterogeneous produces a meaningful change in system multiplication;
2. If a change in multiplication is determined to exist, evaluate the magnitude of the change against other system parameters in search of useful correlations;
3. Evaluate the presence or lack of correlation.

## 5.3 CASE STUDIES

Based on previous work, the effect on neutron multiplication in critical model simulations of twenty-percent enriched uranium due to heterogeneity has been demonstrated. The smallest particle size at which an observable effect is approximately 500  $\mu\text{m}$ . This result was shown to be consistent with previous experiments and nuclear safety guidance commonly used in the field of nuclear criticality safety. It is therefore of interest to investigate the presence or absence of similar effects in enrichments higher and lower than twenty percent, but still in the range of what is commonly referred to as “high-assay, low-enriched uranium” or HALEU.

### 5.3.1 USE OF EVALUATED BENCHMARKS

In support of this investigation, a subset of benchmarks was selected from the ICSBEP Handbook [4] from a set of previously-selected benchmarks [2] for further evaluation specific to this work. In the handbook, these benchmarks are identified by fuel isotope, fuel physical form, and neutron spectrum. For example, LEU-MET-THERM-004 indicates that the fuel is low-enriched uranium (LEU) metal (MET) with a thermal neutron spectrum (THERM). The number assigned to each benchmark is sequential based on the order in which the number is assigned to the evaluation. In this work, four benchmark series were selected based on their enrichment: IEU-COMP-INTER-003 [5], IEU-COMP-MIXED-002 [6], IEU-COMP-THERM-001 [7], and IEU-COMP-THERM-015 [8].

#### 5.3.1.1 IEU-COMP-INTER-003

IEU-COMP-INTER-003 documents a series of experiments using an equimolar ratio of uranium tetrafluoride ( $\text{UF}_4$ ) and Teflon ( $\text{CF}_2$ ) which were performed at the ORNL in the mid-1950s. The enrichment of the uranium was approximately 37.5 wt.% U-235. The fuel material and the moderator material was pressed into blocks of various sizes which could be arranged into a variety of critical configurations using a split-table apparatus. A total of fourteen critical configurations were made during the experiment series with a variety of hydrogen-to-uranium (H/U) ratios. The mass of fuel and moderator in each configuration varied based on the arrangement and size of the blocks used. The critical configurations in the experimental series were generally cubic in shape, although one case was arranged into a pseudocylinder and one was an irregular rectangular parallelepiped. A complete description of the experiments and the benchmark configurations is provided in the reference [5].



### 5.3.1.2 IEU-COMP-MIXED-002

A set of experiments similar to IEU-COMP-INTER-003 was performed using the same style of blocks, but with a variety of enrichment. This experimental series is documented as IEU-COMP-MIXED-002. In this experimental series, blocks using depleted (0.2 wt.%) uranium were added to the configurations to produce critical experiments over a range of enrichment. Critical configurations were achieved at enrichments of 30, 25, 18.8, and 12.5 wt.% U-235. Each of these critical configurations had a generally cubic shape with less variation than the similar IEU-COMP-INTER-003 experiments. A complete description of the experiments and the benchmark configurations is provided in the reference [6].

### 5.3.1.3 IEU-COMP-THERM-001

Twenty-nine critical configurations were evaluated experimentally using the (presumably) same split-table apparatus at ORNL in the mid-1940s which used alternating arrays of ‘H’ cubes and ‘U’ cubes arranged into a cuboid structure. The ‘H’ cubes were cubes of polyethylene, and the ‘U’ cubes were 30 wt.% enriched uranium fluoride-polytetrafluoroethylene ( $\text{UF}_4\text{-(CF}_2\text{)}_n$ ). Most of the critical experiments in this series also had a paraffin reflector. A complete description of the experiments and the benchmark configurations is provided in the reference [7].

### 5.3.1.4 IEU-COMP-THERM-015

A series of experiments were conducted at Aldermaston and Dounreay in the United Kingdom during the 1950s and 1960s using uranium oxide ( $\text{UO}_2$ ) and wax to simulate uranium oxyfluoride ( $\text{UO}_2\text{F}_2$ ) solutions. These experiments used solid  $\text{UO}_2$  and wax cubes in a variety of rectangular configuration. The enrichment of uranium in these experiments was 30.14 wt.% and the proportions of wax and  $\text{UO}_2$  were varied over a range of H/U ratio. A complete description of the experiments and the benchmark configurations is provided in the reference [8].

## 5.4 METHODS

### 5.4.1 USE OF BENCHMARKS

The benchmark model specifications from the ICSBEP handbook were used to generate models for use in the Monte Carlo computation code MCNP version 6.2 [9] [10]. All cases in this work were evaluated using nuclear data from the ENDF/B-VIII.0 cross section library [11] with 100,000 particles per generation and 550 cycles, discarding the first 50 cycles to ensure source convergence and minimize statistical errors. These benchmark models are used to establish a baseline for comparison with the transformed models.

### 5.4.2 TRANSFORMATIONS

In order to evaluate the effects of heterogeneity in the selected benchmarks, a transformation is applied which changes the homogeneous material specifications into an equivalent-mass heterogeneous system. The heterogeneous system is a regular lattice of uranium metal spheres with the same isotopic ratio as the original benchmark, surrounded by moderating material. The moderating material is similarly transformed, with the same mass and composition as the original benchmarks. This transformation is performed by conversion of the benchmark material specifications into the total mass of each isotope and then dividing the mass into the volume of the fuel and moderator to produce new fuel and moderator atom densities for use in the heterogeneous models. The overall model geometry remains unchanged, including conservation of total system volume, except for the changes in material specification within the fuel and moderator regions.

The mass of fuel and moderator for each system was determined using dimensional analysis. In each case, the atomic number density given in the benchmark specification for each isotope was multiplied by the volume of the cell(s) containing the isotope to determine its mass (Equation 5.1). Attention was given to conserving the total number of atoms during the transformation for each of the two regions of interest (fuel and moderator). Variations and uncertainties in these values could produce unwanted bias which could affect the results. Similarly, the original benchmark geometry was maintained during the transformations. Truncation of fuel regions by placement of the particles was evaluated early in the development of the transformation process and determined not to have a particular impact on the cases being evaluated, but it is recognized that similar transformations have produced notable bias in other work.

$$m^i = N_{material(benchmark)}^i \times V_{cell(benchmark)} \quad (5.1)$$

where:

- $m^i$  = mass for isotope  $i$  in the transformation
- $N_{material(benchmark)}^i$  = benchmark homogeneous material density for isotope  $i$
- $V_{cell(benchmark)}$  = benchmark cell volume containing the homogeneous material specification

For fuel (uranium isotopes), the total fuel mass is divided by an assumed material density (18.95 g·cm<sup>-3</sup>) to obtain the volume of fuel in the transformed system. The fuel volume is then divided by the volume of a 500 μm diameter sphere to obtain the number of spheres needed to complete the transformation to a regular lattice (Equation 5.2).

$$n_{fuel} = m_{fuel} \div 18.95 \text{ g} \cdot \text{cm}^{-3} \div 6.545\text{e-}05 \text{ cm}^3 \quad (5.2)$$

where:

- $n_{fuel}$  = number of fuel particles in the transformation
- $m_{fuel}$  = total fuel mass
- 18.95 g · cm<sup>3</sup> = assumed fuel density
- 6.545e-05 cm<sup>3</sup> = volume for a 500 μm diameter sphere

In parallel, the volume of the moderating material is obtained by subtracting the computed fuel volume from the total cell volume containing the homogenous fuel/moderator mixtures specified in the benchmarks. The moderator volume is then used to re-compute the material number densities of non-fuel isotopes.

$$N_{mod}^{transformed} = m_{mod}^{benchmark} \div (v_{total} - v_{fuel}) \quad (5.3)$$

where:

- $N_{mod}^{transformed}$  = number density of moderating material
- $m_{mod}^{benchmark}$  = computed mass of moderating material
- $v_{total}$  = total volume of cells containing homogeneous material specification
- $v_{fuel}$  = computed fuel volume

After the new material densities are computed, the benchmark models are modified by replacing the homogeneous material specifications with a repeated lattice of fuel spheres surrounded by the non-fuel moderating materials. The lattice parameter,  $x$ , is determined by dividing the number of fuel particles into the volume of the lattice and taking a cube root. This parameter establishes the size of an individual repeated cell within the lattice. The volume surrounding the fuel particle in the lattice is then filled with the material specification for the moderating material derived above. The modified cases are re-run in MCNP using 100,000 particles per generation over 550 cycles with the first 50 cycles discarded to ensure source convergence and minimize statistical error.

### 5.4.3 COMPARISONS

To determine the effect of the heterogeneity transformation, the unmodified benchmark model is compared to the transformed model using the effective multiplication parameter,  $k_{\text{eff}}$ . Nominally, the benchmark models have a  $k_{\text{eff}}$  of approximately 1.0, and it is expected that the introduction of heterogeneity will introduce a departure from the nominal value which can be demonstrated as the “heterogeneity effect”. This method is effective because the models have the same mass of fuel and moderating materials and the same general geometry, with the only change being the distribution of the fuel materials into discrete particles in a regular lattice, as opposed to a homogenized mixture of fuel and moderator.

### 5.4.4 CORRELATIONS

#### 5.4.4.1 GRAPHICAL ANALYSIS

After the differences in  $k_{\text{eff}}$  ( $\Delta k$ ) (Eq. 5.4) between the nominal and transformed models is determined, the resulting  $\Delta k$  is used to determine if there are useful correlations across several parameters. The first method used is graphical analysis. The parameters and  $\Delta k$  are plotted across the various cases to see if a visual correlation can be established. This method is useful to determine if there are first-order correlations, but it is also subject to bias in the way the data is presented. Careful selection of axes and scale are needed to ensure that false correlations are not established due to poor presentation of the data.

$$\Delta k = k_{\text{eff,benchmark}} - k_{\text{eff,modified}} \quad (5.4)$$

#### 5.4.4.2 MATHEMATICAL CORRELATIONS

To determine whether there are useful correlations using a more robust method, Pearson's correlation coefficient is used (Equation 5.5) [12]. The Pearson coefficient is a convenient measure which is used to determine whether or not a linear correlation exists between two sets of paired variables,  $x$  and  $y$ . The coefficient is generally interpreted as a measure of the strength of the linear relationship and gives a value between -1 and 1. A value of 0 indicates that there is no correlation in the observed values, and a value of 1 or -1 means that there is a perfect linear relationship.

$$r_{xy} = \frac{\sum_{i=1}^n (x_i - \bar{x})(y_i - \bar{y})}{\sqrt{\sum_{i=1}^n (x_i - \bar{x})^2} \sqrt{\sum_{i=1}^n (y_i - \bar{y})^2}} \quad (5.5)$$

where:

$r_{xy}$  = sample correlation coefficient

$n$  = sample size

$x_i$  =  $i$ -th value of sample  $x$

$\bar{x}$  = mean value of sample  $x$

$y_i$  =  $i$ -th value of sample  $y$

$\bar{y}$  = mean value of sample  $y$

Because the coefficient relies on sample size, there must be sufficient data from which to draw a conclusion regarding the existence or non-existence of a correlation within the population ( $\rho$ ). Consequently, there are computed critical values, based on sample size, above which it can be said with varying degrees of confidence that a correlation does, in fact, exist. These values have been computed and tabulated for use in these types of applications [13]. Based on the degrees of freedom in a given correlation, in this case  $N - 2$ , where  $N$  is the number of data pairs in the calculation, the value of the sample correlation coefficient,  $r_{obs}$  shows that the comparison is statistically correlated if it is greater than the computed critical value,  $r_{critical}$ . As an example from the reference, we set the null hypothesis,  $H_0$ , as "no correlation exists" or  $\rho = 0$ , and the alternative hypothesis,  $H_1$  as "the populations are correlated" or  $\rho \neq 0$ . The null hypothesis is rejected and the alternative hypothesis is accepted when the sample correlation coefficient exceeds the critical correlation coefficient.

$$H_0 : \rho = 0, H_1 : \rho \neq 0, \alpha = 0.05, df = 30$$

$$r_{critical} = \pm 0.3494; \text{ If } |r_{obs}| \geq |r_{critical}| \text{ then reject } H_0$$

where:

$H_0$	= null hypothesis
$H_1$	= alternative hypothesis
$\rho$	= population correlation coefficient
$\alpha$	= confidence interval
$r_{critical}$	= critical correlation coefficient
$r_{obs}$	= sample correlation coefficient

#### 5.4.4.3 APPLICATION OF PEARSON'S COEFFICIENT

Preliminary work not included in this report using Spearman's rank correlation showed that *some* correlation existed between the various paired variables, but that particular correlation does not provide information on the nature of the correlation. Selection of Pearson's coefficient for this work was primarily driven by the fact that it does not require particularly large data sets and was therefore appropriate given the availability of data. Importantly, note that the use of Pearson's coefficient to reveal linear correlations does not necessarily imply that there is a particular reason based in first principles that the relationship *should* be linear. Consequently, additional work evaluating the particular nature of the correlations between the paired variables is needed to determine the precise nature of the relationship. Such work, however, will require larger data sets than are currently available.

The use of Pearson's correlation coefficient in this work is applied in three ways. For data sets where the enrichment is constant throughout the set, the data are evaluated over all cases included in the set. This includes all cases of IEU-COMP-INTER-003, IEU-COMP-THERM-001, and IEU-COMP-THERM-015. The paired variables used in the correlation are the hydrogen-to-uranium ratio ( $H/U^{235}$ ) and the difference in  $k_{eff}$  ( $\Delta k$ ).

The second application of the correlation includes separate evaluations within the benchmark series IEU-COMP-MIXED-002, based on different enrichments. This data set is unique because it has variance in both  $H/U^{235}$  and in enrichment. Fortunately, the variations are consistent enough that there are sub-sets of data within this larger set that separate comparisons can be made. The first sub-set uses Cases 2 through 6 and the paired variables of  $H/U^{235}$  and  $\Delta k$  at an enrichment of 18.8 wt. % and the second sub-set uses the same paired variables for Cases 7-9 at 12.5 wt. %.

The third application of the correlation uses Cases 1, 2, 3, and 7 of IEU-COMP-MIXED-002 at an approximately constant  $H/U^{235}$  of 13.75 to 14.06. For this data set, the paired variables are enrichment

and  $\Delta k$ . Because of this opportunity, this data set is considered to be the most significant of the four in this work, despite the very small sample size.

## 5.5 RESULTS

### 5.5.1 MODELS AND TRANSFORMATIONS

The computed  $k_{\text{eff}}$  and  $\Delta k$  results for the nominal and transformed models are shown in Tables 5.1 through 5.4. Also shown is a summary of the  $H/U^{235}$  and enrichment for each evaluated case.

Table 5.1. IEU-COMP-INTER-003 Results and Parameters.

Case	Nominal $k_{\text{eff}}$	Transformed $k_{\text{eff}}$	$\Delta k$	$H/U^{235}$ ratio	$U^{235}/U$
ICI-003-01	$1.01194 \pm 0.00010$	$1.01219 \pm 0.00009$	0.00025	0.11	0.375
ICI-003-02	$1.01579 \pm 0.00010$	$1.01940 \pm 0.00010$	0.00361	0.11	0.375
ICI-003-03	$1.01659 \pm 0.00010$	$1.01700 \pm 0.00010$	0.00041	0.21	0.375
ICI-003-04	$1.01675 \pm 0.00011$	$1.01729 \pm 0.00011$	0.00054	1.35	0.375
ICI-003-05	$1.01568 \pm 0.00011$	$1.01632 \pm 0.00011$	0.00064	2.55	0.375
ICI-003-06	$1.01344 \pm 0.00012$	$1.01480 \pm 0.00011$	0.00136	6.14	0.375
ICI-003-07	$1.01625 \pm 0.00012$	$1.01716 \pm 0.00011$	0.00091	4.84	0.375
ICI-003-08	$1.01860 \pm 0.00012$	$1.01939 \pm 0.00012$	0.00079	4.82	0.375
ICI-003-09	$1.01192 \pm 0.00016$	$1.01169 \pm 0.00015$	-0.00023	4.75	0.375
ICI-003-10	$1.01430 \pm 0.00019$	$1.01489 \pm 0.00019$	0.00059	7.14	0.375
ICI-003-11	$1.01519 \pm 0.00013$	$1.01693 \pm 0.00013$	0.00174	10.58	0.375
ICI-003-12	$1.01499 \pm 0.00028$	$1.01608 \pm 0.00027$	0.00109	13.62	0.375
ICI-003-13	$1.01312 \pm 0.00013$	$1.01354 \pm 0.00013$	0.00042	16.60	0.375
ICI-003-14	$1.01316 \pm 0.00013$	$1.01357 \pm 0.00013$	0.00041	17.11	0.375

### 5.5.2 OBJECTIVE

The objective of this work is to establish whether or not correlations between  $H/U^{235}$  or enrichment and  $\Delta k$  resulting from heterogeneity exist, and to what degree the correlations, if any, exist. The computed results for the transformations and calculation of correlation coefficients are shown in Table 5.5. Similarly, the graphical representations of the evaluated parameters appear in the Figures.

Table 5.2. IEU-COMP-MIXED-002 Results and Parameters.

Case	Nominal $k_{\text{eff}}$	Transformed $k_{\text{eff}}$	$\Delta k$	H/U <sup>235</sup> ratio	U <sup>235</sup> /U
ICM-002-01	1.03231 $\pm$ 0.00031	1.03467 $\pm$ 0.00028	0.00236	13.98	0.3
ICM-002-02	1.03408 $\pm$ 0.00027	1.03675 $\pm$ 0.00027	0.00267	13.57	0.25
ICM-002-03	1.03659 $\pm$ 0.00027	1.03710 $\pm$ 0.00028	0.00051	13.65	0.188
ICM-002-04	1.02515 $\pm$ 0.00028	1.02477 $\pm$ 0.00026	-0.00038	16.36	0.188
ICM-002-05	1.02789 $\pm$ 0.00027	1.02909 $\pm$ 0.00027	0.00120	6.23	0.188
ICM-002-06	1.01573 $\pm$ 0.00021	1.01753 $\pm$ 0.00022	0.00180	2.60	0.188
ICM-002-07	1.02403 $\pm$ 0.00024	1.02512 $\pm$ 0.00025	0.00109	14.06	0.125
ICM-002-08	1.02845 $\pm$ 0.00026	1.02940 $\pm$ 0.00024	0.00095	14.32	0.125
ICM-002-09	1.00929 $\pm$ 0.00023	1.01054 $\pm$ 0.00024	0.00125	7.32	0.125

Table 5.3. IEU-COMP-THERM-001 Results and Parameters.

Case	Nominal $k_{\text{eff}}$	Transformed $k_{\text{eff}}$	$\Delta k$	H/U <sup>235</sup> ratio	U <sup>235</sup> /U
ICT-001-01	1.00247 $\pm$ 0.00012	1.00570 $\pm$ 0.00012	0.00323	7.92	0.2983
ICT-001-02	1.00343 $\pm$ 0.00012	1.00639 $\pm$ 0.00012	0.00296	15.85	0.2983
ICT-001-03	0.99870 $\pm$ 0.00013	1.00068 $\pm$ 0.00012	0.00198	31.69	0.2983
ICT-001-04	1.00031 $\pm$ 0.00012	1.00131 $\pm$ 0.00013	0.00100	63.38	0.2983
ICT-001-05	1.00711 $\pm$ 0.00011	1.00537 $\pm$ 0.00011	-0.00174	221.85	0.2983
ICT-001-06	1.00469 $\pm$ 0.00013	1.00688 $\pm$ 0.00012	0.00219	31.69	0.2983
ICT-001-07	1.00252 $\pm$ 0.00013	1.00466 $\pm$ 0.00012	0.00214	31.69	0.2983
ICT-001-08	1.00013 $\pm$ 0.00012	1.00212 $\pm$ 0.00012	0.00199	31.69	0.2983
ICT-001-09	1.00811 $\pm$ 0.00012	1.01057 $\pm$ 0.00012	0.00246	15.85	0.2983
ICT-001-10	1.00246 $\pm$ 0.00013	1.00540 $\pm$ 0.00012	0.00294	15.86	0.2983
ICT-001-11	1.00091 $\pm$ 0.00013	1.00396 $\pm$ 0.00012	0.00305	15.86	0.2983
ICT-001-12	1.00105 $\pm$ 0.00012	1.00368 $\pm$ 0.00012	0.00263	15.85	0.2983
ICT-001-13	1.00120 $\pm$ 0.00013	1.00205 $\pm$ 0.00013	0.00085	63.38	0.2983
ICT-001-14	1.00127 $\pm$ 0.00012	1.00231 $\pm$ 0.00013	0.00104	63.38	0.2983
ICT-001-15	1.00253 $\pm$ 0.00012	1.00317 $\pm$ 0.00012	0.00064	63.38	0.2983



Table 5.4. IEU-COMP-THERM-015 Results and Parameters.

Case	Nominal $k_{\text{eff}}$	Transformed $k_{\text{eff}}$	$\Delta k$	H/ $U^{235}$ ratio	$U^{235}/U$
ICT-015-01	$0.98168 \pm 0.00010$	$0.99016 \pm 0.00009$	0.00848	16.22	0.3014
ICT-015-02	$0.99801 \pm 0.00009$	$1.00083 \pm 0.00009$	0.00282	39.11	0.3014
ICT-015-03	$1.00072 \pm 0.00009$	$1.00380 \pm 0.00010$	0.00308	81.04	0.3014
ICT-015-04	$1.00099 \pm 0.00010$	$0.99923 \pm 0.00009$	-0.00176	8.13	0.3014
ICT-015-05	$0.99958 \pm 0.00009$	$0.99848 \pm 0.00008$	-0.00110	8.13	0.3014
ICT-015-06	$0.99987 \pm 0.00009$	$0.99982 \pm 0.00009$	-0.00005	16.22	0.3014
ICT-015-07	$0.99899 \pm 0.00009$	$1.00167 \pm 0.00008$	0.00268	16.23	0.3014
ICT-015-08	$0.99455 \pm 0.00010$	$1.01039 \pm 0.00009$	0.01584	39.11	0.3014
ICT-015-09	$0.99538 \pm 0.00009$	$1.00934 \pm 0.00009$	0.01396	39.11	0.3014
ICT-015-10	$0.99150 \pm 0.00009$	$1.00948 \pm 0.00009$	0.01798	39.11	0.3014
ICT-015-11	$0.99699 \pm 0.00009$	$1.01397 \pm 0.00009$	0.01698	81.04	0.3014
ICT-015-12	$0.98661 \pm 0.00010$	$1.01343 \pm 0.00009$	0.02682	81.04	0.3014
ICT-015-13	$0.99995 \pm 0.00009$	$1.01289 \pm 0.00009$	0.01294	81.04	0.3014
ICT-015-14	$0.99504 \pm 0.00008$	$1.01225 \pm 0.00010$	0.01721	81.04	0.3014
ICT-015-15	$0.99453 \pm 0.00008$	$1.01188 \pm 0.00009$	0.01735	81.09	0.3014
ICT-015-16	$0.99443 \pm 0.00009$	$1.00841 \pm 0.00009$	0.01398	81.24	0.3014
ICT-015-17	$0.99383 \pm 0.00009$	$1.00992 \pm 0.00009$	0.01609	81.24	0.3014
ICT-015-18	$0.99898 \pm 0.00010$	$1.00516 \pm 0.00009$	0.00618	81.24	0.3014
ICT-015-19	$1.00032 \pm 0.00010$	$1.00063 \pm 0.00008$	0.00031	8.12	0.3014
ICT-015-20	$0.99212 \pm 0.00010$	$1.00349 \pm 0.00008$	0.01137	8.12	0.3014
ICT-015-21	$0.99895 \pm 0.00010$	$0.99872 \pm 0.00008$	-0.00023	8.13	0.3014
ICT-015-22	$0.98830 \pm 0.00011$	$0.99849 \pm 0.00008$	0.01019	8.13	0.3014
ICT-015-23	$0.99536 \pm 0.00008$	$1.00197 \pm 0.00008$	0.00661	16.22	0.3014
ICT-015-24	$0.99454 \pm 0.00009$	$1.00122 \pm 0.00008$	0.00668	16.23	0.3014
ICT-015-25	$0.99223 \pm 0.00009$	$1.01128 \pm 0.00009$	0.01905	39.11	0.3014
ICT-015-26	$0.99401 \pm 0.00009$	$1.01301 \pm 0.00009$	0.01900	81.04	0.3014
ICT-015-27	$0.99795 \pm 0.00009$	$1.00717 \pm 0.00009$	0.00922	81.04	0.3014
ICT-015-28	$0.99722 \pm 0.00009$	$1.01351 \pm 0.00010$	0.01629	81.04	0.3014

### 5.5.3 CORRELATIONS USING H/U-235

#### 5.5.3.1 GRAPHICAL ANALYSIS

Figure 5.1 shows the paired data for  $H/U^{235}$  and  $\Delta k$  associated with IEU-COMP-INTER-003 at 37.5% enrichment. These data appear to have some correlation, but are not as well-paired as expected for a well-correlated system. Figures 5.2 and 5.3 show similar subsets of the data for IEU-COMP-MIXED-002 at 12.5% and 18.8% enrichment, respectively. These data do appear to be well-correlated based on the relative shape of each curve, but clearly there is only a modest amount of data in each subset from which to draw a conclusion. Figure 5.4 shows the paired data for IEU-COMP-THERM-001, which appears to be extremely well-correlated. In addition to the entire data set showing a graphical correlation, there are visible sub-sets in the data which could be extracted (Cases 1 through 5, for example) which might show an even stronger correlation than the entire data set. Finally, Figure 5.5 shows the paired data for IEU-COMP-THERM-015 at 30.14% enrichment. These data show that a correlation probably exists, but is again, not clearly well-correlated.

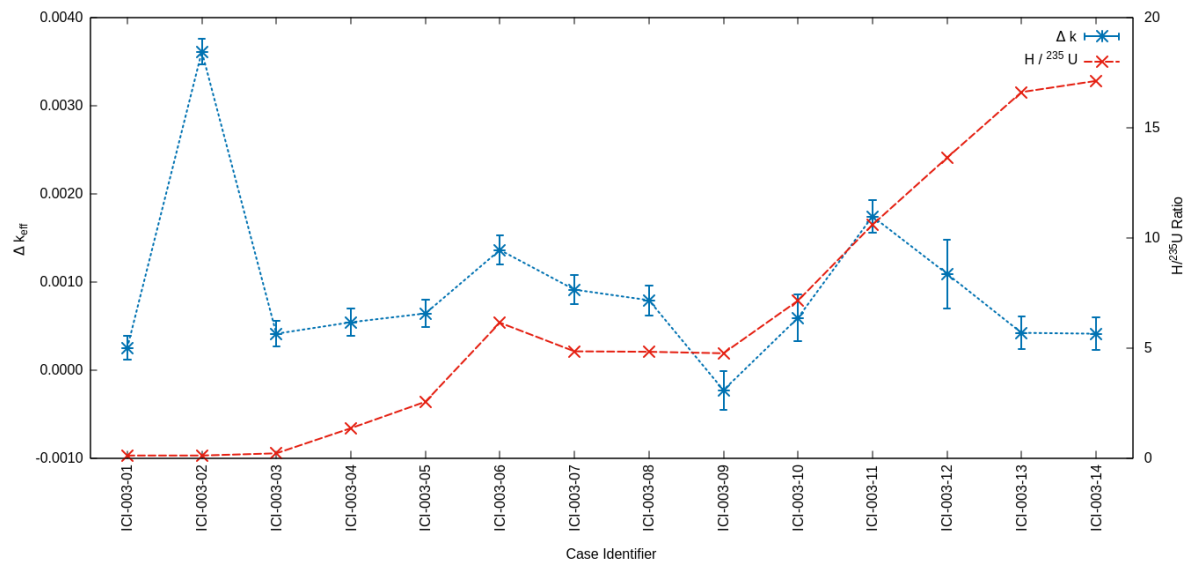


Figure 5.1. A graph showing Delta- $k_{\text{eff}}$  and  $H-^{235}\text{U}$  ratio by case number for the IEU-COMP-INTER-003 data set with 37.5 percent uranium enrichment.

Figure 5.6 shows the subset of data that are compared using enrichment as a parameter instead of  $H/U^{235}$ . While the data show that there may be a correlation, it is not entirely clear from the graphical analysis that such a correlation exists or not. Two scatterplots of data are shown in Figures 5.7 and 5.8. These plots are included for completeness, to show that the IEU-COMP-INTER-003 data set does

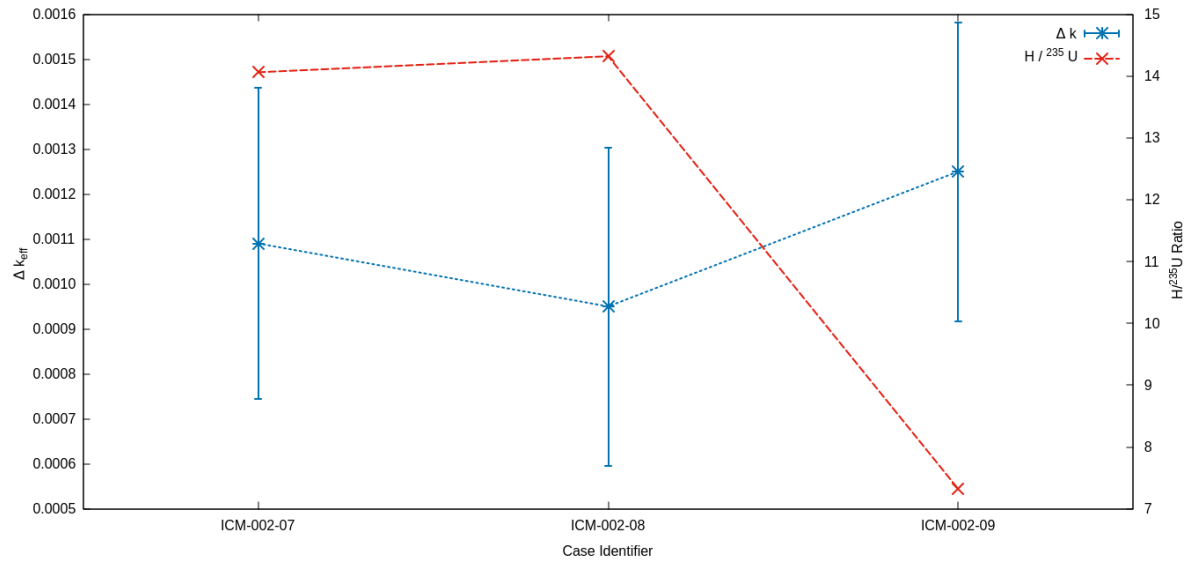


Figure 5.2. A graph showing  $\Delta k_{\text{eff}}$  and  $\text{H-}^{235}\text{U}$  ratio by case number for a portion of the ICM-002 data set with 12.5 percent uranium enrichment.

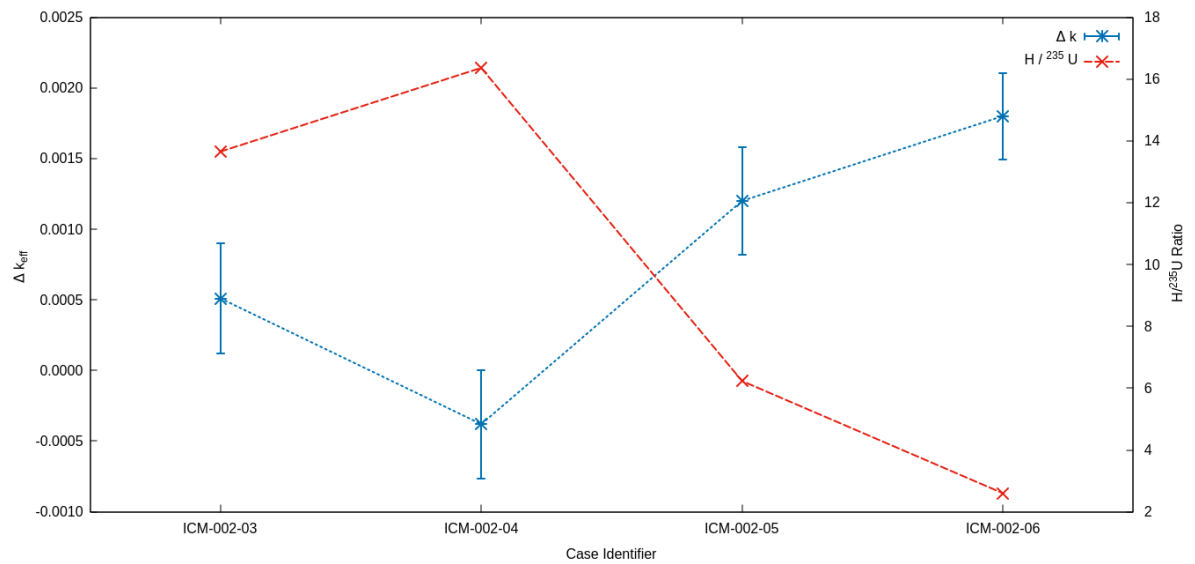


Figure 5.3. A graph showing  $\Delta k_{\text{eff}}$  and  $\text{H-}^{235}\text{U}$  ratio by case number for a portion of the ICM-002 data set with 18.8 percent uranium enrichment.

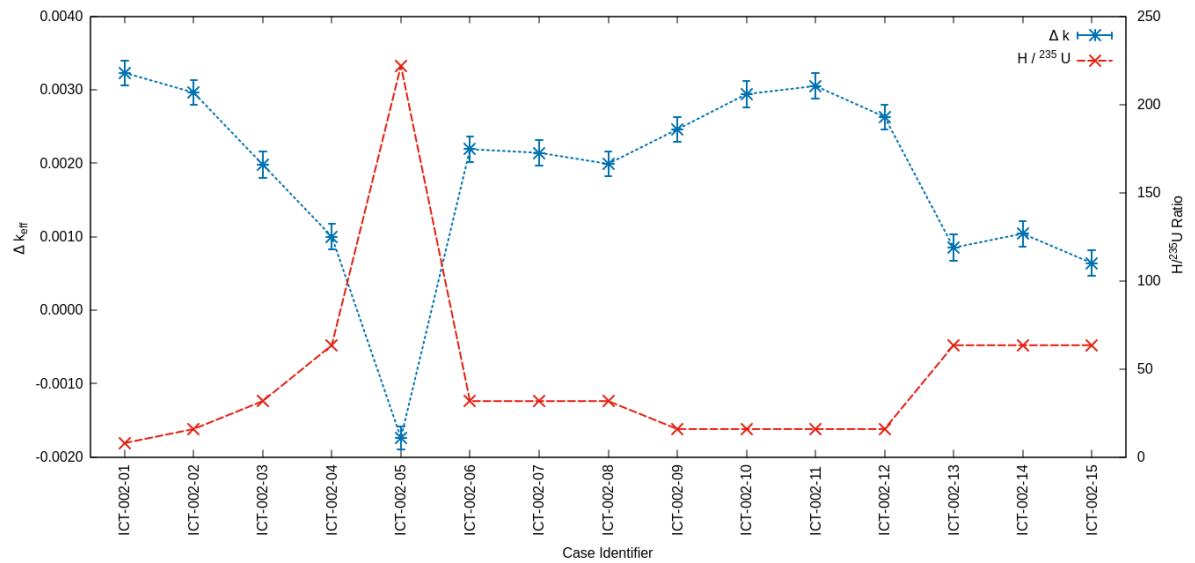


Figure 5.4. A graph showing Delta- $k_{\text{eff}}$  and  $H\text{-}^{235}\text{U}$  ratio by case number for a portion of the ICT-001 data set with 29.83 percent uranium enrichment.

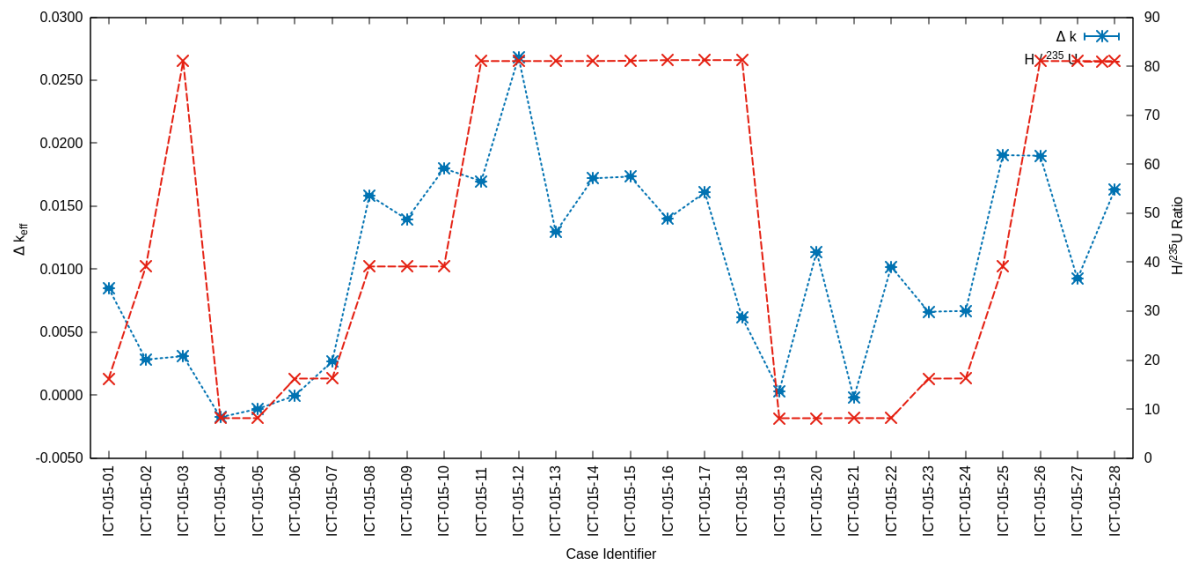


Figure 5.5. A graph showing Delta- $k_{\text{eff}}$  and  $H\text{-}^{235}\text{U}$  ratio by case number for a portion of the ICT-015 data set with 30.14 percent uranium enrichment.

not appear to have any correlation, and that the IEU-COMP-MIXED-002 enrichment correlation is more strongly supported by the graphical analysis scatterplot tool than by a side-by-side comparison of parameters.

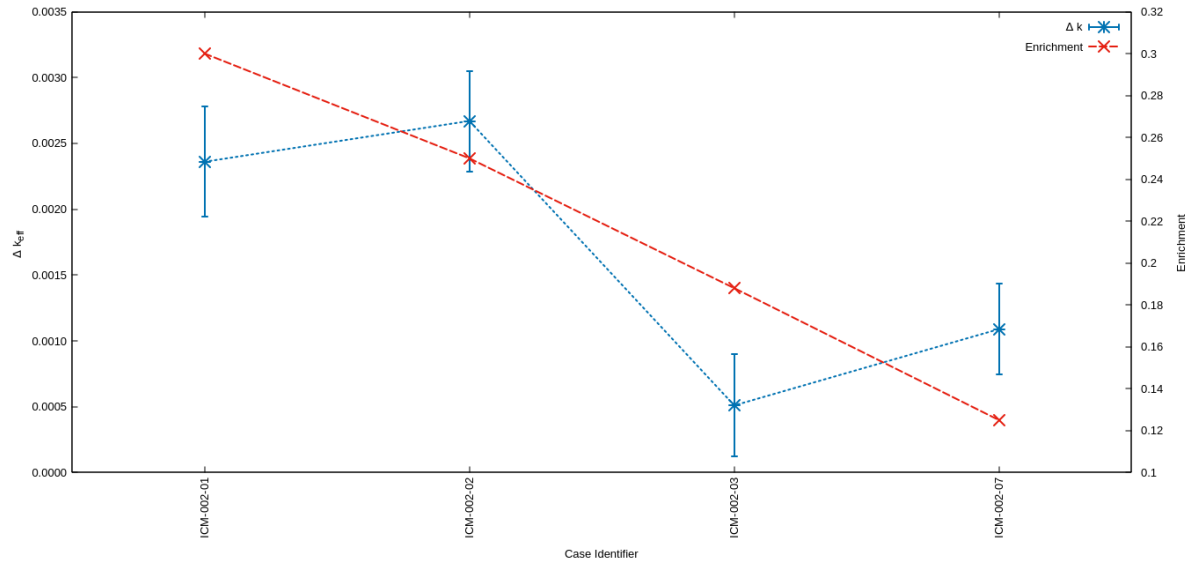


Figure 5.6. A graph showing Delta- $k_{\text{eff}}$  and Uranium Enrichment by case number for a portion of the ICM-002 data set.

## SCATTERPLOTS

### 5.5.3.2 CORRELATION COEFFICIENTS

As shown in Table 5.5, several of the evaluated cases are very well correlated. IEU-COMP-THERM-001 and IEU-COMP-THERM-015 have computed Pearson's coefficients that greatly exceed the critical value with a 99.9% confidence interval. Similarly, and despite the small data set, IEU-COMP-MIXED-002 Cases 3-6 (18.8% enrichment) exceeds its critical value at the 95% confidence interval. These results align closely with the expectations produced from the graphical analysis, Figures 5.4, 5.5, and 5.2. The other IEU-COMP-MIXED-002 data sets show some *potential* to be correlated, but did not exceed the critical value at the 80% confidence interval. Consequently, it is plausible that a correlation exists in these data sets, but there is not sufficient data to clearly establish such a correlation. The final data set, IEU-COMP-INTER-003 clearly has a very low or no correlation. Its very small correlation coefficient combined with the low critical value due to its relatively large sample size show with a high degree of confidence that a correlation does not exist for this data set.

<sup>1</sup>The R-value is statistically significant when greater than or equal to the critical value for the given confidence interval. The critical values are determined based on the number of samples within the population and are tabulated in [13]. The

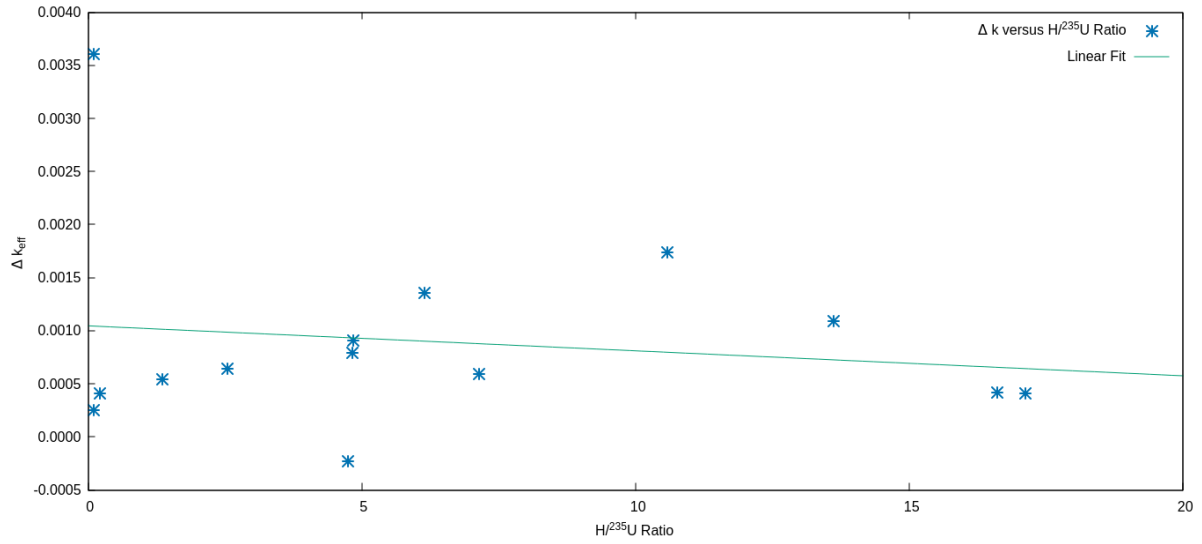


Figure 5.7. A scatterplot showing Delta-k<sub>eff</sub> and H-<sup>235</sup>U ratio by case number for a portion of the ICI-003 data set with 37.5 percent uranium enrichment.

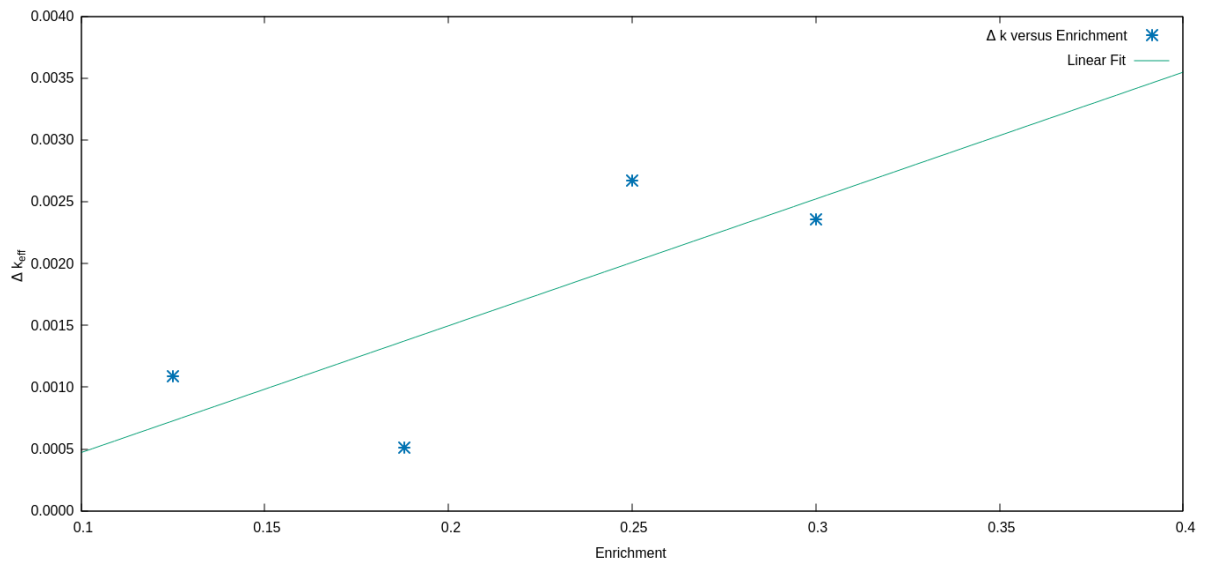


Figure 5.8. A scatterplot showing Delta-k<sub>eff</sub> versus Uranium Enrichment for a portion of the ICM-002 data set..

Table 5.5. Correlation Results.

Benchmark Series	Cases	Variables	R-Value	Critical Values <sup>1</sup>		
				0.2	0.05	0.001
IEU-COMP-INTER-003	1-14	H/U <sup>235</sup> to $\Delta k$	-0.14723	0.3646	0.5324	0.7800
IEU-COMP-MIXED-002	3-6	H/U <sup>235</sup> to $\Delta k$	-0.97393	0.8000	0.9500	0.9990
IEU-COMP-MIXED-002	7-9	H/U <sup>235</sup> to $\Delta k$	-0.89959	0.9511	0.9969	0.9999
IEU-COMP-MIXED-002	1-3 and 7	Enrichment to $\Delta k$	0.75872	0.8000	0.9500	0.9990
IEU-COMP-THERM-001	1-15	H/U <sup>235</sup> to $\Delta k$	-0.94552	0.3507	0.5140	0.7604
IEU-COMP-THERM-015	1-28	H/U <sup>235</sup> to $\Delta k$	0.62058	0.2546	0.3809	0.5974

## 5.6 DISCUSSION

### 5.6.1 THE HETEROGENEITY EFFECT

The results of this work demonstrate that, for the evaluated critical systems, a meaningful heterogeneity effect exists when the homogeneous material specifications are modestly transformed into equivalent-mass heterogeneous systems. The separation of fuel mass from the moderator mass and subsequent rearrangement produced in nearly all cases a change in the multiplication factor of the system. This result demonstrates a fact that is relatively well known in nuclear criticality safety that a heterogeneous system is substantially different in its nuclear characteristics from a homogeneous system. The fact that this phenomenon can be demonstrated using existing evaluations of critical benchmarks should be considered valuable as an observation in itself. A word of caution, however, on this point should be emphasized. The evaluated critical benchmarks documented in the ICSBEP handbook have been thoroughly reviewed and vetted; manipulations which create models which are similar but are substantially different should be carefully evaluated before use in practical nuclear criticality safety work. As an academic tool, however, the use of evaluated benchmarks in this manner should be encouraged to exploit the opportunity of using past critical experiments to explore and demonstrate real nuclear phenomena (such as the effect of heterogeneity).

### 5.6.2 INTERPRETATIONS OF CORRELATION

The primary objective of this work is to establish whether or correlations exist between the magnitude of the heterogeneity effect and other nuclear parameters of the evaluated systems. In this regard, this

---

critical values listed correspond to an 80, 95, and 99.9 percent probability that the paired values under evaluation are linearly correlated.

work is resoundingly successful. Using graphical analysis and mathematical correlations, it is shown that there is a relationship between the magnitude of the heterogeneity effect and the  $H/U^{235}$  ratio in these systems, and there is *probably* a relationship between the magnitude of the effect and enrichment. Interestingly, however, the effect does not appear to be correlated at the highest enrichment in the examination range.

In support of this observation, examination of the minimum critical mass for uranium systems as shown in the literature [14] shows that a convergence between homogeneous and heterogeneous systems is likely. Figure 5.9 is a graph showing the minimum critical mass for three types of systems: unreflected spheres, reflected homogeneous spheres, and reflected heterogeneous spheres. The data shown on the graph are values derived from historical experimental data and associated interpolations and extrapolations. Of particular interest is the bottom dashed line, which shows an extrapolation beyond five percent enrichment. If this particular extrapolation is accurate, it would indicate that the homogeneous and heterogeneous systems converge at some point. Comparison on a volume basis, however, shows a different story. Figure 5.10 shows the minimum critical volume over the same range of enrichment. It is readily apparent that, on a volume basis, the heterogeneity effect should always be present because the interpolated graphs for homogeneous and heterogeneous systems never converge.

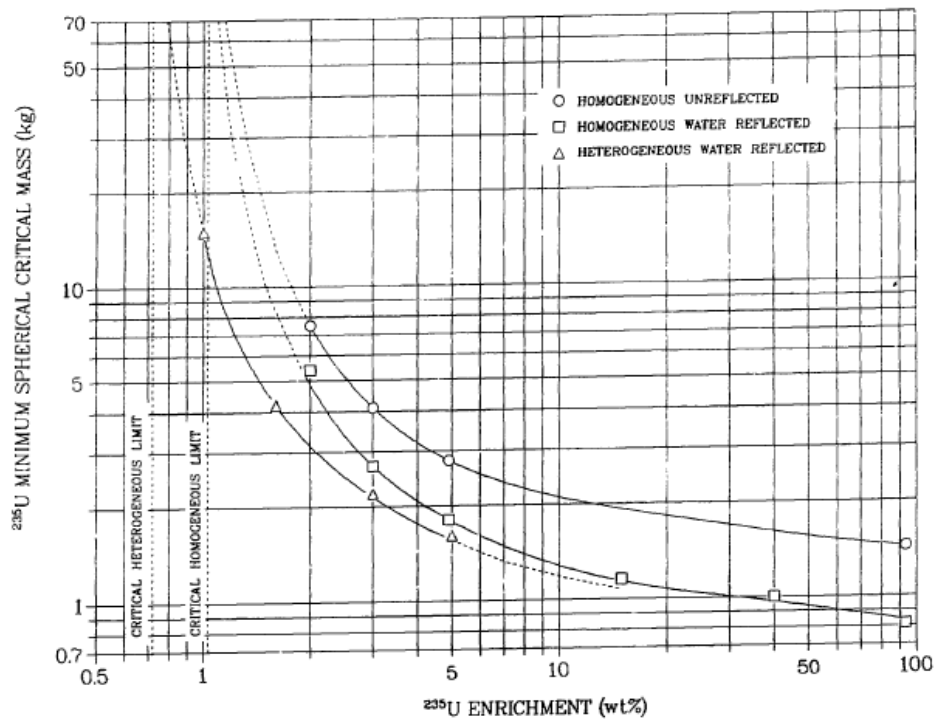


Figure 5.9. Figure 22 from LA-10860, showing the minimum critical mass of uranium systems over the full range of enrichment.



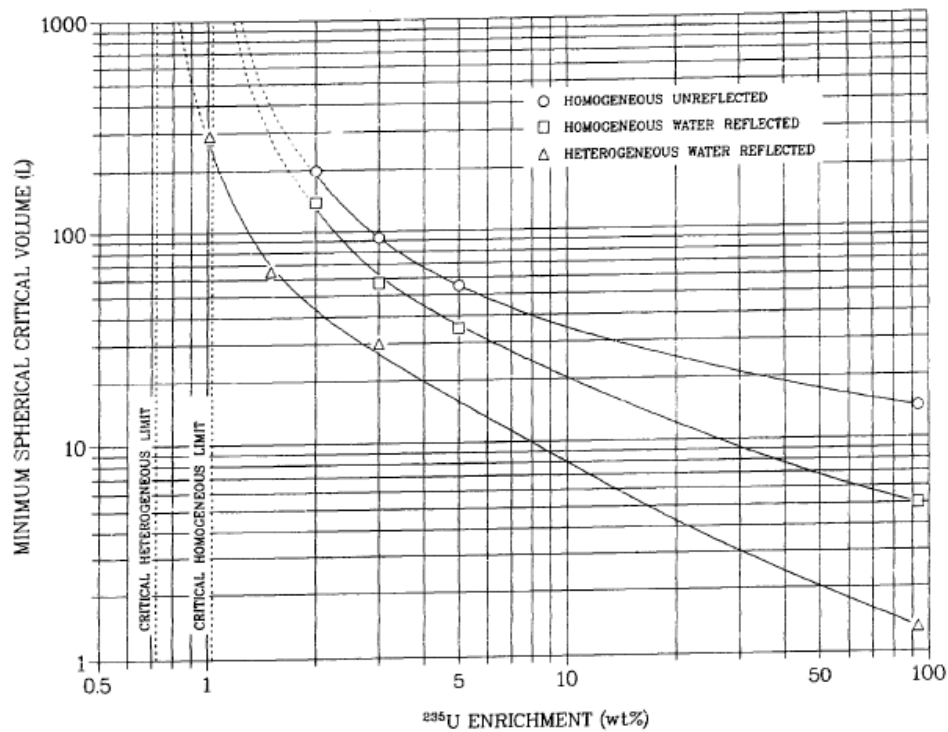


Figure 5.10. Figure 23 from LA-10860, showing the minimum critical volume of uranium systems over the full range of enrichment.

For further discussion on this point, we turn to Anomalies of Nuclear Criticality, Section 8 [15]. In this section, a discussion exists that asserts that above 34% enrichment, heterogeneous systems are bounded in critical volume by equivalent-mass single-unit systems. Figure 5.11 shows the minimum critical volume for homogeneous and heterogeneous systems of uranium and water over a range of enrichment, which is equivalent to Figure 5.10 with the added curve showing the volume of single-unit metal systems. The important feature on this figure is the transition point, which occurs at 34% enrichment. For enrichments higher than this value, heterogeneity appears to become strongly dependent on the presence of moderator. If Figures 5.10 and 5.11 are overlaid, one would see that the curves of Figure 5.10 extend into the region to the right and above the single-unit curve in Figure 5.11. Based on this information, one would expect that a low-moderation system would behave more like a single unit and would be insensitive to small changes in mass distribution, and for a higher-moderation system, there could be a large difference, similar to Figure 5.10. This behavior is borne out by the lack of correlation for the IEU-COMP-INTER-003 system. Based on the higher enrichment and relative lack of moderation, this particular system behaves more like the single-unit system presented in Figure 5.11, rather than the systems shown in Figure 5.10. A re-examination of Figure 5.1 using a different perspective shows that the  $\Delta k$  for the entire series is actually relatively constant despite the change in  $\text{H}/\text{U}^{235}$  ratio, which would

be expected for a system that is generally insensitive to heterogeneity. It is possible that, if a similar system were evaluated at higher levels of moderation, a correlation would emerge. This observation serves to reinforce the position that the heterogeneity effect in HALEU systems is worthy of further study and consideration, particularly by expanding the range of evaluation and correlations discovered in the course of this work.

## 5.7 FUTURE WORK

Clearly, there is an abundance of future work created by these results. A more thorough examination of the ICSBEP handbook for other useful benchmark evaluations would be a logical next step. Additionally, the creation of systematic and regular (in the geometric sense) models specifically designed for a more comprehensive look into the correlations between moderator ratio and enrichment and heterogeneity would likely produce a wealth of useful and interesting data. Such a systematic approach could be used to fill in the gaps, so to speak, in the evaluated benchmark data and confirm or disprove the probable, but inconclusive, correlations discovered herein. Of particular interest would be extension of the IEU-COMP-INTER-003 system to higher values of H/U-235 ratio to see if there is a particular cutoff in this ratio where the correlation disappears.

Similarly, expansion of the method discussed in this work to include an evaluation of correlations between the heterogeneity effect and other neutron spectral indices is planned. Given that the systems evaluated in this work are under-moderated, it is entirely possible that other indications, such as ANECF or a more detailed examination of the entire neutron energy spectrum, would produce stronger correlations or may give rise to further discovery. Additional parametric studies which may be considered are variations in particle size, particle distribution, and fuel density which may influence the presence or strength of the observed correlations. These parametric studies may be useful for modeling specific fuel types, such as those which utilize small particles embedded in a moderator matrix by design.

Further development of the nature of the correlations will be conducted. As discussed in Section 5.4.4.3, the use of Pearson's coefficient is a rather crude tool which is primarily used for linear correlations. It is highly likely that the particular relationship of the paired variables in this evaluation is non-linear, which means more advanced correlation techniques would be useful. Development of larger data sets for this purpose will be needed. These data could then be used to establish useful guidelines for nuclear criticality safety professionals as the nuclear industry graduates from low-enriched to high-assay, low-enriched fuel in the twenty-first century.

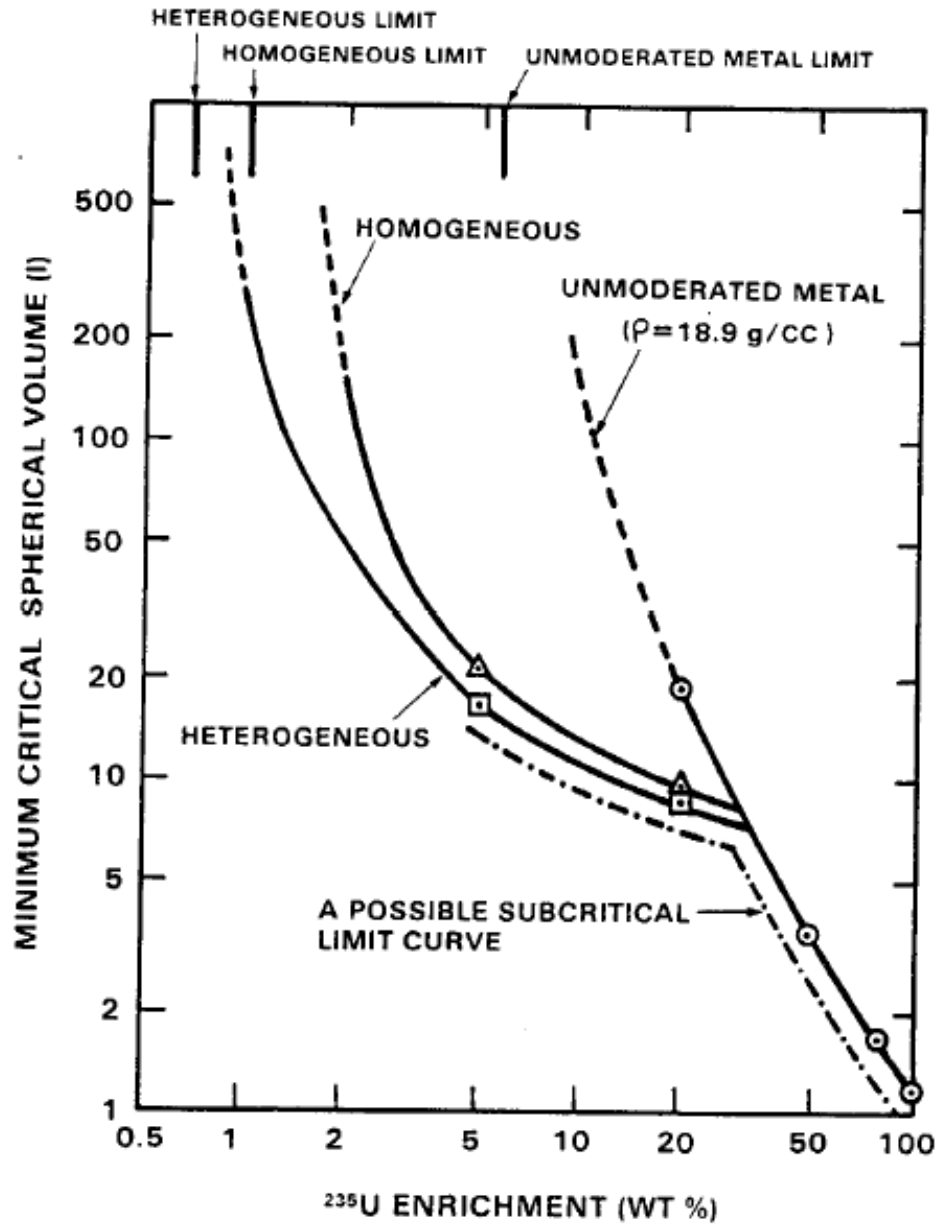


Figure 11. Minimum Critical Volume vs. Uranium Enrichment

Figure 5.11. Figure 11 from PNNL-19176, showing the minimum critical volume of homogeneous and heterogeneous uranium-water systems over the range of enrichment.

## 5.8 SUMMARY REMARKS

Major results and implications include -

- The heterogeneity effect in HALEU systems was confirmed using slightly-modified evaluated criticality safety benchmarks;
- A correlation between the moderator ratio ( $H/U^{235}$ ) and the magnitude of the heterogeneity effect was confirmed in the evaluated systems;
- A correlation between enrichment and the magnitude of the heterogeneity effect is strongly suspected, but could not be confirmed;
- The heterogeneity effect disappears in the system evaluated at 37.5%, which is consistent with expectations.

As part of the goals of this work, it was desired to determine if, using an evaluated benchmark model, useful models could be generated to evaluate the effect of heterogeneity in HALEU systems. This work demonstrates that this goal was successful. Evaluated benchmark models were modified to introduce a small degree of heterogeneity which produced new values of the effective multiplication factor,  $k_{\text{eff}}$ , that were used to produce correlated results between the new models and the baseline benchmark models. Success in accomplishing this goal shows that there are potentially many more uses for evaluated benchmark experiments beyond the typical use of validation of nuclear data and modeling codes.

The correlation established in this work between the moderator ratio ( $H/U^{235}$ ) and the magnitude of the heterogeneity effect is extremely important in two ways: (1) it shows that there is not an easily discernible rule which can be generally applied to these systems, such as that suggested in the literature ("heterogeneous systems have lower critical volume than homogeneous systems"), and (2) it shows that there is much more information which can be gleaned from this particular type of evaluation. In particular, the bias generated during the benchmark evaluation process as systems are homogenized or de-homogenized is generally not captured as part of the evaluation. This research strongly suggests that the nuclear criticality safety community would be well-served to expand the evaluation of such biases and to include them as supplemental information during the benchmark evaluation process.

Similarly, it appears as though there may be a similar set of arguments for the correlation between heterogeneity and enrichment, but this work did not produce sufficient statistical evidence to definitively show that such a correlation exists. The implication here is that more work is necessary to determine whether or not such a correlation exists.

Finally, the moderator ratio correlation disappeared in cases evaluated above 37.5% enrichment,

which was consistent with expectations following the literature review. This work provides more supporting evidence that there is, indeed, a “breakpoint” in enrichment above which nuclear criticality safety rules can safely ignore the effects of system heterogeneity. While this observation is not particularly relevant for HALEU applications, it may become much more significant as more advanced fuels are explored in the future.

## REFERENCES

- [1] Joseph A. Christensen and R. A. Borrelli. “Evaluations of the Effect of Heterogeneity in HALEU Systems Using Modified Critical Benchmarks”. In: *Nuclear Science and Engineering* 196.11 (2022), pp. 1333–1348. DOI: 10.1080/00295639.2022.2087832. eprint: <https://doi.org/10.1080/00295639.2022.2087832>. URL: <https://doi.org/10.1080/00295639.2022.2087832>.
- [2] Joseph A. Christensen and R. A. Borrelli. “Nuclear Criticality Safety Aspects for the Future of HALEU: Evaluating Heterogeneity in Intermediate-Enrichment Uranium Using Critical Benchmark Experiments”. In: *Nuclear Science and Engineering* 195.3 (2021), pp. 300–309. DOI: 10.1080/00295639.2020.1819143. eprint: <https://doi.org/10.1080/00295639.2020.1819143>. URL: <https://doi.org/10.1080/00295639.2020.1819143>.
- [3] Joseph A. Christensen and R. A. Borrelli. “Parametric Study of Minimum Critical Volume for High-Assay Low-Enriched Uranium (20%) in Spherical Geometry Against Particle Size”. In: *Nuclear Science and Engineering* 196.1 (2022), pp. 98–108. DOI: 10.1080/00295639.2021.1940066. eprint: <https://doi.org/10.1080/00295639.2021.1940066>. URL: <https://doi.org/10.1080/00295639.2021.1940066>.
- [4] Nuclear Energy Agency. *International Handbook of Evaluated Criticality Safety Benchmark Experiments*. NEA No. 7520. Paris: OECD Nuclear Energy Agency, July 2020.
- [5] Karla R. Elam. *Unreflected UF<sub>4</sub>-CF<sub>2</sub> blocks with 37.5% <sup>235</sup>U*. In: *International Handbook of Evaluated Criticality Safety Benchmark Experiments*. [DVD]. Tech. rep. IEU-COMP-INTER-003. Nuclear Energy Agency, 2019.
- [6] Karla R. Elam. *Unreflected UF<sub>4</sub>-CF<sub>2</sub> blocks with uranium of 30, 25, 18.8, and 12.5% <sup>235</sup>U*. In: *International Handbook of Evaluated Criticality Safety Benchmark Experiments*. [DVD]. Tech. rep. IEU-COMP-MIXED-002. Nuclear Energy Agency, 2019.
- [7] Virginia F. Dean. *Critical arrays of polyethylene-moderated U(30)F<sub>4</sub>-polytetrafluoroethylene one-inch cubes*. In: *International Handbook of Evaluated Criticality Safety Benchmark Experiments*. [DVD]. Tech. rep. IEU-COMP-THERM-001. Nuclear Energy Agency, 2019.
- [8] James P. Dyrda, Nigel P. Tancock, and Matthew D. Eaton. *Single cores of 30.14% <sup>235</sup>U enriched UO<sub>2</sub>/wax mixtures—bare and with single reflector materials*. In: *International Handbook of Evaluated Criticality Safety Benchmark Experiments*. [DVD]. Tech. rep. IEU-COMP-THERM-015. Nuclear Energy Agency, 2019.

- [9] C.J. Werner, et al. *MCNP6.2 Release Notes*. Tech. rep. LA-UR-18-20808. Los Alamos National Laboratory, 2018.
- [10] C.J. Werner (ed.) *MCNP Users Manual - Code Version 6.2*. Tech. rep. LA-UR-17-29981. Los Alamos National Laboratory, 2017.
- [11] D.A. Brown et al. “ENDF/B-VIII.0: The 8th Major Release of the Nuclear Reaction Data Library with CIELO-project Cross Sections, New Standards and Thermal Scattering Data”. In: *Nuclear Data Sheets* 148 (2018). Special Issue on Nuclear Reaction Data, pp. 1–142. ISSN: 0090-3752. DOI: <https://doi.org/10.1016/j.nds.2018.02.001>. URL: <https://www.sciencedirect.com/science/article/pii/S0090375218300206>.
- [12] David Freedman, Robert Pisani, and Roger Purves. “Statistics (international student edition)”. In: *Pisani, R. Purves, 4th edn. WW Norton & Company, New York* (2007).
- [13] Bart L. Weathington, Christopher J.L. Cunningham, and David J. Pittenger. *Understanding Business Research*. First. John Wiley & Sons, Inc., 2012.
- [14] H. C. Paxton and N. L. Pruvost. *Critical dimensions of systems containing  $^{235}\text{U}$ ,  $^{239}\text{Pu}$ , and  $^{233}\text{U}$* . Tech. rep. LA-10860-MS. Los Alamos National Laboratory, 1987.
- [15] Clayton, E.D. *Anomalies of Nuclear Criticality*. Tech. rep. PNNL-19176. Pacific Northwest Laboratory, 2010.

## CHAPTER 6: SUMMARY AND CONCLUSIONS

### 6.1 SUMMARY AND CONCLUSIONS

#### 6.1.1 ESTABLISH RESEARCH BASELINE FOR USE OF NUCLEAR CRITICALITY SAFETY BENCHMARKS

In Chapter 2, specific objectives were established and achieved. The primary purpose of this work was to establish a baseline understanding of the nature and scope of a heterogeneous nuclear system. This scope was accomplished by the formal evaluation of an historical critical experiment and documentation of the results of this evaluation in the ICSBEP handbook.

The specific experiment selected for this benchmark was a system of LEU fuel rods in water. Using the available experimental records and informed assumptions, a detailed model of the system of experimental configurations was developed in the neutronics modeling code MCNP and the particular characteristics of the experimental system were examined using perturbation of experimental parameters to determine the effect on the measured  $k_{\text{eff}}$ . After the experiments and associated uncertainty were evaluated, a simplified benchmark model of the experiment was built and simplification biases were quantified. The benchmark  $k_{\text{eff}}$  and experimental  $k_{\text{eff}}$  were compared across a number of similar neutronics codes and data libraries and were found to be satisfactory. The overall results of the project are shown in Tables 2.46 and 2.47.

This work created the opportunity for further exploration of the effect of heterogeneity in uranium-water systems in two ways. The first is that it demonstrates a method by which a systematic evaluation of experimental uncertainty and simplification of experimental models can create a useful baseline for further analysis. The second way is that it revealed, during the simplification process, that there is a connection between the experimental parameter of hydrogen-to-uranium ratio (H/U) and the bias introduced when converting the detailed model to the simplified model. Initially, during this process, the bias introduced when attempting to homogenize the discrete model into a uranium-water mixture was deemed to be large and therefore unacceptable under the guidelines of the benchmark evaluation project. Upon closer examination, however, it was observed that the bias was dependent on physical experimental parameters and should encourage additional consideration. This observation led to further examination and the additional work performed throughout this project.



### 6.1.2 COMPLETE AN EVALUATION OF HISTORICAL DATA TO DEMONSTRATE THE EFFECTS OF HETEROGENEITY

The work performed for Chapter 3 closely examined several parameters important to NCS that are particularly relevant to heterogeneity. This work focused specifically on HALEU due to its renewed importance in the industry and the increased potential, described in the literature, for criticality accidents in fuel cycle facility applications. The work documented in this chapter shows a method by which a detailed examination of heterogeneity in uranium-water systems can be performed in a generalized model, and it compares the results of the methodology to results published in literature.

In particular, two specific parameters found in the literature were explored. A frequently-encountered value for particle size, 127  $\mu\text{m}$ , is considered the ‘breakpoint’ between a homogeneous and a heterogeneous uranium-water system. The second parameter is the ratio between equivalent-mass homogeneous and heterogeneous system critical volume. This ratio can be used in NCS applications to establish safe handling volumes for systems whose homogeneous critical parameters are known, but may be subject to heterogeneity through changes in process conditions.

The method and results used in this chapter largely confirm the results found in the literature at a higher degree of precision. It was determined that the particle size limit was likely to be an overly conservative extrapolation of experimental results and lacked some foundational basis. It was also determined that the safety margin recommendations found in some literature for the volume ratio are sufficient for safety, but may have the potential to be relaxed if sufficient additional evidence is developed.

The determination of the minimum critical volume for twenty percent enriched LEU (HALEU) using the method described in this chapter matches the literature well for homogeneous cases. Similarly, the particle size at which the distinction between the homogeneous cases and the heterogeneous case is in the appropriate range to match the experiment which forms the basis for the current recommendation. These factors effectively validate the method and support its extension to the specific determination of the minimum volume for heterogeneous systems, which satisfies a particular need in the current NCS methodology.

### 6.1.3 INVESTIGATE THE EFFECTS OF HETEROGENEITY USING CRITICAL BENCHMARKS

In Chapters 4 and 5, the algorithms and applications developed in Chapter 3 are applied to critical benchmark experiments found in the ICSBEP handbook [1] within the parametric range of interest.

### 6.1.3.1 IDENTIFY CANDIDATE BENCHMARKS

Chapter 4 defines the selection criteria used to down-select benchmarks from the handbook. In particular, the criteria are used to select benchmarks with specific parameters which were likely to generate useful data following application of the heterogeneity algorithms. Of the thousands of available benchmarks, only a handful met the desired selection criteria. This step was necessary because the evaluation of heterogeneity effects in critical systems relies on known “good” data from critical experiments and the quantified uncertainty from the benchmark evaluation process to ensure relevant data are generated. It is fortunate that sufficient candidate benchmark evaluations were available for this analysis, but the relative scarcity of qualifying benchmarks highlights the need for more work in this area.

### 6.1.3.2 EVALUATE SELECTED BENCHMARKS

Finally, in Chapter 5, the methodology developed in Chapter 3 for evaluation of a generalized HALEU system is directly applied to evaluated critical benchmarks. In this chapter, heterogeneity is induced in the models by replacement of homogeneous fuel-moderator regions with equivalent-mass heterogeneous regions with a particle size known to induce changes in  $k_{\text{eff}}$  in the general model, 500  $\mu\text{m}$ . The difference in multiplication factor is measured between the homogeneous and heterogeneous models and evaluations are conducted. The first evaluation was graphical analysis, which is a *prima facie* (“at first glance”) approach relying on subjective judgement to identify visual correlations. While powerful, this approach is subject to certain biases in how the data are presented. To combat these biases, rigorous statistical analysis were applied to the data to ensure the visual correlations are sufficiently reliable to present conclusions. For this approach, Pearson’s coefficient is used to measure the degree of linear correlation between the parameters of interest.

The results of the graphical analysis were visually very interesting and showed a generally high degree of correlation between the heterogeneity bias and two parameters, the enrichment of the system and the moderator-to-fuel ratio. The corresponding statistical analysis using Pearson’s coefficient largely confirmed the graphical analysis, but not with a high degree of certainty in all cases. The general conclusion is that there is a correlation between the heterogeneity bias and both enrichment and the moderator-to-fuel ratio, but this was not statistically confirmed in all the evaluated cases, primarily due to limited data availability. Therefore, it is possible that the correlated cases are not in the general case and can be dismissed, but it is also possible, and more likely based on the graphical analysis, that there is in fact a strong correlation which would be revealed when more data are made available.

## 6.2 IMPLICATIONS AND APPLICATIONS

The immediate effects of this work are threefold. Improved precision and accuracy regarding the particular details of heterogeneity for HALEU applications are an obvious improvement to the decades-old NCS guidance that exists in the literature today. The particle-size threshold of 127  $\mu\text{m}$  is a useful tool for practitioners of NCS, but the newly-created knowledge that there exists some observable margin between this recommended value and the value (400  $\mu\text{m}$ ) obtained in the course of this work may prove useful when conducting analyses of nuclear processes moving forward. Similarly, having additional data on the minimum critical volume for twenty-percent enriched systems, both homogeneous and heterogeneous, and the method by which the data were generated, is certainly going to improve the reliability of safety analysis work for these systems.

The second way this work is bound to have an immediate impact is by creating the realization that there is a tremendous opportunity for improved data generation and collection across the entire spectrum of enrichment for these systems. The work generated in Chapter 3 interfaces with the drawing shown from *Anomalies* [2] directly at the twenty-percent enrichment point. If one considers the minimum critical volume shown in Figure 3.5 and rotate it to intersect with Figure 3.1 at twenty-percent enrichment, it can be easily observed that there is a tremendous amount of space in which similar analysis can be conducted across the entire range of enrichment from, at least, six to thirty-four percent. Such an analysis, especially if it were maintained in a reliable database, would be absolutely invaluable to NCS analysts.

Finally, the presentation of this work should highlight for nuclear safety professionals the dire need for improved quality and quantity of data for NCS. While this work is not intended as a criticism of ongoing efforts to preserve and develop nuclear experimental data through efforts such as the ICSBEP, it is apparent that there is much more work that *can* be done in this area. Development and collection of correlation data for experimental parameters, and not just a binary view of acceptable or unacceptable simplification biases should be a priority for anyone working in this field. The experimental facilities available in the mid-twentieth century are, quite literally, history and are unlikely to return. Therefore, the collection, preservation, and analysis of any and all available data which can be used to ensure the safe development of nuclear technology through the next century must be an absolute priority. This work creates a pathway by which existing data can be used to expand and evaluate even limited experimental data into useful conclusions for NCS applications.

### 6.3 FUTURE WORK

Several obvious follow-on objectives arise from this work in order to continue the exploration of the impacts of an industry transition to HALEU in the United States and abroad. First, continued development and formalization of the algorithms used herein is paramount. As discussed in Chapter 3, the study of heterogeneity involved the use of several disjointed code systems and the development of a set of arguably bespoke methods. These methods could easily be expanded and implemented in a robust, validated, code system. Such an endeavor would accomplish two goals: expansion of the evaluation across an entire range of enrichment from six to thirty-four percent U-235 and validation to ensure that the results of such an analysis are robust and useful for real-world NCS applications. Implementation of the described methodology into a single concise code system would likely produce a tool with usefulness across the nuclear industry in safety applications.

Additionally, a systematic evaluation using a validated computational tool would be of great benefit to efforts to preserve and further evaluate legacy data in nuclear engineering. The ability to perform critical nuclear experiments is severely limited based on the availability of funding and the nature of hazards produced from such experiments. As can be seen throughout this work, reliance on data generated in the mid-twentieth century, often poorly preserved, is extremely commonplace in nuclear criticality safety applications. In order to ensure advancement in the field of NCS, it is a priority to preserve critical experiment data through efforts like the ICSBEP; the methods described in this work could easily be expanded as an extension of this priority. Of course, if critical experiments could be conducted to evaluate the effects of heterogeneity using direct measurements, they absolutely should be.

Another particular future-work objective appearing in this work is the expansion of the ICSBEP methodology. As discussed in Chapter 1, the effect of heterogeneity was observed during the conduct of work in Chapter 2, but it was dismissed as oppositional to the overall objective. That is, because the bias observed when the heterogeneous experiment was ‘simplified’ to a homogeneous model was too large, it was discarded and not recorded; this was an unforced error. What should have happened is that the bias should have been recorded and explored further at the time to demonstrate a potential relationship between the bias and the experimental parameters (in this case, moderator-to-fuel ratio). The work described in Chapter 4 and 5 shows that there is much more data which can be extracted from even the existing benchmark evaluations. It is likely that there are many, many benchmark evaluations in the handbook that have ‘hidden’ correlations awaiting discovery and exploration. Future benchmark experiment evaluations should ensure that careful analysis of systemic bias is conducted.

Finally, the work of Goertzel and Morfitt deserve a benchmark evaluation. Morfitt’s dissertation [3]

almost certainly contains sufficient detail of his experimental findings to produce a quality benchmark experiment evaluation. Again, in keeping with data preservation goals, this particular experiment can provide a myriad of useful data for future nuclear engineering applications. It might even be possible that a rigorous examination of this experiment and a renewed look at Goertzel's analytical solution method may give rise to more advanced methodologies to evaluate critical nuclear systems, especially considering that their work was conducted in an age where modern computational systems simply didn't exist.

## 6.4 CLOSING REMARKS

As discussed in Chapter 1, the work of supporting the advancement of reactor designs and expansion of the nuclear industry causes NCS practitioners in the nuclear fuels industry to face difficult dilemma. On one hand, nuclear safety is the highest priority for any fuel cycle facility, as the consequences of a nuclear criticality accident are dire. On the other, production of fuels with higher enrichment must be economically competitive in order to meet the growing demand for advanced nuclear applications, lest the technology be abandoned prematurely as "too expensive". While it is convenient to proclaim that nuclear safety will always triumph in these circumstances, history has shown that this is not always the case [4].

Many of the historical criticality accidents are the indirect result of time and schedule pressures driven by production demands. Often, the margins applied to nuclear systems for safety reasons are restrictive and unwieldy, which makes them subject to bypass by operations personnel who may not understand the particular details or importance of the rules. By reducing safety margins, however, the risk associated with the activities increases. Therefore, it is often the choice of safety professionals to apply conservative, and perhaps overly-conservative, margins to every activity, especially in the face of uncertainty. Combating this uncertainty and providing validated and reliable data to safety analysts is one way to simultaneously meet the objectives of protecting human lives from the consequences of a nuclear criticality accident and meeting production goals for advanced nuclear fuels, which was the overall objective of this work.

In order to manage the competing demands of safety and production, it is fundamentally necessary that NCS professionals have reliable tools and data to ensure that nuclear safety objectives are never compromised and that they are able to effectively manage increased demand rates for complex and higher-enrichment fuels. This work shows that there are avenues by which even historical data can be used to dramatically improve the knowledge base used in NCS at a relatively low cost by using

existing tools to extend the evaluation of historical critical experiments. Consequently, it follows that further development of these types of tools will open the door for NCS practitioners to always ensure that nuclear criticality accidents are prevented while reducing the conservatism baked-in to the existing guidance which has a strong potential to shrink production margins to unmanageable levels.

## REFERENCES

- [1] Nuclear Energy Agency. *International Handbook of Evaluated Criticality Safety Benchmark Experiments*. NEA No. 7520. Paris: OECD Nuclear Energy Agency, July 2020.
- [2] Clayton, E.D. *Anomalies of Nuclear Criticality*. Tech. rep. PNNL-19176. Pacific Northwest Laboratory, 2010.
- [3] J.W. Morfitt. *Minimum Critical Mass and Uniform Thermal Neutron Core Flux in an Experimental Reactor*. Ph.D. Thesis. Report number Y-1023. Declassified November 22, 1957. Oak Ridge, TN: United States Atomic Energy Commission, Dec. 1953.
- [4] H. C. Paxton and N. L. Pruvost. *Critical dimensions of systems containing  $^{235}\text{U}$ ,  $^{239}\text{Pu}$ , and  $^{233}\text{U}$* . Tech. rep. LA-10860-MS. Los Alamos National Laboratory, 1987.

## APPENDIX A: TYPICAL INPUT LISTINGS

Monte Carlo N-Particle (MCNP) version 5.1.51 calculations were utilized for calculating results in this evaluation. The Evaluated Neutron Data File library ENDF/B-VII.0 was utilized in analysis of the experiment and benchmark model biases and uncertainties. The MCNP5 calculations were performed with 750 generations with 100,000 neutrons per generation. The keff estimates did not include the first 50 generations and the statistical uncertainty in  $k_{\text{eff}}$  is 0.00010.

### A.1 EXAMPLE MCNP INPUT DECK FOR CASE 1

```

LEUMT 4 4.27cm Spaced Triangular Lattice
c
c Simplified Model
c Experiment Number T-4.27-35
c 35 Rods, Water Height 62.00 cm
c
c
c *****
c |                               Cell Cards                               |
c *****
c
c
c Universe 1 is a FUELED lattice Element
c
101 1 4.7804-02  -001                               u=1 imp:n=1
102 3 0.099988  001 -004 049                         u=1 imp:n=1
103 3 0.099988  001 005 -006                         u=1 imp:n=1
105 3 0.099988  001 #102 #103 #104                   u=1 imp:n=1
104 3 0.099988  001 070 -071                         u=1 imp:n=1
c
c Universe 2 is an EMPTY lattice Element
c
201 3 0.099988  -001                               u=2 imp:n=1
202 3 0.099988  001 -004 049                         u=2 imp:n=1

```





```

3 3 3 3 3 3 3 3 3 3 3 3 3 3 3 3 3 3 3 3 3 3 &
3 3 3 3 3 3 3 3 3 3 3 3 3 3 3 3 3 3 3 3 3 3 &
3 3 3 3 3 3 3 3 3 3 3 3 3 3 3 3 3 3 3 3 3 3 &
3 3 3 3 3 3 3 3 3 3 3 3 3 3 3 3 3 3 3 3 3 3 &
3 3 3 3 3 3 3 3 3 3 3 3 3 3 3 3 3 3 3 3 3 3 &
3 3 3 3 3 3 3 3 3 3 3 3 3 3 3 3 3 3 3 3 3 3 &
3 3 3 3 3 3 3 3 3 3 3 3 3 3 3 3 3 3 3 3 3 3 &

```

```
imp:n=1
```

```
c
```

```
502 0 003 -023 ((-051 052 -053 054):(-055 051 -053 054):(-051 052 &
-057 053):(-052 056 -053 054):(-051 052 -054 058)) &
```

```
fill=4 imp:n=1
```

```
c
```

```
401 3 0.099988 -002 u=9 imp:n=1
402 3 0.099988 002 -004 049 u=9 imp:n=1
403 3 0.099988 002 005 -006 u=9 imp:n=1
404 3 0.099988 002 #402 #403 #405 u=9 imp:n=1
405 3 0.099988 002 070 -071 u=9 imp:n=1
406 0 -059 051 -061 053 003 -023 fill=9 imp:n=1
```

```
c
```

```
411 3 0.099988 -024 u=6 imp:n=1
412 3 0.099988 024 -004 049 u=6 imp:n=1
413 3 0.099988 024 005 -006 u=6 imp:n=1
414 3 0.099988 024 #412 #413 #415 u=6 imp:n=1
415 3 0.099988 024 070 -071 u=6 imp:n=1
416 0 -052 060 -061 053 003 -023 fill=6 imp:n=1
```

```
c
```

```
421 3 0.099988 -025 u=7 imp:n=1
422 3 0.099988 025 -004 049 u=7 imp:n=1
423 3 0.099988 025 005 -006 u=7 imp:n=1
424 3 0.099988 025 #422 #423 #425 u=7 imp:n=1
425 3 0.099988 025 070 -071 u=7 imp:n=1
447 0 -052 060 -054 062 003 -023 fill=7 imp:n=1
```

```

c
431 3 0.099988 -026 u=8 imp:n=1
432 3 0.099988 026 -004 049 u=8 imp:n=1
433 3 0.099988 026 005 -006 u=8 imp:n=1
434 3 0.099988 026 #432 #433 #435 u=8 imp:n=1
435 3 0.099988 026 070 -071 u=8 imp:n=1
448 0 -059 051 -054 062 003 -023 fill=8 imp:n=1
c
c
701 3 0.099988 ((-004 049):(005 -006):(70 -71)) -059 055 -053 054 imp:n=1
702 3 0.099988 -059 055 -053 054 #701 003 -023 imp:n=1
c
703 3 0.099988 ((-004 049):(005 -006):(70 -71)) -051 052 -061 057 imp:n=1
704 3 0.099988 -051 052 -061 057 #703 003 -023 imp:n=1
c
705 3 0.099988 ((-004 049):(005 -006):(70 -71)) -056 060 -053 054 imp:n=1
706 3 0.099988 -056 060 -053 054 #705 003 -023 imp:n=1
c
707 3 0.099988 ((-004 049):(005 -006):(70 -71)) -051 052 -058 062 imp:n=1
708 3 0.099988 -051 052 -058 062 #707 003 -023 imp:n=1
c
601 3 0.099988 -031 030 -040 (059:-060:061:-062) #801 #830 #831 &
#832 #833 #834 #835 #836 #837 #838 #839 #840 #841 #842 #843 imp:n=1
602 3 0.099988 -059 060 -061 062 023 -040 imp:n=1
c
801 3 0.099988 (-003 027 -059 060 -061 062) imp:n=1
c
811 3 0.099988 ((-392 39 -059 060 -061 062) &
((-059 352):(060 -362):(-061 372):(062 -382))) imp:n=1
812 3 0.099988 (392 -027 -059 035 -061 382):(392 -027 060 -036 &
-061 382):(392 -027 -061 037 -059 060):(392 -027 -38 62 -59 60) imp:n=1
813 3 0.099988 (-391 039 -059 035 -061 382):(-391 039 060 -036 &
-061 382):(-391 039 -061 037 -059 060):(-391 039 -38 62 -59 60) imp:n=1

```

814 3 0.099988 (-392 391 035 -351 -371 381):(-392 391 -036 361 &  
-371 38):(-392 391 -371 37 -351 361):(-392 391 -038 381 361 -351) imp:n=1

c

820 3 0.099988 (-027 039 -035 036 -037 038) imp:n=1

821 3 0.099988 (-392 391 -352 351 -372 382):(-392 391 -361 362 -372 &  
382):(-392 391 -372 371 -352 362):(-392 391 -381 382 -352 362) imp:n=1

c

830 3 0.099988 -039 080 -081 072 -073 074 imp:n=1

831 3 0.099988 -080 075 -073 074 -081 0711 imp:n=1

832 3 0.099988 -080 075 -073 074 -0711 0712 imp:n=1

833 3 0.099988 -080 075 -073 074 -0712 0713 imp:n=1

834 3 0.099988 -080 075 -073 074 -0713 0714 imp:n=1

835 3 0.099988 -080 075 -073 074 -0714 0715 imp:n=1

836 3 0.099988 -080 075 -073 074 -0715 0716 imp:n=1

837 3 0.099988 -080 075 -073 074 -0716 0717 imp:n=1

838 3 0.099988 -080 075 -073 074 -0717 0718 imp:n=1

839 3 0.099988 -080 075 -073 074 -0718 0719 imp:n=1

840 3 0.099988 -080 075 -073 074 -0719 0720 imp:n=1

841 3 0.099988 -080 075 -073 074 -0720 0721 imp:n=1

842 3 0.099988 -080 075 -073 074 -0721 0722 imp:n=1

843 3 0.099988 -080 075 -073 074 -0722 072 imp:n=1

c

850 3 0.099988 030 -075 -059 060 -061 062 imp:n=1

c

802 0 ((-030 033):031) -032 -034 033 imp:n=1

c

c

803 0 (040 -031):(031 034):032:-033 imp:n=0

c \*\*\*\*\*

c | Surface Cards |

c \*\*\*\*\*

c

```

001 cz 1.245          $ fuel cylinder
002 c/z 25.4 25.4 0.28125 $ steel rod support
024 c/z -25.4 25.4 0.28125 $ steel rod support
025 c/z -25.4 -25.4 0.28125 $ steel rod support
026 c/z 25.4 -25.4 0.28125 $ steel rod support
c
c
003 pz 0.0           $ bottom plane
004 pz 1.27          $ lower lattice plate top
049 pz 0.635         $ lower lattice plate bottom
005 pz 29.365        $ upper lattice plate bottom
006 pz 30.635        $ upper lattice plate top
070 pz 55.0
071 pz 55.635
c
010 p 1 1.73205 0 4.27
011 p -1 1.73205 0 -4.27
012 p 1 1.73205 0 -4.27
013 p -1 1.73205 0 4.27
014 px 2.135
015 px -2.135
c
051 px 23.485        $ support rod cell boundaries
052 px -23.485
053 py 23.485
054 py -23.485
c
055 px 29.9          $ inner lattice boundaries
056 px -29.9
057 py 29.9
058 py -29.9
c
059 px 30.48         $ outer lattice boundaries

```

```

060 px -30.48
061 py 30.48
062 py -30.48
c
023 pz 60.0          $ fuel rod top
c
027 pz -2.54        $ tabletop bottom
028 px 28.48        $ table legs
029 px -28.49
030 pz -16.51       $ tank bottom inside
c
031 cz 58.3         $ tank I.D.
032 cz 59.2525      $ tank O.D.
033 pz -16.98625    $ tank bottom outside
034 pz 100          $ tank top
c
035 px 20.32
0351 px 20.79625
0352 px 30.00375
036 px -20.32
0361 px -20.79625
0362 px -30.00375
037 py 20.32
0371 py 20.79625
0372 py 30.00375
038 py -20.32
0381 py -20.79625
0382 py -30.00375
039 pz -7.62        $ steel angle bottom
0391 pz -7.14375    $ steel support inside (bot)
0392 pz -3.01625    $ steel support inside (top)
c
080 pz -12.7        $ table 2" middle

```

081 px 33.02  
 0711 px 20.32  
 0712 px 17.78  
 0713 px 12.7  
 0714 px 10.16  
 0715 px 5.08  
 0716 px 2.54  
 0717 px -2.54  
 0718 px -5.08  
 0719 px -10.16  
 0720 px -12.7  
 0721 px -17.78  
 0722 px -20.32  
 072 px -33.02  
 073 py 33.02  
 074 py -33.02  
 075 pz -15.24

c

c

040 pz 62.0 \$ water height

c

c \*\*\*\*\*

c | Data Cards |

c \*\*\*\*\*

c

c

m2 6000.70c 3.5790-2 &  
 1001.70c 5.7255-2 1002.70c 8.5896-06 &  
 8016.70c 1.4310-2 8017.70c 5.7264-06 \$ Plexiglas

mt2 poly.10t

c

m4 6000.70c 3.2210-04 &

26054.70c 3.4444-03 26056.70c 5.4021-02 &  
 26057.70c 1.2482-03 26058.70c 1.6486-04 &  
 25055.70c 1.7604-03 15031.70c 7.0256-05 &  
 16032.70c 4.2989-05 16033.70c 3.3931-07 &  
 16034.70c 1.9047-06 16036.70c 9.0484-09 &  
 14028.70c 1.1910-03 14029.70c 6.0306-05 &  
 14030.70c 4.0032-05 24050.70c 7.6866-04 &  
 24052.70c 1.4806-02 24053.70c 1.6787-03 &  
 24054.70c 4.1702-04 28058.70c 5.6091-03 &  
 28060.70c 2.1603-03 28061.70c 9.3925-05 &  
 28062.70c 2.9908-04 28064.70c 7.6623-05 &  
 7014.70c 3.4397-04 7015.70c 1.2774-06 \$ SS304  
 c  
 m5 6000.70c 5.9039-04 &  
 26054.70c 4.9447-03 26056.70c 7.7551-02 &  
 26057.70c 1.7919-03 26058.70c 2.3667-04 \$ Carbon Steel  
 c  
 m3 8016.70c 3.3329-02 1001.70c 6.6658-02 \$ Water  
 mt3 lwtr.10t  
 c  
 m1 92234.70c 1.8465-05 92235.70c 2.3941-03 92238.70c 4.5391-02  
 c  
 c  
 kcode 100000 1.0 50 750  
 ksrc -12.81 0 15 -8.54 0 15 -4.27 0 15 0 0 15 4.27 0 15 8.54 0 15 &  
 12.81 0 15 -10.675 3.70 15 -6.405 3.70 15 -2.135 3.70 15 &  
 2.135 3.70 15 6.405 3.70 15 10.675 3.70 15 -8.54 7.40 15 -4.27 7.40 15 &  
 0 7.40 15 4.27 7.40 15 8.54 7.40 15 -6.405 11.10 15 -2.135 11.10 15 &  
 2.135 11.10 15 -10.675 -3.70 15 -6.405 -3.70 15 -2.135 -3.70 15 &  
 2.135 -3.70 15 6.405 -3.70 15 10.675 -3.70 15 -8.54 -7.40 15 &  
 -4.27 -7.40 15 0 -7.40 15 4.27 -7.40 15 8.54 -7.40 15 -2.135 -11.10 15 &  
 2.135 -11.10 15 6.405 -11.10 15 &  
 -12.81 0 45 -8.54 0 45 -4.27 0 45 0 0 45 4.27 0 45 8.54 0 45 &



```
12.81 0 45 -10.675 3.70 45 -6.405 3.70 45 -2.135 3.70 45      &
2.135 3.70 45 6.405 3.70 45 10.675 3.70 45 -8.54 7.40 45 -4.27 7.40 45 &
0 7.40 45 4.27 7.40 45 8.54 7.40 45 -6.405 11.10 45 -2.135 11.10 45    &
2.135 11.10 45 -10.675 -3.70 45 -6.405 -3.70 45 -2.135 -3.70 45      &
2.135 -3.70 45 6.405 -3.70 45 10.675 -3.70 45 -8.54 -7.40 45          &
-4.27 -7.40 45 0 -7.40 45 4.27 -7.40 45 8.54 -7.40 45 -2.135 -11.10 45 &
2.135 -11.10 45 6.405 -11.10 45
```

```
print
```

APPENDIX B: SELECTED PORTIONS OF THE LETTER  
FROM E. B. JOHNSON TO G. E. WHITESIDES



INTERNAL CORRESPONDENCE

NUCLEAR DIVISION

POST OFFICE BOX X, OAK RIDGE, TENNESSEE 37831

To (Name) G. E. Whitesides Date February 16, 1968  
 Company  
 Location  
 Originating Dept.  
 Answering letter date  
 Copy to Subject

*Dear Elliott*

Enclosed are draft copies of our data on lattices of U(4.89) rods in water. I hope the tables are self-explanatory in the absence of text. However, there are a few facts which are not specifically included.

The rods are unclad metal, each  $30.00 \pm 0.01$  cm long. Two coaxial rods go into the 60-cm-high lattices. There was a water reflector at least 15 cm thick on all sides of each lattice. The tabular data summary indicates the reactivity for each near-critical lattice.

We are extending these measurements to include rods 0.76 cm (0.30 in.) in diameter and intend to use an even smaller diameter. Limited measures of the criticality of lattices of rods of each diameter in aqueous boron solution, in dilute U(4.98)O<sub>2</sub>F<sub>2</sub> solution, and in the uranyl fluoride solutions containing boron are also in progress. We will send you these data in draft form as they are completed if you are interested. Eventually, of course, there will be a report containing all this information.

We are interested in the results of any use you make of these data.

E. B. Johnson

EBJ:mw

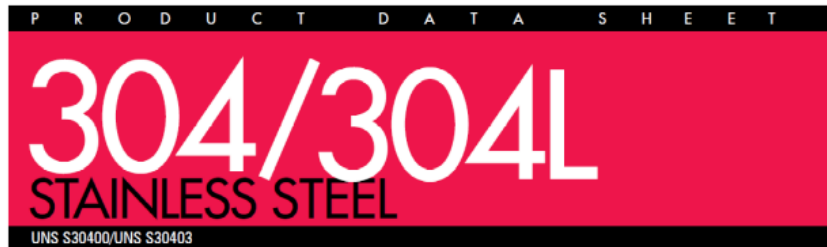
*Ely*

Critical Lattices of U(4.89) Rods in Water  
 Rod Diameter: 2.49 cm (0.982 in.)  
 Triangular Pattern<sup>a</sup>

Lattice Spacing (cm)	Surface	Center	Lattice Height (cm)	Total Number of Rods	Mass of <sup>235</sup> U (kg)	Volume of Water Volume of Uranium	Concentration (g of <sup>235</sup> U/liter)	Reactivity of Submerged Lattice (cents)
1.78			30	50	6.772	2.232	286.0	~21
			60	34	9.210			Subcritical
				35	9.481			~37
2.23			30	45	6.095	2.949	234.0	Subcritical
				46	6.231			~18
			60	31	8.398			-9.8
				32	8.669			102
2.73			30	49	6.637	3.830	191.3	~33
				48	6.502			Subcritical
			60	31	8.398			Subcritical
				32	8.669			~92
3.53			30	73	9.888	5.424	143.9	~16
				72	9.752			-2.9
			60	39	10.565			9.6
				38	10.294			Subcritical

a. Incomplete outer rings consisted of rods symmetrically placed on the six faces.

# APPENDIX C: MATERIAL DATA SHEET FOR STAINLESS STEEL



AK Steel Type 304 is a variation of the basic 18-8 grade, Type 302, with a higher chromium and lower carbon content. Lower carbon minimizes chromium carbide precipitation due to welding and its susceptibility to intergranular corrosion. In many instances, it can be used in the "as-welded" condition, while Type 302 must be annealed in order to retain adequate corrosion resistance.

Type 304L is an extra low-carbon variation of Type 304 with a 0.03% maximum carbon content that eliminates carbide precipitation due to welding. As a result, this alloy can be used in the "as-welded" condition, even in severe corrosive conditions. It often eliminates the necessity of annealing weldments except for applications specifying stress relief. It has slightly lower mechanical properties than Type 304.

Typical uses include architectural moldings and trim, kitchen equipment, welded components of chemical, textile, paper, pharmaceutical and chemical industry processing equipment.

#### AVAILABLE FORMS

AK Steel produces Type 304 Stainless Steel in thicknesses from 0.01" to 0.25" (0.025 to 6.35 mm) max. and widths up to 48" (1219 mm). For other thicknesses and widths, inquire.

#### COMPOSITION

	Type 304 %	Type 304L %
Carbon	0.08 max.	0.03 max.
Manganese	2.00 max.	2.00 max.
Phosphorus	0.045 max.	0.045 max.
Sulfur	0.030 max.	0.030 max.
Silicon	0.75 max.	0.75 max.
Chromium	18.00-20.00	18.0-20.0
Nickel	8.00-12.00	8.0-12.0
Nitrogen	0.10 max.	0.10 max.
Iron	Balance	Balance

#### SPECIFICATIONS

AK Steel Types 304 and 304L Stainless Steels are covered by the following specifications:

Type 304	Type 304L
AMS 5513	AMS 5511
ASTM A 240	ASTM A 240
ASTM A 666	ASTM A 666

#### MECHANICAL PROPERTIES

Typical Room Temperature Mechanical Properties

	UTS ksi (MPa)	0.2% YS ksi (MPa)	Elongation % in 2" (50.8 mm)	Hardness Rockwell
Type 304L	85 (586)	35 (241)	55	B80
Type 304	90 (621)	42 (290)	55	B82

## AK STEEL 304/304L STAINLESS STEEL DATA SHEET

### PHYSICAL PROPERTIES

Density, 0.29 lbs/in<sup>3</sup>  
8.03 g/cm<sup>3</sup>

Electrical Resistivity, microhm-in  
(microhm-cm)  
68°F (20°C) – 28.4 (72)  
1200°F (659°C) – 45.8 (116)

Specific Heat, BTU/lb/°F (kJ/kg•K)  
32 - 212°F (0 - 100°C) – 0.12 (0.50)

Thermal Conductivity, BTU/hr/ft<sup>2</sup>/ft/°F  
(W/m•K)  
at 212°F (100°C) – 9.4 (16.2)  
at 932°F (500°C) – 12.4 (21.4)

Mean Coefficient of Thermal Expansion,  
in/in/°F (µm/m•K)  
32 - 212°F (0 - 100°C) –  $9.4 \times 10^{-6}$  (16.9)  
32 - 600°F (0 - 315°C) –  $9.6 \times 10^{-6}$  (17.3)  
32 - 1000°F (0 - 538°C) –  $10.2 \times 10^{-6}$  (18.4)  
32 - 1200°F (0 - 649°C) –  $10.4 \times 10^{-6}$  (18.7)

Magnetic Permeability, H – 200  
Oersteds, Annealed - 1.02 max.

Modulus of Elasticity, ksi (MPa)  
 $28.0 \times 10^3$  (193 x 10<sup>3</sup>) in tension  
 $11.2 \times 10^3$  (78 x 10<sup>3</sup>) in torsion

Melting Range, °F (°C) – 2550 - 2650  
(1399 - 1454)

### CORROSION RESISTANCE

These steels exhibit excellent resistance to a wide range of atmospheric, chemical, textile, petroleum and food industry exposures.

### OXIDATION RESISTANCE

The maximum temperature to which Types 304 and 304L can be exposed continuously without appreciable scaling is about 1650°F (899°C). For intermittent exposure, the maximum exposure temperature is about 1500°F (816°C).

### HEAT TREATMENTS

Type 304 is non-hardenable by heat treatment. Annealing: Heat to 1900 - 2050°F (1038 - 1121°C), then cool rapidly. Thin strip sections may be air cooled, but heavy sections should be water quenched to minimize exposure in the carbide precipitation region.

Stress Relief Annealing: Cold worked parts should be stress relieved at 750°F (399°C) for 1/2 to 2 hours.

### FORMABILITY

Types 304 and 304L have very good drawability. Their combination of low yield strength and high elongation permits successful forming of complex shapes. However, these grades work harden rapidly. To relieve stresses produced in severe forming or spinning, parts should be full annealed or stress-relief annealed as soon as possible after forming.

### WELDABILITY

The austenitic class of stainless steels is generally considered to be weldable by the common fusion and resistance

techniques. Special consideration is required to avoid weld "hot cracking" by assuring formation of ferrite in the weld deposit. Types 304 and 304L are generally considered to be the most common alloys of this stainless class. When a weld filler is needed, AWS E/ER 308, 308L or 347 are most often specified. Types 304 and 304L Stainless Steels are well known in reference literature and more information can be obtained in this way.

### METRIC CONVERSION

Data in this publication are presented in U.S. customary units. Approximate metric equivalents may be obtained by performing the following calculations:

Length (inches to millimeters) –  
Multiply by 25.4

Strength (ksi to megapascals or  
meganeutons per square meter) –  
Multiply by 6.8948

Temperature (Fahrenheit to Celsius) –  
(°Fahrenheit - 32) Multiply by 0.5556

Density (pounds per cubic inch to  
kilograms per cubic meter) –  
Multiply by 27,670

The information and data in this product data sheet are accurate to the best of our knowledge and belief, but are intended for general information only. Applications suggested for the materials are described only to help readers make their own evaluations and decisions, and are neither guarantees nor to be construed as express or implied warranties of suitability for these or other applications.

Data referring to mechanical properties and chemical analyses are the result of tests performed on specimens obtained from specific locations with prescribed sampling procedures; any warranty thereof is limited to the values obtained at such locations and by such procedures. There is no warranty with respect to values of the materials at other locations.

AK Steel and the AK Steel logo are registered trademarks of AK Steel Corporation.



Customer Service 800-331-9090

AK Steel Corporation  
3221 Centre Pointe Drive  
West Chester, OH 45389

www.aksteel.com

© 2007 AK Steel Corporation

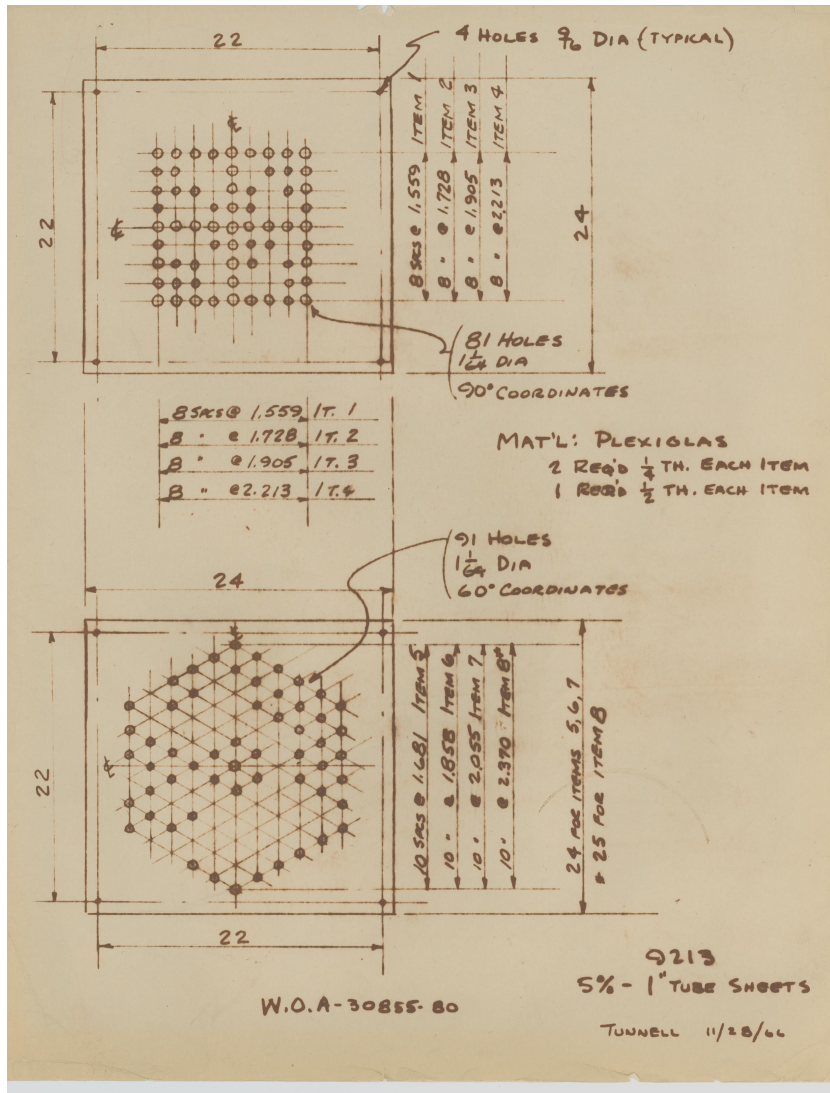


7100-0096 7/07






# APPENDIX F: LATTICE PLATE ASSEMBLY DRAWING







## APPENDIX H: LATTICE PLATE ASSEMBLY DRAWING

 **INTERNAL CORRESPONDENCE**

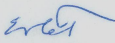
**NUCLEAR DIVISION** POST OFFICE BOX X, OAK RIDGE, TENNESSEE 37831

To (Name) E. Maeyens Date August 22, 1966  
Company Y-12 Originating Dept. Critical Experiments Facility  
Location Bldg. 9723-14 Answering letter date

Copy to E. B. Johnson ✓ Subject 5% Rods, Work Order A-30822-00

Please refer to memo of August 12, 1966 requesting that the 5% metal rods be machined to 15.750 in. length. We wish to revise this dimension to  $11.811 \pm 0.010$  in. length for all three sizes.

It is our understanding that the 1-in.-diam size will be cut to length first, and we ask that we be notified if a change is made in this procedure.

  
W. C. Tunnell

WCT:ff